UNIVERSIDADE FEDERAL DA BAHIA
FACULDADE DE MEDICINA
FUNDAÇÃO OSWALDO CRUZ
INSTITUTO GONÇALO MONIZ

UFBA

FIOCRUZ

Programa de Pós-Graduação em Patologia

TESE DE DOUTORADO

MICROSCOPIA CONFOCAL DE REFLECTÂNCIA (MCR) NO DIAGNÓSTICO DE NEOPLASIAS DA PELE

NAIARA ABREU FRAGA BRAGHIROLI

Salvador – Bahia

2018

UNIVERSIDADE FEDERAL DA BAHIA
FACULDADE DE MEDICINA
FUNDAÇÃO OSWALDO CRUZ
INSTITUTO GONÇALO MONIZ

Programa de Pós-Graduação em Patologia

MICROSCOPIA CONFOCAL DE REFLECTÂNCIA (RCM) NO DIAGNÓSTICO DE NEOPLASIAS DA PELE

NAIARA ABREU FRAGA BRAGHIROLI

Orientador: Prof. Dr. Harold S. Rabinovitz
Co-orientador: Prof. Dr. Luiz Antônio Rodrigues de Freitas

Tese apresentada ao Curso de Pós-Graduação em Patologia Humana para a obtenção do grau de Doutor.

Salvador – Bahia

2018

Ficha Catalográfica elaborada pela Biblioteca do
Instituto Gonçalo Moniz / FIOCRUZ - Salvador - Bahia.

Braghiroli, Naiara Abreu Fraga
B813m Microscopia confocal de reflectância (RCM) no diagnóstico de neoplasias da pele. / Naiara Abreu Fraga Braghiroli. - 2018.
88 f. : il. ; 30 cm.

Orientador: Prof. Dr. Luiz Antônio Rodrigues de Freitas, Laboratório de Patologia Estrutural e Molecular.
Tese (Doutorado em Patologia) – Universidade Federal da Bahia, Faculdade de Medicina. Fundação Oswaldo Cruz, Instituto Gonçalo Moniz, 2018.

1. Microscopia confocal. 2. Câncer de pele. 3. Carcinoma basocelular. 4. Carcinoma espinocelular. 5. Ceratose seborreica. I. Título.

CDU 616-006.8

Título da Tese: " **MICROSCOPIA CONFOCAL DE REFLECTÂNCIA (MCR) NO DIAGNÓSTICO DE NEOPLASIAS DA PELE"**

NAIARA ABREU FRAGA BRAGHIROLI

FOLHA DE APROVAÇÃO

Salvador, 25 de julho de 2018

COMISSÃO EXAMINADORA

Dr. Pedro Dantas Oliveira
Professor
UFS

Dra. Juliana Dumet Fernandes
Professora
UFBA

Dr. Paulo Roberto Lima Machado
Professor
UFBA

Dr. Eduardo Antonio Gonçalves Ramos
Professor Adjunto
UFBA

Dr. Luiz Antonio Rodrigues de Freitas
Pesquisador
IGM/Fiocruz

APOIO E FONTES DE FINANCIAMENTO

Agradecimentos à Universidade de Miami (Miami-Florida/USA) e à Skin & Cancer Associates (Plantation-Florida/USA) pela disponibilização do aparelho de Microscopia Confocal 1500 e 3000, permissão para utilização de bancos de dados, bem como a aprovação do Parecer do Comitê de Ética (Institutional Review Board)/ Liberação do IRB para realização de estudos retrospectivos em dermatoscopia e microscopia confocal de reflectância.

Dedico esse trabalho a todos os pesquisadores e estudiosos que acreditam no valor da dedicação, da disciplina e da persistência; e, como prêmio, podem ver o fruto do seu esforço se tornar benefício à saúde de um outro ser.

AGRADECIMENTOS

Agradeço à Deus, pela minha existência, com suas bênçãos e desafios que me promovem a oportunidade de evoluir como ser humano.

Ao Prof. Dr. Harold S. Rabinovitz, por me acolher em seu serviço de forma tão generosa e por me incentivar diariamente, com seu exemplo, a ser uma profissional ética e competente. Agradeço o seu suporte incondicional na elaboração e execução dos meus projetos. Exemplo de mestre, na profissão e na vida. À Maggie Oliviero e toda à equipe do serviço de dermatologia da Skin & Cancer Associates meus agradecimentos pelo acolhimento e amizade.

Ao Prof. Dr. Luíz Antônio Rodrigues de Freitas, pela confiança em mim depositada, aceitando o desafio de orientar-me à distância e pela oportunidade de realização de um sonho.

À Profa. Dra. Maria Clara B. F. Melro Braghiroli, agradeço pelo apoio, incentivo, e, principalmente, pela inspiração. Agradeço por abraçar como seu esse projeto, auxiliando em todas as etapas, principalmente na redação final do trabalho.

Aos meus pais, Hermenegildo e Diacuí, e minha irmã Larissa, pelo apoio e suporte eterno e incondicional. Pela formação de meu caráter, por sempre me incentivarem, com seus exemplos, a seguir o caminho certo, mesmo que mais longo e desafiante. Por plantar em mim a semente da ética e respeito ao próximo. Valores que irei passar aos meus filhos, Maria Cecilia e João Pedro, a primeira, minha fonte de luz na vida e o segundo, que ainda é tão pequeno, mas já muito amado e me transforma em uma pessoa melhor. Razões do meu viver.

Ao meu esposo João, meu amor, melhor amigo, meu companheiro de vida. Agradeço a cumplicidade, força e apoio diário.

Aos bons préstimos da biblioteca do Instituto Gonçalo Moniz- IGM/FIOCRUZ, em especial a senhora Ana Maria Fiscina Vaz Sampaio.

Aos pacientes, razão principal desse projeto.

“ A tarefa não é tanto ver aquilo que ninguém viu,

mas pensar o que ninguém ainda pensou

sobre aquilo que todo mundo vê”

Arthur Schopenhauer

BRAGHIROLI, Naiara Abreu Fraga. Microscopia confocal de reflectância (RCM) no diagnóstico de neoplasias da pele. 88 f. il. Tese (Doutorado em Patologia) – Universidade Federal da Bahia. Fundação Oswaldo Cruz, Instituto Gonçalo Moniz, Salvador, 2018.

RESUMO

INTRODUÇÃO: Desde sua introdução na prática da clínica médica, a Microscopia Confocal de Reflectância (MCR) vem contribuindo no diagnóstico não invasivo de neoplasias benignas e malignas da pele. Ela tem sido utilizada como ferramenta auxiliar em lesões com achados equívocos ao exame clínico e dermatoscópico. A MCR tem reduzido substancialmente a necessidade de realização de biópsias de lesões benignas, especialmente em locais anatômicos de difícil acesso cirúrgico. Os resultados obtidos tem demonstrado excelente correlação com os aspectos histológicos, articulando-se como uma ponte entre a dermatoscopia e a histopatologia. Os aprimoramentos tecnológicos na funcionalidade e dimensões das sondas, e a subsequente disponibilização de equipamentos mais compactos, como o Vivascope 1500 e o Vivascope 3000, vêm, progressivamente, revolucionando a abordagem médica das neoplasias cutâneas. Assim, a MCR é atualmente reconhecida como uma ferramenta adjunta no diagnóstico *in vivo* não invasivo de neoplasias cutâneas, na delimitação de margens tumorais e no monitoramento da resposta ao tratamento não cirúrgico do câncer de pele. **OBJETIVO:** O presente trabalho tem como objetivo o estabelecimento de critérios na MCR de lesões cutâneas equívocas, e correlaciona as características observadas com os aspectos histológicos, no sentido de validar uma ferramenta diagnóstica não invasiva, que permita diferenciar, com significativa precisão, as neoplasias benignas e malignas da pele. **CONCLUSÕES:** Os aspectos morfológicos observados à MCR na avaliação das estruturas da pele mostram equivalência com os achados histológicos, permitindo plena comparação entre as imagens da microscopia confocal e as imagens histopatológicas. O equipamento de MCR com pistola portátil (*handheld*) (HH-RCM) permite o acesso a áreas anatômicas curvadas e pode ser aplicado diretamente à superfície cutânea, sem a necessidade do anel de fixação, tornando o exame da microscopia confocal mais factível e rápido. O modelo HH-RCM é capaz de diagnosticar com precisão pápulas solitárias faciais inespecíficas, dentre elas: carcinoma basocelular (CBC), tricoblastoma desmoplásico, carcinoma escamocelular (CEC), hiperplasia sebácea e nevo melanocítico intradérmico. O equipamento tradicional para realização da MRC, assim como o modelo portátil HH-RCM, demonstram um alto valor preditivo positivo no diagnóstico do CBC. O modelo tradicional mostra um valor preditivo negativo maior que o modelo portátil, devido ao seu campo de visão mais largo, oferecendo uma visão da arquitetura total das lesões maiores que 1,0 mm. A MCR se mostrou precisa no diagnóstico de ceratose seborréica clonal, enquanto que, ao exame clínico e à dermatoscopia, aparenta aspecto semelhante ao melanoma maligno da pele. A mucinose dérmica focal, apesar de clinicamente se assemelhar ao CBC, mostra características na MCR que permitem sua diferenciação do CBC. A MCR permite caracterizar o CEC pigmentado pela presença do padrão de favo de mel atípico nas camadas granulosa e espinhosa da epiderme, associado a presença dos pequenos círculos brilhosos ao redor das papilas dérmicas. O padrão de distribuição dos vasos ao nível da junção dermo-epidérmica e derme papilar é relevante para o diagnóstico do CEC cutâneo. O sinal da “casa de botão” na MCR associado ao padrão de favo de mel atípico ao nível epidérmico é importante no diagnóstico do CEC *in situ*.

Palavras-chaves: Microscopia confocal de reflectância; Câncer de pele; Carcinoma basocelular; Carcinoma espinocelular; Ceratose seborréica clonal; Lesões equívocas cutâneas; Mucinose dérmica focal; Neoplasia cutânea; Tricoepitelioma desmoplásico.

BRAGHIROLI, Naiara Abreu Fraga. Reflectance confocal microscopy (RCM) in the diagnosis of neoplasm of the skin. 88 f. il. Tese (Doutorado em Patologia) – Universidade Federal da Bahia. Fundação Oswaldo Cruz, Instituto Gonçalo Moniz, Salvador, 2018.

ABSTRACT

INTRODUCTION: Since its first introduction in a medical practice, Reflectance Confocal Microscopy (RCM) has been contributing as a non-invasive diagnostic tool for assessment of benign and malignant neoplasms of the skin. RCM has also been used as an adjunct tool for diagnosing equivocal cutaneous lesions that lack characteristic clinical or dermoscopic features. Use of RCM has led to a substantially decreased number of benign lesion biopsies, especially in anatomic areas with limited surgical access. Multiple published studies show a tight correlation between the RCM and histologic features, positioning RCM as a bridge between the dermoscopy and histology. The development of more compact equipment with smaller probes, such as Vivascope 1500 and Vivascope 3000, has led to improved medical assessment of cutaneous neoplasms. Many authorities consider RCM an important in vivo non-invasive adjunct diagnostic tool for the diagnosis of skin lesions, as well as the delineation of tumoral margins during surgery and for monitoring of the non-surgical treatment for skin cancers. **OBJECTIVE:** This study proposes RCM diagnostic criteria of equivocal cutaneous lesions and their histological correlation and validates RCM as a non-invasive diagnostic tool that allows accurate differentiation between benign and malignant neoplasms of the skin. **CONCLUSION:** The morphologic aspects of the skin's structures observed in RCM evaluation correlate well with their corresponding histologic findings. The handheld RCM (HH-RCM) allows for fast evaluation of skin lesions located in curved anatomic areas of the body and face without the necessity of the ring for fixation, allowing evaluation of lesions that otherwise could not be evaluated with the bigger traditional RCM probe. The HH-RCM can precisely diagnose nonspecific solitary facial papules, such as basal cell carcinoma (BCC), desmoplastic trichoblastoma, squamous cell carcinoma (SCC), sebaceous hyperplasia and intradermal melanocytic nevi. Similarly, the wide probe RCM equipment, has shown a high positive predictive value for the diagnosis of BCC. The wide probe RCM shows a higher negative predictive value compared to the HH- RCM for the diagnosis of BCC likely due to its larger field of view, which allows the evaluation of the whole architecture of lesions larger than 1,0 mm. The RCM has also proven very useful in the diagnosis of clonal seborrheic keratosis. This benign skin growth often has clinical and dermoscopic features that can mimic malignant melanoma. Focal dermal mucinosis, although clinically similar to BCC, has different RCM characteristics that allows their differentiation. The RCM findings for pigmented SCC include an atypical honeycomb pattern at the level of the spinous-granular layers and small bright circles around the dermal papillae. The pattern of distribution of the vessels at the dermal-epidermal junction and papillary dermis showing the "buttonhole" sign is specific for SCC. The buttonhole sign associated with the atypical honeycomb pattern at the spinous-granular layer is an important feature for the diagnosis of SCC in situ.

Keywords: Reflectance confocal microscopy; Skin cancer; Basal cell carcinoma; Spinous cell carcinoma; Clonal seborrheic keratosis; Equivocal skin lesions; Focal dermal mucinosis; Skin neoplasm; Desmoplastic trichoepithelioma

LISTAS DE ABREVIATURAS E SIGLAS

BCC	Basal cell carcinoma**.** Leia-se CBC
CBC	Carcinoma basocelular
CEC	Carcinoma escamocelular
CSC	Ceratose Seborréica Clonal
CSK	Leia-se CSC
HH-RCM	Hand-held Reflectance Confocal Microscopy
HS	Hiperplasia sebácea
JDE	Junção dermo-epidérmica
LPLK	Lichen planus-like keratosis. Leia-se ceratose liquenóide
MCR	Microscopia Confocal de Reflectância
MDF	Mucinose Dérmica Focal
RCM	Leia-se MCR
SCC	Leia-se CEC
TBD	Tricoblastoma desmoplásico
VPP	Valor preditivo positivo
VPN	Valor preditivo negativo

SUMÁRIO

1. INTRODUÇÃO

A tecnologia da microscopia confocal de reflectância (MCR) foi criada em 1955, por Marvin Minsky. Sua patente foi obtida em 1957, e descrevia a possibilidade de se realizar a análise de superfícies, com visualização instantânea de imagens ampliadas com alta resolução, permitindo uma varredura da área, no plano horizontal, ao se mover o ponto sob iluminação do objeto em exame.

A primeira publicação científica com dados e imagens geradas pelo microscópio confocal foi de autoria de M. David Eggar e Petran, em 1967**;** os autores relatam o projeto e a construção do microscópio confocal. Em 1969, e depois em 1971, Davidovits e Egger publicaram os primeiros estudos utilizando o microscópio confocal com varredura a laser na avaliação do tecidos orgânicos, utilizando fragmento de nervo *ex vivo* (DAVIDOVITS et al., 1969).

A análise de tecidos vivos, contudo, foi iniciada anos após, em 1980, quando diversos grupos de pesquisas desenvolveram os primeiros estudos em material proveniente de organismos humanos e de outros animais (GONZÁLEZ et al., 2003).

O mapeamento de pele humana com uso da MCR foi realizado em 1995, por Rajadhyaksha e colaboradores, pioneiros na obtenção de imagens de alta resolução, instantâneas e não-destrutivas da pele. (RAJADHYAKSHA et al., 1995).

A MCR fornece imagens com detalhamento a nível celular do tecido cutâneo, no sentido horizontal, em camadas paralelas à superfície da pele. Assim, distingue-se dos aspectos habituais da histologia convencional, que analisa os cortes de tecido no sentido vertical, perpendicular à superfície.

O princípio da MRC envolve o uso de uma fonte de luz pontual que ilumina um ponto focal na pele. A imagem refletida (reflectância) é então visualizada em um detector após passar por um pequeno orifício, permitindo, assim, que somente a área em foco (confocal) seja detectada. Para criar uma imagem da arquitetura completa da lesão estudada, o ponto iluminado pelo feixe de luz é mapeado, permitindo uma seção virtual de uma camada fina horizontal (microscopia) *in vivo,* com uma resolução lateral de 8x8 milímetros (mm). No plano vertical, MCR permite a visualização da epiderme e derme papilar, com um limite de profundidade em torno de 200-250 micrômetros. A tecnologia da MCR se baseia no uso de laser de

baixa potência (laser de diodo) que emite luz infra-vermelha de 830 nanômetros (nm). A seção óptica das imagens da MCR é comparável à resolução das imagens histopatológicas de 30 X.

A MCR apresenta a vantagem de facultar a adoção da conduta clínica em fase antecipada ao exame histopatológico, com a possibilidade de realização do exame *in vivo* e em tempo real, sem dano à pele, fornecendo uma avaliação de toda a arquitetura da lesão estudada numa seção horizontal.

As descrições obtidas pela MCR são importantes para orientar a definição das margens de segurança nas ressecções cirúrgicas, posto que fornecem melhor delimitação das lesões. Também a MCR contribui no direcionamento dos recortes das secções de espécimens para os exames anatomo-patológicos. Assim, constitui um elemento auxiliar para a histopatologia, que habitualmente avalia uma área limitada do espécimen no plano vertical.

As imagens fornecidas pela MCR na avaliação de lesões cutâneas são de coloração preta e branca. Os padrões visualizados são baseados na diferença de refração das várias estruturas da pele. Estruturas com alta refratividade aparecem brancas e brilhosas, enquanto estruturas não reflectantes aparecem escuras/pretas. A melanina produz o maior contraste, com um índice de refração de 1.7, permitindo a identificação de melanócitos e queratinócitos pigmentados individuais, assim como melanófagos. A queratina também tem alto índice de refração (IR=1.5), permitindo a identificação de neoplasias queratinocíticas da pele. Colágeno e células inflamatórias, também se apresentam iluminados na MCR. (QUE et al., 2015)

Existem dois tipos de equipamentos de MCR atualmente disponíveis para o diagnóstico de lesões dermatológicas. O modelo de sonda larga (VIVASCOPE 1500; CaliberID, Rochester, NY) compõe as seções ópticas em um mosaico de imagens, permitindo um campo de visão de 838 mm^2. O modelo portátil (Vivascope 3000; CaliberID, Rochester, NY), introduzido na prática dermatológica em 2011, tem uma sonda de pequenas dimensões, o que permite a avaliação de lesões em áreas curvadas da face e áreas anatomicamente de difícil acesso. Este modelo fornece um campo limitado de visão de 131 mm^2.

Exemplos dos modelos Vivascope 1500 e Vivascope 3000, com suas respectivas sondas:

A B

Vivascope 1500, modelo tradicional. A) Visão geral. B) Sonda larga sendo acoplada ao anel de metal fixado sobre a pele a ser avaliada.

C D

Vivascope 3000, modelo portátil. C) Visão geral. D) Sonda pequena de fácil mobilização.

A sonda portátil se mostrou particularmente útil no diagnóstico de pápulas faciais solitárias. Apresentou uma sensibilidade de 93% e especificidade de 78% no diagnóstico do carcinoma basocelular. (FRAGA-BRAGHIROLI et al., 2014; CASTRO et al., 2015)

Desde sua introdução na prática clínica, a MCR vem contribuindo como um precioso apoio no diagnóstico não invasivo de neoplasias benignas e malignas da pele. Ela tem sido utilizada como ferramenta auxiliar em lesões com achados equívocos por ocasião do exame clínico e também no dermatoscópico. Assim, a MCR tem reduzido a necessidade de realização de biópsias de lesões benignas, especialmente em locais anatômicos de difícil acesso cirúrgico, em regiões complexas do ponto de vista funcional (a exemplo das pálpebras), e nas áreas esteticamente sensíveis. Neste sentido, a resolutividade da MCR mitiga a ansiedade inerente a um processo cirúrgico e a espera por um diagnóstico definitivo, e ademais, diminui os custos para o paciente e para o serviço público de saúde.

Apesar do curto período de experiência médica com utilização da MCR na clínica dermatológica, pode-se já afirmar que os resultados obtidos até no momento tem demonstrado excelente correlação com os aspectos histológicos, articulando-se como uma ponte entre a dermatoscopia e a patologia. Torna-se imprescindível, por conseguinte, a sistematização destes resultados com estabelecimento de critérios diagnósticos que facultem a interpretação dos aspectos morfológicos observados nos diferentes tipos de enfermidades da pele e dos estágios evolutivos das lesões.

Na literatura especializada já se encontram descrições de alguns padrões morfológicos obtidos em exames realizados por MCR, que permitem a configuração de elementos importantes para o raciocínio diagnóstico.

Evidenciamos a vantagem de utilizar os recursos da MCR na avaliação do carcinoma basocelular pigmentado ao examinar um paciente com fototipo cutâneo V. Devido a coloração mais escura da pele, os achados clínicos e dermatoscópicos do CBC pigmentado são mais difíceis de serem apreciados, porém este dado não influenciou a interpretação das imagens da MCR, sendo possível a identificação da ilha tumoral, rodeada por estruturas em fenda escuras ao nível da junção dermo-epidérmica (STEPHENS et al., 2013).

De forma pioneira, em 2013, descrevemos a presença dos múltiplos

pequenos círculos brilhosos localizados na junção dermo-epidérmica, como um critério na MCR para o diagnóstico do carcinoma espinocelular pigmentado. Este aspecto descrito se correlaciona com os pequenos círculos marrons visualizados na dermatoscopia, os quais correspondem aos queratinócitos basais pigmentados atípicos, localizados ao redor das papilas dérmicas, observados na histopatologia (FRAGA-BRAGHIROLI et al., 2013).

Com base nas considerações e dados supracitados, depreende-se a necessidade de se ampliar os conhecimentos sobre o efetivo potencial diagnóstico da MCR na prática médica.

O presente trabalho lida com o estabelecimento de critérios na microscopia confocal de reflectância de lesões cutâneas equívocas, e correlaciona as características observadas com os aspectos histológicos, no sentido de validar uma ferramenta diagnóstica não invasiva, que permita diferenciar, com significativa precisão, as neoplasias benignas e malignas da pele.

2. JUSTIFICATIVA E HIPÓTESE

Até a presente data, o método “padrão ouro” para diagnóstico de neoplasias cutâneas da pele é a biópsia e a subsequente análise histológica. No entanto, a retirada cirúrgica de lesões de grandes dimensões, mormente as localizadas em áreas anatômicas complexas, como a face, demanda a adoção de condutas que reduzam as perdas funcionais e estéticas.

A MCR tem o potencial de evitar remoções desnecessárias de lesões, principalmente na face, onde sequelas funcionais são importantes, e também os pacientes são mais relutantes com o resultado estético.

Tem também a MCR as funções de guiar as incisões nas biópsias de lesões complexas, de mapear as margens pré-cirúrgicas e intra-operatórias, além de monitorar a resposta tumoral nas terapias não-invasivas.

O conjunto destes benefícios se reflete no aprimoramento do diagnóstico diferencial, evitando a ressecção desnecessária de lesões benignas, ou a melhor delimitação da lesão, reduzindo a área de tecido excisado e as respectivas sequelas. Trata-se, portanto, de evitar um grande número de procedimentos traumáticos e psicologicamente importantes, além de reduzir os impactos sociais e os custos financeiros da atenção à saúde, neste setor.

A utilização da Microscopia Confocal de Reflectância (MCR) *in vivo* é recente na prática médica. Atualmente, poucos Serviços de Dermatologia no Brasil dispõem destes equipamentos, e todos encontram-se localizados na região Sul-Sudeste do país; nenhum Serviço da rede pública ou particular dispõe desta tecnologia na região Norte-Nordeste. No entanto, considerando-se as evidentes vantagens advindas do ponto de vista médico e, também, social e econômico, é de se prever que logo sejam adquiridos e instalados novos equipamentos de MCR, disponibilizando os procedimentos pertinentes para o Sistema Único de Saúde – SUS em todas as regiões do país.

Os parâmetros básicos referentes às técnicas e métodos descritos no presente trabalho tem o potencial de ampliar sua aplicação em diversas outras enfermidades e condições clínicas. Neste sentido, justifica-se plenamente o investimento na

formação de profissionais e nas pesquisas sobre MCR *in vivo,* de forma a propiciar continuados avanços no desenvolvimento deste importante campo médico-científico.

HIPÓTESES

A MCR é uma ferramenta diagnóstica não invasiva que diferencia com precisão as neoplasias benignas e malignas da pele.

Há correlação precisa entre os achados da MCR com as características observadas na avaliação histopatológica.

3. OBJETIVOS

3.1 OBJETIVO GERAL

Analisar padrões morfológicos de neoplasias benignas e malignas da pele observados por microscopia confocal de reflectância

3.2 OBJETIVOS ESPECÍFICOS

1. Descrever a técnica da MCR aplicada na prática médica da dermatologia.

2. Descrever os aspectos morfológicos observados à MCR na pele normal e nos tumores de pele mais prevalentes.

3. Demonstrar a utilidade da MCR no diagnóstico de lesões cutâneas equívocas ao exame clínico e dermatoscópico.

4. Descrever os achados na MCR do carcinoma espinocelular pigmentado, e não pigmentado, e sua correlação histopatológica.

5. Comparar a sensibilidade, especificidade, valor preditivo positivo e valor preditivo negativo dos equipamentos de MCR - Vivascope 1500 versus Vivascope 3000 - no diagnóstico do carcinoma basocelular.

6. Descrever os aspectos morfológicos das lesões cutâneas equívocas observadas na MCR e correlacioná-los com os achados histopatológicos.

4. METODOLOGIA

A Metodologia utilizada no presente trabalho encontra-se descrita em cada um dos artigos científicos publicados, inseridos no Capítulo 5 - RESULTADOS

5. RESULTADOS

5.1 ARTIGO DE REVISÃO

Through the looking glass: Basics and principles of reflectance confocal microscopy.

Syril Keena T. Que, **Naiara Fraga-Braghiroli**, Jane M. Grant-Kels, Harold S. Rabinovitz, Margaret Oliviero, Alon Scope.

Journal of the American Academy of Dermatology 2015. Vol. 3 Number 2.

Situação- Artigo Publicado

Esta revisão descreve os princípios básicos da microscopia confocal de reflectância, suas aplicações no diagnóstico das neoplasias cutâneas, assim como suas limitações.

O artigo tem também o objetivo de descrever as característica da pele normal na MCR, além dos achados associados às neoplasias dermatológicas benignas e malignas mais prevalentes.

Os autores descrevem os aspectos morfológicos confocais de lesões benignas, analisando a ceratose seborréica, lentigo solar, hiperplasia sebácia e nevo melanocítico. Dentre as neoplasias malignas, os autores descrevem as características do carcinoma basocelular, carcinoma espinocelular e do melanoma.

REVIEWS

Through the looking glass: Basics and principles of reflectance confocal microscopy

Syril Keena T. Que, MD,[a] Naiara Fraga-Braghiroli, MD,[b] Jane M. Grant-Kels, MD,[a] Harold S. Rabinovitz, MD,[b] Margaret Oliviero, ARNP, MSN,[b] and Alon Scope, MD[c,d]
Farmington, Connecticut; Miami, Florida; Tel Aviv, Israel; and New York, New York

Reflectance confocal microscopy (RCM) offers high-resolution, noninvasive skin imaging and can help avoid obtaining unnecessary biopsy specimens. It can also increase efficiency in the surgical setting by helping to delineate tumor margins. Diagnostic criteria and several RCM algorithms have been published for the differentiation of benign and malignant neoplasms. We provide an overview of the basic principles of RCM, characteristic RCM features of normal skin and cutaneous neoplasms, and the limitations and future directions of RCM. (J Am Acad Dermatol 2015;73:276-84.)

Key words: basal cell carcinoma; cutaneous oncology; melanoma; noninvasive imaging; reflectance confocal microscopy; squamous cell carcinoma; tumors/neoplasm.

In this rapidly developing medical/technological era, noninvasive imaging devices have emerged as useful tools for diagnosing cutaneous neoplasms. Reflectance confocal microscopy (RCM) provides high-resolution, noninvasive imaging and can be used as an adjunct to the management of skin cancers. Herein, we describe for the general dermatologist the basic principles of RCM, detail its potential applications and current limitations, and discuss RCM features of both normal skin and cutaneous neoplasms.

Abbreviations used:

BCC: basal cell carcinoma
DEJ: dermoepidermal junction
RCM: reflectance confocal microscopy
SCC: squamous cell carcinoma

FUNDAMENTALS OF REFLECTANCE CONFOCAL MICROSCOPY

In vivo RCM is a noninvasive optical imaging technique that provides high-resolution images of skin. RCM relies on a low-power laser that emits near-infrared light (830 nm). To attain a lateral resolution of about 1 μm, RCM allows only light back-reflected from a desired focal point within the skin to pass back through a gating pinhole and enter the detector. The basic RCM optical section image is comparable to high magnification histopathology at about ×30; the advantage of RCM compared to histopathology is that optical sections can be obtained in vivo, with no disruption of the skin. Output images are horizontal and parallel to the surface of the skin, visually sectioned in a manner resembling histopathologic specimens in Mohs micrographic surgery.[1] RCM can image the epidermis and papillary dermis but is limited to an imaging depth of about 200 μm.

The wide-probe RCM (VivaScope 1500; CaliberID, Rochester, NY) stitches optical sections into larger mosaic images, allowing a field of view of 8 × 8 mm. The recent introduction of the handheld RCM (VivaScope 3000; CaliberID) has enabled imaging of lesions on concave surfaces, which are typically difficult to image using the bulky

From the Departments of Dermatology at the University of Connecticut Health Center,[a] Farmington, University of Miami Miller School of Medicine,[b] Miami, and Sheba Medical Center and Sackler Faculty of Medicine,[c] Tel Aviv University; and the Dermatology Service,[d] Memorial Sloan Kettering Cancer Center, New York.

Supported by the European Commission Marie Curie FP7 Reintegration Grant to Dr Scope (PIRG07-GA-2010-268359). Dr Rabinovitz has received equipment and funding for a fellowship program from Lucid Inc.

Dr Rabinovitz is an investigator in a study coordinated by Lucid Inc, manufacturer of a commercial confocal microscope. The other authors have no conflicts of interest to declare.

Accepted for publication April 23, 2015.

Correspondence to: Syril Keena T. Que, MD, University of Connecticut Health Center, Department of Dermatology, 21 South Rd, Farmington, CT 06032. E-mail: keenaq@gmail.com.

Published online June 4, 2015.
0190-9622/$36.00

© 2015 by the American Academy of Dermatology, Inc.

http://dx.doi.org/10.1016/j.jaad.2015.04.047

J Am Acad Dermatol
Volume 73, Number 2

wide-probe RCM. Because of its narrow probe, however, the handheld RCM has a field of view limited to 1 × 1 mm.[2] In its current form, the dimensions of the wide-probe RCM imaging station are 30 × 23 × 54 in (76.2 × 58.4 × 137.2 cm); this device can be stowed at the corner of a standard examination room and can be mobilized between examination rooms.

Traditionally, RCM images obtained in the dermatologic setting are black and white, and patterns visualized stem from differences in the reflection of various tissue structures. Highly reflective structures appear bright/white, while nonreflective structures appear dark. Melanin produces the strongest contrast (reflection index = 1.7).[3] The high magnification and resolution of RCM, coupled with the strong reflectivity of melanin, allow for the recognition of individual cells, such as melanocytes and pigmented keratinocytes. Melanin-containing histiocytes (melanophages) are also easily seen on RCM. Keratin is another strong endogenous reflector (reflection index = 1.5), which allows for imaging of keratinocytic neoplasms. In addition, collagen and inflammatory cells strongly reflect RCM light and appear bright in RCM images.[4]

CAPSULE SUMMARY

- Reflectance confocal microscopy provides high-resolution noninvasive skin imaging.
- This review describes the basic principles of reflectance confocal microscopy, its applications in cutaneous oncology, and its limitations.
- As reflectance confocal microscopy continues to evolve, its use in clinical practice can potentially increase a dermatologist's efficiency and diagnostic capability.

POTENTIAL CLINICAL APPLICATIONS OF REFLECTANCE CONFOCAL MICROSCOPY

RCM can be used as an adjunctive diagnostic tool for lesions that display equivocal clinical and dermoscopic features and can increase the physician's and patient's confidence about whether a biopsy specimen is mandated, especially in cosmetically sensitive areas or in anatomic sites from which biopsy specimens are difficult to obtain. RCM has been reported in the bedside evaluation of the oral and genital mucosa[5] and eyelid tumors,[6] with a reported sensitivity of 100% and a specificity of 69.2% for skin cancers on the eyelid as a whole, including basal cell carcinoma (BCC), squamous cell carcinoma (SCC), and melanoma.

In the setting of dermatologic surgery, RCM allows for the preoperative diagnosis of skin cancer and can also define surgical margins before excision or between stages of Mohs micrographic surgery.[7-20] According to 1 study, RCM has a sensitivity of 96.6% and a specificity of 89.2%, with a positive predictive value of 93.0% and a negative predictive value of 94.7% for detecting BCCs during Mohs micrographic surgery.[15] Another study cites the sensitivity and specificity of detecting BCCs as 86% and 99%, respectively.[16] There is also reported benefit in using RCM to delineate poorly defined melanocytic lesions, such as lentigo maligna.[21] Of note, RCM is helpful only when neoplastic aggregates are located in the epidermis or papillary dermis; in cases of recurrent BCC or SCC, the neoplastic aggregates are often located in the reticular dermis and may be out of the range of detection of RCM. In such cases, RCM can be used to confirm the presence of a tumor, but a negative RCM examination cannot rule out the possibility of recurrence.

Another indication for RCM is the monitoring of an individual's response to nonsurgical therapies. RCM has been used to monitor the treatment efficacy of imiquimod for actinic keratoses,[22] BCC,[23] and lentigo maligna,[24] and the effect of cryotherapy for superficial BCCs.[25] When BCCs were treated with imiquimod, RCM revealed tumor clearance or a reduction in tumor size, with results corresponding well to histopathologic findings.[23] Again, caution should be taken when interpreting a negative result on RCM, because neoplastic aggregates may be present deeper than the imaging range of RCM. Regular follow-up skin examinations are indicated to assess for recurrent neoplasms.

BASIC TERMINOLOGY AND REFLECTANCE FOCAL MICROSCOPY FINDINGS

Obtaining the correct diagnosis with RCM requires some level of training and experience, and RCM is operator-dependent, as is any morphology-based diagnostic modality. Nevertheless, a few simple algorithms have been designed for the diagnosis of benign and malignant neoplasms, and consensus terminology for RCM has been published.[26]

Normal skin features on RCM are presented below. Please see Table I for a summary.

Suprabasal epidermis

The stratum corneum appears as a highly refractive surface with visible furrows that represent

Table I. List of basic reflectance confocal microscopy patterns

Epidermis	
Honeycomb pattern	Normal pattern of keratinocytes of the granular and spinous layers formed by bright polygonal outlines of keratinocytes (cytoplasm and intercellular borders) with dark central nuclei
Cobblestone pattern	Normal pattern of basal keratinocytes at the suprapapillary plates and a variant of the normal pattern of the spinous-granular layers in darkly pigmented skin; closely set pigmented keratinocytes appear as bright round cells separated by a less refractive polygonal outline
Disarranged pattern	Focal or diffuse loss of the normal patterns of the spinous-granular layers (ie, honeycomb or cobblestone) characterized by unevenly distributed bright cells and granular particles
Cells in Pagetoid pattern	Presence of bright round or dendritic nucleated cells at suprabasal layers of the epidermis
Dermoepidermal junction	
Edged vs. nonedged papillae	Edged—Dermal papillae demarcated by a rim of bright cells (pigmented basal keratinocytes and melanocytes) Nonedged—Dermal papillae without a demarcated rim of bright cells, but separated by a series of large reflecting cells
Ringed pattern	A low-magnification pattern composed of bright thin rim of cells surrounding dark dermal papillae, seen when there is predominance of "edged papillae" at the dermoepidermal junction. Mostly seen in nevi with histopathologically identified lentiginous or small-nested junctional proliferation of melanocytes
Meshwork pattern	A low-magnification pattern composed of interconnecting bright thickened tubular structures. At higher magnifications, there is enlargement of the interpapillary spaces (rete ridges) by bright cell aggregates; outlines of individual cells are often indiscernible. Mostly seen in nevi with predominantly nested junctional proliferation of melanocytes
Papillary dermis	
Dense nest/cluster	Well-demarcated oval to round aggregate of compactly clustered large bright cells (melanocytes)
Clod pattern	A low-magnification pattern composed of predominance of dense compact nests/clusters of melanocytes within the superficial dermis. Mostly seen in nevi with predominantly dermal, large nested proliferation of melanocytes
Cerebriform cluster	Confluent aggregates of low reflecting polygonal or elongated structures separated by a low reflecting rim, resulting in a cerebriform appearance, in which cellular nuclei and contour cannot be usually distinguished—correlates with aggregates of atypical melanocytes in the dermis, mostly seen in nodules of primary or skin metastasis of melanoma

skin folds (Fig 1, *A*). This layer of skin appears bright because of the dense content of keratin, which backscatters light at the air–stratum corneum interface. The stratum granulosum and spinosum appear as a honeycomb pattern, whereby nuclei appear dark while the keratin-containing cytoplasm appears as granular-bright polygonal outlines, with regular spacing between keratinocytes (Fig 1, *B*).

Basal epidermis/dermoepidermal junction

The refractivity of keratinocytes at the basal layer depends upon an individual's skin type: lighter skin types (Fitzpatrick skin types I and II) have basal keratinocytes with low refractivity; darker skin types (Fitzpatrick skin types III-VI) have highly refractive cytoplasm. The RCM pattern of normal skin is therefore most readily seen in individuals with Fitzpatrick skin types III and higher. At the basal layer of the epidermis, at the level of the suprapapillary plates, a cobblestone pattern is often seen, appearing as aggregates of small refractive cells (Fig 1, *C*). These are basal keratinocytes whose nuclear contours appear brighter than the cytoplasm because of the supranuclear melanin cap; cobblestone is the inverse pattern of the symmetric honeycomb pattern seen higher up in the epidermis. Lower sections through the basal layer of the epidermis have a ringed circular pattern of bright small cells (ie, pigmented basal keratinocytes and few basal melanocytes) around darker dermal

J Am Acad Dermatol
Volume 73, Number 2

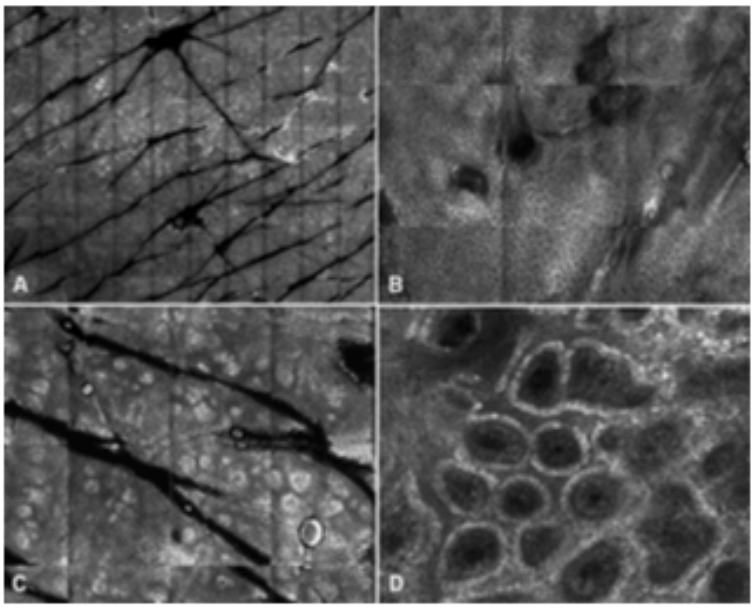

Fig 1. Normal skin imaged with reflectance confocal microscopy (VivaScope 1500; CaliberID, Rochester, NY). **A**, Dark furrows representing the skin folds (dermatoglyphics) visible at the surface of the epidermis. **B**, Regular honeycomb pattern at the spinous-granular layer of the epidermis. **C**, Cobblestone pattern visible at the suprabasal layer in a patient with Fitzpatrick skin type IV. **D**, Edged papillae at the dermoepidermal junction.

papillae, a pattern that has been termed "edged papillae" (Fig 1, *D*).[27]

Papillary dermis

The papillary dermis has fibrillar collagen bundles laid out as coils and rings or in a parallel arrangement. Superficial papillary blood vessels can be identified. While performing real-time RCM imaging, one can readily see blood cells coursing through the vessels.

REFLECTANCE CONFOCAL MICROSCOPY FEATURES OF BENIGN CUTANEOUS NEOPLASMS

Seborrheic keratosis

On RCM, seborrheic keratoses typically have the following features: epidermal projections and keratin-filled invaginations at the lesion surface; keratin-filled pseudocysts and a regular honeycomb pattern at the epidermal layers; densely packed, round to polymorphous dermal papillae and elongated bright cords with bulbous projections at the dermoepidermal junction (DEJ); dilated round and linear blood vessels; and melanophages in the papillary dermis (Fig 2).[28]

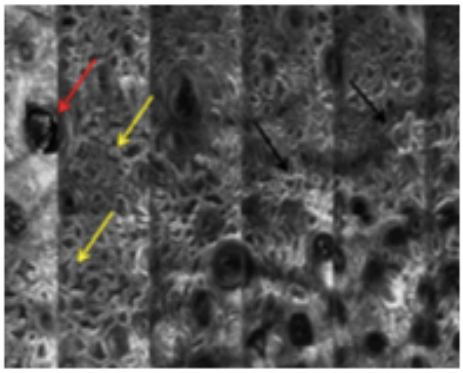

Fig 2. Seborrheic keratosis. Mosaic reflectance confocal microscopy image (VivaScope 1500; CaliberID, Rochester, NY; 2.5 × 1.5 mm) at the level of the dermoepidermal junction. Note the keratin-filled invaginations (*red arrow*), elongated bright tubular cords with bulbous projections at the dermoepidermal junction (*yellow arrows*), and the round to polymorphous, well-circumscribed dermal papillae (*black arrows*).

Solar lentigo

Solar lentigines on RCM show an increased density of dermal papillae, elongated to irregularly

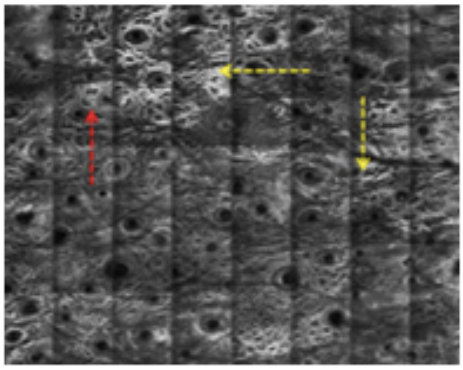

Fig 3. Solar lentigo. Mosaic reflectance confocal microscopy image (VivaScope 1500; CaliberID, Rochester, NY; 4 × 3.5 mm) at the level of the dermoepidermal junction. Note the polycyclic papillae (*red arrow*) and the interconnecting bright cords (*yellow arrows*).

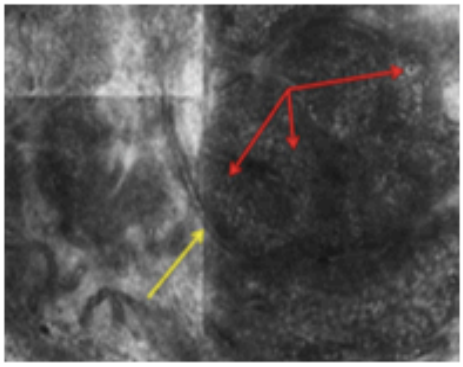

Fig 4. Sebaceous hyperplasia. Reflectance confocal microscopy image (VivaScope 1500; CaliberID, Rochester, NY; 1.0 × 0.5 mm) at the level of the papillary dermis. Note the enlarged lobules with refractive cuboidal cells with dark central nuclei and granular bright cytoplasm (*red arrows*) and the blood vessels around the lobules of sebaceous cells (*yellow arrows*).

shaped and rimmed by bright, monomorphic cells (pigmented basal keratinocytes).[29] Notably, solar lentigines display overlapping features with flat seborrheic keratosis, showing interconnecting bright cords (ie, polycyclic papillary contours) at the DEJ. These correspond to anastomosing rete ridges on histopathologic examination (Fig 3).[30]

Sebaceous hyperplasia

Sebaceous hyperplasia appear on RCM as enlarged lobules with refractive cuboidal cells containing dark central nuclei, granular bright cytoplasm, and dilated sebaceous ducts.[31] A dilated central follicular infundibulum is often seen (Fig 4).[32]

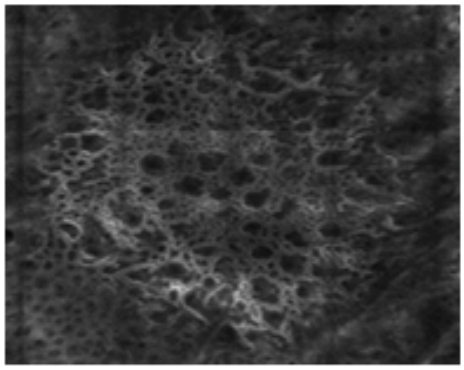

Fig 5. Melanocytic nevus. Mosaic reflectance confocal microscopy images (VivaScope 1500; CaliberID, Rochester, NY; 2 × 2 mm) at the dermoepidermal junction. Note the ringed pattern characterized by dermal papillae rimmed by regular bright cells.

Melanocytic nevi

Melanocytic nevi present an overall regular pattern at the DEJ and papillary dermis on mosaic RCM images (akin to low-magnification microscopy). RCM patterns typically seen in nevi include the ringed, meshwork, and clod patterns. Ring-patterned nevi have dermal papillae rimmed by regular bright cells (melanocytes and pigmented basal keratinocytes) and sometimes small junctional nests; ringed nevi on RCM correspond histopathologically to nevi with mostly lentiginous or small-nested junctional proliferation of melanocytes (Fig 5). Meshwork-patterned nevi have interconnecting rete ridges with elongated junctional nests corresponding on histopathology to nevi with a predominantly nested junctional proliferation of melanocytes (Fig 6). Clod-patterned nevi feature nests of melanocytes that fill and expand the dermal papillae, corresponding on histopathology to nevi with a predominantly dermal proliferation of melanocytes (Fig 7).[33]

REFLECTANCE CONFOCAL MICROSCOPY FEATURES OF MALIGNANT CUTANEOUS NEOPLASMS

Basal cell carcinomas

BCCs appear on RCM as neoplastic aggregates at the DEJ or papillary dermis, appearing as "dark silhouettes"—hyporeflective, dark areas outlined by bright fibroplastic stroma—or as "bright tumor islands"—elongated or polycyclic, cord-like structures surrounded by cleft-like dark spaces. These

J Am Acad Dermatol
Volume 73, Number 2

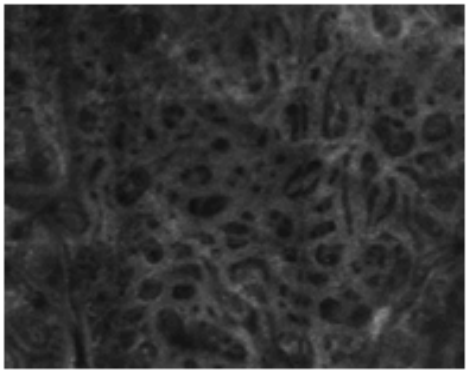

Fig 6. Melanocytic nevus. Mosaic reflectance confocal microscopy images (VivaScope 1500; CaliberID, Rochester, NY; 1.5 × 1.5 mm) at the dermoepidermal junction. Note the meshwork pattern characterized by interconnecting thickened rete ridges with elongated junctional nests.

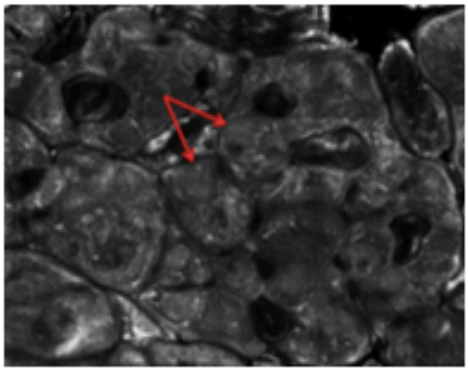

Fig 7. Melanocytic nevus. Mosaic reflectance confocal microscopy images (VivaScope 1500; CaliberID, Rochester, NY; 2 × 2 mm) at the dermoepidermal junction. Note the clod-patterned nevus characterized by nests of melanocytes that fill and expand the dermal papillae (*arrows*).

dark clefts on RCM contain mucin and are equivalent to the clefts seen around the neoplastic aggregates on histopathologic examination. The neoplastic aggregates on RCM often feature "peripheral palisading" of nuclei at the periphery of tumor islands. The dermis in BCC shows dilated and tortuous "linear blood vessels" that course en face, parallel to the horizontal plane of RCM imaging (Fig 8).[34,35]

Squamous cell carcinoma

Under RCM, SCC presents a disarranged or atypical honeycomb pattern in the epidermis. Round nucleated bright cells in a pagetoid pattern correspond on histopathologic examination to

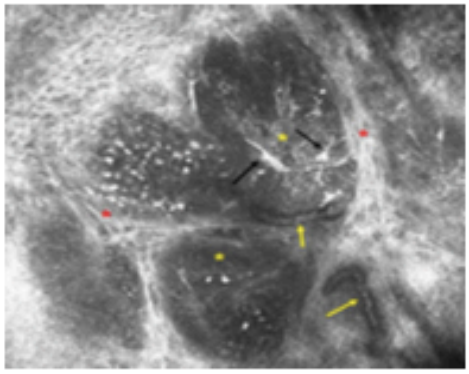

Fig 8. Basal cell carcinoma. Reflectance confocal microscopy image (VivaScope 3000; CaliberID, Rochester, NY) at the level of the papillary dermis. Note the bright fibroplastic dermal stroma composed of thick collagen bundles (*red asterisks*) and dilated and tortuous linear blood vessels (*yellow arrows*) surround the bright tumor islands (*yellow asterisks*). The tumor islands harbor bright stellate cells (*black arrows*) with dendritic extension that correspond to melanocytes.

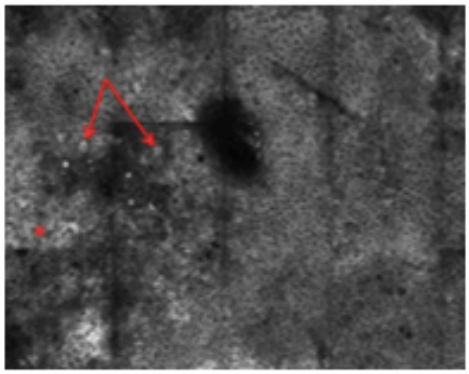

Fig 9. Squamous cell carcinoma. Mosaic reflectance confocal microscopy image (VivaScope 1500; CaliberID, New York, NY; 2 × 1.5 mm) at the level of the spinous-granular layers. Note the disarranged epidermis and an atypical honeycomb pattern characterized by keratinocytes of different sizes and shapes (*red asterisk*) and round nucleated bright cells in a pagetoid pattern corresponding to discohesive atypical keratinocytes (*red arrows*).

dyskeratotic, atypical keratinocytes in the suprabasal epidermis. In the dermal papillae, looping, round blood vessels can be observed.[36] While there is some overlap in the RCM features of SCCs and actinic keratoses, a disarranged epidermal pattern at the spinous-granular layer and the presence of neoplastic aggregates in the dermis are highly suggestive of SCC (Fig 9).[37] Notably, imaging of

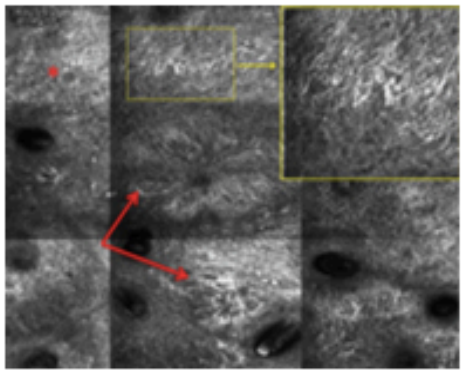

Fig 10. Melanoma in situ on the nose of a 69-year-old man. Mosaic reflectance confocal microscopy image (VivaScope 1500; CaliberID, New York, NY; 1.5 × 1.5 mm) showing an oblique view through the spinous-granular and basal layers of epidermis. Note the sheet of dendritic cells around hair follicles (*red arrows*) and the disarranged pattern of the spinous-granular layer of the epidermis (*red asterisk*). Inset: sheets of bright nucleated and dendritic cells, representing infiltration of the spinous layer of the epidermis by atypical melanocytes in pagetoid spread.

markedly hyperkeratotic SCC with RCM is greatly limited by the strong back-reflectance of the dense keratin at the surface of the tumor.

Melanoma

The RCM features of melanoma include architectural and cellular attributes. First, melanomas often have an asymmetric distribution of pattern and brightness and a focal loss of a DEJ pattern. Scanning for key RCM features by anatomic layer, in the suprabasal layers of the epidermis, bright round nucleated or dendritic cells are seen; these correspond on histopathologic examination to atypical melanocytes in a pagetoid pattern. A widespread infiltration of the epidermis by melanocytes in a pagetoid pattern is often associated with a disarranged epidermal pattern of the spinous-granular layers. At the DEJ, nonedged contours of the dermal papillae, loss of the papillary dermal contours, and infiltration by atypical bright round or dendritic cells are often seen. Junctional nests in melanomas show variability in size, brightness, shape, and spacing. In the papillary dermis, irregularly shaped nests with heterogeneity in brightness can be seen. Many of the nests are discohesive. In nodular melanomas, low-refractivity cerebriform clusters of melanocytes can be seen in the papillary dermis (Fig 10). One metaanalysis found an overall per-lesion sensitivity of 93% (95% confidence interval [CI], 89-96%) and a specificity of 76% (95% CI, 68-83%) for detecting melanomas on RCM.[38]

RCM is useful in the diagnosis of amelanotic to light-colored melanomas, which are often difficult to diagnose by clinical appearance or dermoscopy. In 1 study, specificity in the diagnosis of light-colored melanoma was improved by using RCM compared with dermoscopy (84% vs 39%, respectively).[39] There are several accounts for the utility of RCM in light-colored melanomas. First, atypical melanocytes may still be seen under RCM because even microscopic amounts of melanin can produce cellular contrast. Second, subcellular organelles, such as melanosomes—whose size (about 500 nm) is comparable to that of the wavelength of RCM light (830 nm)—will appear bright under RCM images. Third, in 85% of amelanotic melanomas, hyporeflective pagetoid cells may be identified under RCM.[40] Finally, additional features suggestive of amelanotic melanomas include a disarranged pattern of the epidermis, nonedged or absent dermal papillae, and large pleomorphic bright nucleated cells twice the size of basal keratinocytes, compatible with atypical melanocytes.[41]

Because of its high sensitivity for detecting melanomas at early stages, RCM reduces the risk of referring a melanoma for monitoring and subsequently losing a patient to follow-up. It can also decrease the number of unnecessary biopsy specimens obtained for benign melanocytic lesions. In 1 study, RCM-assisted diagnosis reduced the number of benign lesions sent for excision, based on suspicious clinical and dermoscopic criteria, by more than half; only 197 of 424 examined suspect benign lesions were excised after examination by RCM.[42]

CURRENT LIMITATIONS AND FUTURE DIRECTIONS

RCM is an evolving technology with several limitations. First, RCM imaging depth is confined to the epidermis and papillary dermis, which may result in false negatives, because tumors extending to or originating in the reticular dermis and subcutaneous fat may be missed. In lesions with marked epidermal thickening, including acral surfaces, the view of RCM is further limited to the epidermis alone. Additional barriers to the penetration of RCM light are hyperkeratosis, reflective creams (eg, sunscreen) or surface particles not removed before imaging, and an uneven skin surface, which may trap air bubbles; these barriers may degrade RCM image quality. Second, an interpreter of RCM faces the challenge of distinguishing between cells with a similar

reflection index and shape, such as Langerhans cells versus dendritic melanocytes at the spinous layer. Third, the high cost of the current devices (the US retail price is $98,500 for the wide-probe RCM [VivaScope 1500] and $69,500 for the handheld RCM [VivaScope 3000]), the duration of time for imaging a single lesion, and the training and experience needed for RCM-based diagnosis may serve as additional barriers to the adoption of this technology. Incorporation of RCM with teledermatology may make RCM more practical for obtaining a rapid diagnosis; in the ideal scenario, a physician could capture RCM images of a lesion and send these images to a remote RCM-trained dermatologist or pathologist for immediate evaluation. RCM readers should have strong basis in dermatopathology, because many RCM diagnostic features correlate well with histopathologic diagnostic criteria.

There are several technological developments that appear promising for the future use of RCM. First, with regard to potentially reducing both the size and the cost of the device, RCM devices that image skin using line-scanning (rather than point-scanning) lasers are currently being developed.[43] Second, with regard to computer-assisted RCM image analysis and (possibly) 3-dimensional image reconstruction, software is being designed for the automated recognition of skin anatomy and pathology under RCM.[44,45] Third, to improve contrast under confocal imaging—and particularly toward color-enhanced in vivo imaging—fluorescent-based confocal imaging is being tested, using intradermal injection of in vivo dyes, such as indocyanine-green.[46,47] Finally, 1 study has shown feasibility for digitally stained confocal mosaics that mimic the appearance of hematoxylin and eosin–based histopathology; this was achieved by combining reflectance and fluorescent mode confocal imaging and assigning pseudocolors to tissue structures based on their differential enhancement under each confocal mode (akin to the technique of stain–counterstain in histopathology).[48]

In conclusion, the role of RCM has been studied in the clinical setting as an adjunctive tool for identifying cutaneous malignancies, delineating tumor margins, and assessing the response of skin cancers to nonsurgical therapies. New developments continue to make the technology more practical, including the creation of a smaller, handheld RCM device to facilitate its use at bedside and special stains to make RCM images more in line with the appearance of hematoxylin and eosin–stained specimens. Algorithms have been developed for the interpretation of RCM images in their present form, and while formal training courses are not yet available in the United States, the basics of RCM image interpretation are sporadically taught at continuing medical education courses and at short workshops held at national meetings. Future considerations include the incorporation of 3-dimensional imaging and computer reconstruction to further simplify image interpretation and the implementation of a device able to detect lesions at a greater depth than current RCM models.

REFERENCES

1. Nwaneshiudu A, Kuschal C, Sakamoto FH, et al. Introduction to confocal microscopy. *J Invest Dermatol*. 2012;132:e3.
2. Fraga-Braghiroli NA, Stephens A, Grossman D, et al. Use of handheld reflectance confocal microscopy for in vivo diagnosis of solitary facial papules: a case series. *J Eur Acad Dermatol Venereol*. 2014;28:933-942.
3. Kardynal A, Olszewska M. Modern non-invasive diagnostic techniques in the detection of early cutaneous melanoma. *J Dermatol Case Rep*. 2014;8:1-8.
4. Longo C, Zalaudek I, Argenziano G, Pellacani G. New directions in dermatopathology: in vivo confocal microscopy in clinical practice. *Dermatol Clin*. 2012;30:799-814.
5. Debarbieux S, Perrot JL, Erfan N, et al. Reflectance confocal microscopy of mucosal pigmented macules: a review of 56 cases including 10 macular melanomas. *Br J Dermatol*. 2014; 170:1276-1284.
6. Cinotti E, Perrot JL, Campolmi N, et al. The role of in vivo confocal microscopy in the diagnosis of eyelid margin tumors: 47 cases. *J Am Acad Dermatol*. 2014;71:912-918.e2.
7. Tannous Z, Torres A, González S. In vivo real-time confocal reflectance microscopy: a noninvasive guide for Mohs micrographic surgery facilitated by aluminum chloride, an excellent contrast enhancer. *Dermatol Surg*. 2003;29:839-846.
8. Marra DE, Torres A, Schanbacher CF, Gonzalez S. Detection of residual basal cell carcinoma by in vivo confocal microscopy. *Dermatol Surg*. 2005;31:538-541.
9. Schüle D, Breuninger H, Schippert W, et al. Confocal laser scanning microscopy in micrographic surgery (three-dimensional histology) of basal cell carcinomas. *Br J Dermatol*. 2009;161:698-700.
10. Ziefle S, Schüle D, Breuninger H, et al. Confocal laser scanning microscopy vs 3-dimensional histologic imaging in basal cell carcinoma. *Arch Dermatol*. 2010;146:843-847.
11. Patel YG, Nehal KS, Aranda I, et al. Confocal reflectance mosaicing of basal cell carcinomas in Mohs surgical skin excisions. *J Biomed Opt*. 2007;12:034027.
12. Rajadhyaksha M, Menaker G, Flotte T, et al. Confocal examination of nonmelanoma cancers in thick skin excisions to potentially guide Mohs micrographic surgery without frozen histopathology. *J Invest Dermatol*. 2001;117:1137-1143.
13. Kaeb S, Landthaler M, Hohenleutner U. Confocal laser scanning microscopy—evaluation of native tissue sections in micrographic surgery. *Lasers Med Sci*. 2009;24:819-823.
14. Gareau D, Bar A, Snaveley N, et al. Tri-modal confocal mosaics detect residual invasive squamous cell carcinoma in Mohs surgical excisions. *J Biomed Opt*. 2012;17:066018.
15. Gareau DS, Karen JK, Dusza SW, et al. Sensitivity and specificity for detecting basal cell carcinomas in Mohs excisions with confocal fluorescence mosaicing microscopy. *J Biomed Opt*. 2009;14:034012.
16. Bennàssar A, Vilata A, Puig S, Malvehy J. Ex vivo fluorescence confocal microscopy for fast evaluation of tumour margins during Mohs surgery. *Br J Dermatol*. 2014;170:360-365.

17. Karen JK, Gareau DS, Dusza SW, et al. Detection of basal cell carcinomas in Mohs excisions with fluorescence confocal mosaicing microscopy. *Br J Dermatol*. 2009;160:1242-1250.
18. Larson B, Abeytunge S, Seltzer E, et al. Detection of skin cancer margins in Mohs excisions with high-speed strip mosaicing confocal microscopy: a feasibility study. *Br J Dermatol*. 2013; 169:922-926.
19. Longo C, Rajadhyaksha M, Ragazzi M, et al. Evaluating ex vivo fluorescence confocal microscopy images of basal cell carcinomas in Mohs excised tissue. *Br J Dermatol*. 2014;171: 561-570.
20. Chung VQ, Dwyer PJ, Nehal KS, et al. Use of ex vivo confocal scanning laser microscopy during Mohs surgery for nonmelanoma skin cancers. *Dermatol Surg*. 2004;30(12 pt 1): 1470-1478.
21. Curiel-Lewandrowski C, Williams CM, Swindells KJ, et al. Use of in vivo confocal microscopy in malignant melanoma: an aid in diagnosis and assessment of surgical and nonsurgical therapeutic approaches. *Arch Dermatol*. 2004;140:1127-1132.
22. Ulrich M, Krueger-Corcoran D, Roewert-Huber J, et al. Reflectance confocal microscopy for noninvasive monitoring of therapy and detection of subclinical actinic keratoses. *Dermatology*. 2010;220:15-24.
23. Torres A, Niemeyer A, Berkes B, et al. 5% imiquimod cream and reflectance-mode confocal microscopy as adjunct modalities to Mohs micrographic surgery for treatment of basal cell carcinoma. *Dermatol Surg*. 2004;30(12 pt 1):1462-1469.
24. Nadiminti H, Scope A, Marghoob A, et al. Use of reflectance confocal microscopy to monitor response of lentigo maligna to nonsurgical treatment. *Dermatol Surg*. 2010;36:177-184.
25. Ahlgrimm-Siess V, Horn M, Koller S, et al. Monitoring efficacy of cryotherapy for superficial basal cell carcinomas with in vivo reflectance confocal microscopy: a preliminary study. *J Dermatol Sci*. 2009;53:60-64.
26. Scope A, Benvenuto-Andrade C, Agero AL, et al. In vivo reflectance confocal microscopy imaging of melanocytic skin lesions: consensus terminology glossary and illustrative images. *J Am Acad Dermatol*. 2007;57:644-658.
27. Pellacani G, Cesinaro AM, Longo C, et al. Microscopic in vivo description of cellular architecture of dermoscopic pigment network in nevi and melanomas. *Arch Dermatol*. 2005;141: 147-154.
28. Ahlgrimm-Siess V, Cao T, Oliviero M, et al. Seborrheic keratosis: reflectance confocal microscopy features and correlation with dermoscopy. *J Am Acad Dermatol*. 2013;69:120-126.
29. Langley RG, Burton E, Walsh N, et al. In vivo confocal scanning laser microscopy of benign lentigines: comparison to conventional histology and in vivo characteristics of lentigo maligna. *J Am Acad Dermatol*. 2006;55:88-97.
30. Pollefliet C, Corstjens H, Gonzalez S, et al. Morphological characterization of solar lentigines by in vivo reflectance confocal microscopy: a longitudinal approach. *Int J Cosmet Sci*. 2013;35:149-155.
31. Propperova I, Langley RG. Reflectance-mode confocal microscopy for the diagnosis of sebaceous hyperplasia in vivo. *Arch Dermatol*. 2007;143:134.
32. Malvehy J, Puig S. Sebaceous hyperplasia. In: Gonzalez S, Gill M, Halpern AC, eds. *Reflectance confocal microscopy of cutaneous tumors*. London: Informa Healthcare; 2008:164-167.
33. Pellacani G, Scope A, Farnetani F, et al. Towards an in vivo morphologic classification of melanocytic nevi. *J Eur Acad Dermatol Venereol*. 2014;28:864-872.
34. González S, Tannous Z. Real-time, in vivo confocal reflectance microscopy of basal cell carcinoma. *J Am Acad Dermatol*. 2002; 47:869-874.
35. Alarcon I, Carrera C, Tunegano P, et al. Basal cell carcinoma with spontaneous regression: added value of reflectance confocal microscopy when the dermoscopic diagnosis is uncertain. *J Am Acad Dermatol*. 2014;71:e7-e9.
36. Rishpon A, Kim N, Scope A, et al. Reflectance confocal microscopy criteria for squamous cell carcinomas and actinic keratoses. *Arch Dermatol*. 2009;145:766-772.
37. Peppelman M, Nguyen KP, Hoogedoorn L, et al. Reflectance confocal microscopy: non-invasive distinction between actinic keratosis and squamous cell carcinoma. *J Eur Acad Dermatol Venereol*. Available at: http://dx.doi.org/10.1111/jdv.12806. Published online October 30, 2014.
38. Stevenson AD, Mickan S, Mallett S, et al. Systematic review of diagnostic accuracy of reflectance confocal microscopy for melanoma diagnosis in patients with clinically equivocal skin lesions. *Dermatol Pract Concept*. 2013;3:19-27.
39. Guitera P, Pellacani G, Longo C, et al. In vivo reflectance confocal microscopy enhances secondary evaluation of melanocytic lesions. *J Invest Dermatol*. 2009;129:131-138.
40. Losi A, Longo C, Cesinaro AM, et al. Hyporeflective pagetoid cells: a new clue for amelanotic melanoma diagnosis by reflectance confocal microscopy. *Br J Dermatol*. 2014;171: 48-54.
41. Braga JC, Scope A, Klaz I, et al. The significance of reflectance confocal microscopy in the assessment of solitary pink skin lesions. *J Am Acad Dermatol*. 2009;61:230-241.
42. Pellacani G, Pepe P, Casari A, Longo C. Reflectance confocal microscopy as a second-level examination in skin oncology improves diagnostic accuracy and saves unnecessary excisions: a longitudinal prospective study. *Br J Dermatol*. 2014;171:1044-1051.
43. Larson B, Abeytunge S, Rajadhyaksha M. Performance of full-pupil line-scanning reflectance confocal microscopy in human skin and oral mucosa in vivo. *Biomed Opt Express*. 2011; 2:2055-2067.
44. Kurugol S, Dy JG, Brooks DH, Rajadhyaksha M. Pilot study of semiautomated localization of the dermal/epidermal junction in reflectance confocal microscopy images of skin. *J Biomed Opt*. 2011;16:036005.
45. Gareau D. Automated identification of epidermal keratinocytes in reflectance confocal microscopy. *J Biomed Opt*. 2011; 16:030502.
46. Jonak C, Skvara H, Kunstfeld R, et al. Intradermal indocyanine green for in vivo fluorescence laser scanning microscopy of human skin: a pilot study. *PLoS One*. 2011;6:e23972.
47. Skvara H, Kittler H, Schmid JA, et al. In vivo fluorescence confocal microscopy: indocyanine green enhances the contrast of epidermal and dermal structures. *J Biomed Opt*. 2011;16:096010.
48. Gareau DS. Feasibility of digitally stained multimodal confocal mosaics to simulate histopathology. *J Biomed Opt*. 2009;14: 034050.

5.2 ARTIGO ORIGINAL 1

Use of handheld reflectance confocal microscopy for in vivo diagnosis of solitary facial papules: a case series.

N.A. Fraga-Braghiroli, A. Stephens, D. Grossman, H. Rabinovitz, R.P.R. Castro, A. Scope .

Journal of the European Academy of Dermatology and Venereology 2014, 28, 933–942.

Situação- Artigo Publicado

O estudo mostrou a utilização da Microscopia confocal de reflectância de sonda pequena -*hand-held* (HH-RCM) como ferramenta auxiliar no diagnóstico de pápulas faciais solitárias.

Os autores relataram uma série de pacientes que apresentavam lesões equívocas faciais, tanto na avaliação clínica quanto dermatoscópica. O uso da HH-RCM permitiu um diagnóstico preciso e imediato em 100% dos casos.

Os cânceres de pele podem simular lesões cutâneas inespecíficas, constituindo assim um grande desafio para o diagnóstico clínico.

O diagnóstico do câncer de pele não-melanoma quando realizado de forma precoce, e especialmente quando a lesão ainda é pequena, minimiza a chance de eventual comprometimento funcional e estético associado a um procedimento cirúrgico.

A utilização de uma sonda portátil, pequena e de fácil mobilidade, disponível no equipamento HH-RCM, se mostrou ideal na avalição de pequenas lesões em áreas curvadas da face, como nariz, orelhas e região peri-orbital; locais considerados de alta taxa de incidência e recorrência de câncer de pele, considerando-se que não seria possível utilizar o equipamento de MCR regular, devido a suas grandes dimensões.

DOI: 10.1111/jdv.12218 JEADV

ORIGINAL ARTICLE

Use of handheld reflectance confocal microscopy for in vivo diagnosis of solitary facial papules: a case series

N.A. Fraga-Braghiroli,[1,*] A. Stephens,[1] D. Grossman,[1] H. Rabinovitz,[1] R.P.R. Castro,[1] A. Scope[2,3]

[1]Dermatology Department, Skin and Cancer Associations Plantation, Plantation, FL, USA
[2]Dermatology Department, Sheba Medical Center and Sackler Faculty of Medicine, Tel Aviv University, Tel-Aviv, Israel
[3]Dermatology Service, Memorial Sloan-Kettering Cancer Center, New York, NY, USA
*Correspondence: N.A. Fraga-Braghiroli. E-mail: naisrafraga@yahoo.com.br

Abstract

Background Reflectance Confocal Microscopy (RCM) can be useful for evaluation of solitary pink papules that are suspicious for skin cancer. RCM has been challenging to apply to curvy facial areas because of the need for attaining full contact between the skin and RCM probe. A smaller diameter handheld RCM probe has been recently introduced to clinical practice.

Objective To describe the utility of RCM handheld probe as a bedside adjunct for clinical diagnosis of solitary facial papules.

Methods This is a retrospective descriptive case series of six patients presented with a diagnostically equivocal solitary facial papule. All lesions reported were evaluated and imaged clinically, dermoscopically and with handheld RCM, followed by biopsy for histopathological analysis.

Results The series included biopsy-proven basal cell carcinomas (BCCs) ($n = 2$), squamous cell carcinoma ($n = 1$), sebaceous hyperplasia ($n = 1$), desmoplastic trichoepithelioma ($n = 1$) and compound nevus ($n = 1$). Handheld RCM was easy to apply to the curved facial surfaces and allowed for reaching a correct bedside diagnosis.

Conclusion For clinically and dermoscopically equivocal small papules on curved facial surfaces, handheld RCM may be particularly helpful in differentiating benign lesions from skin cancer.

Received: 3 April 2013; Accepted: 21 June 2013

Conflicts of interest

Dr Rabinovitz is an investigator in a study coordinated by Lucid Inc, manufacturer of a commercial confocal microscope. He has received funding for a fellowship programme and equipment from Lucid Inc. He is also a consultant and has received equipment from 3-Gen, manufacturer of a polarized dermatoscope. Drs Fraga-Braghiroli, Stephens, Paula Castro Ramos and Scope and the student Danielle Grossman have no conflicts of interest to declare.

Funding Sources

None declared.

Introduction

Non-melanoma skin cancers (NMSC), including basal cell carcinoma (BCC) and squamous cell carcinoma (SCC) are common on the face. Early diagnosis, when the lesion is small, minimizes the chance of cosmetic and functional impairment from surgical removal. Benign facial lesions, such as melanocytic nevi, sebaceous hyperplasia (SH) and fibrous papules are also common. Differentiation of NMSC from benign facial lesion using clinical and dermoscopic criteria can be quite challenging. This is particularly true when the lesion is small and non-pigmented and when the patient's face is sun-damaged or harbours scars from previous surgery or cryotherapy. In such cases, differential diagnosis relies on subtle clues, such as patient report of change, presence of ulceration or scale and vascular dermoscopic pattern.

Reflectance confocal microscopy (RCM) has been shown to improve diagnostic accuracy in skin cancer screening.[1–3] In addition, RCM was shown to be useful for diagnosis of solitary pink papules or nodules.[4–11] Braga *et al.*[4] reported on a series of patients with clinically and dermoscopically equivocal pink lesions for which RCM examination allowed for accurate diagnosis; they described RCM diagnostic criteria for differentiating benign and malignant neoplasms presenting as pink lesions, including BCC, SCC, amelanotic melanoma and inflamed seborrhoeic keratosis. Guitera *et al.*[5] found that

© 2013 European Academy of Dermatology and Venereology

specificity of diagnosis of light-coloured melanocytic neoplasms was improved by RCM; specificity of melanoma diagnosis was 84% using RCM, compared with specificity of 39% using dermoscopy, without compromise to sensitivity. Improved diagnostic accuracy for light-coloured lesions may be explained by the fact that even scant melanin can produce detectable bright signal under RCM.[5] Guitera *et al.* also reported 100% sensitivity and 88.5% specificity in diagnosis of BCC using RCM.

However, until recently, RCM has been difficult to apply to the face due to curved facial contours, which limit the possibility of attaining full contact between skin and RCM probe. In the absence of full contact, air bubbles accumulate between the RCM probe and skin, interfering with image quality. To this end, handheld RCM (HH-RCM) has been recently introduced to clinical practice. The HH-RCM is small, portable and more accessible for application on curved facial surfaces, including anatomical sites of limited access such as nose, ears and periorbital regions.

The aim of this study was to describe the utility of HH-RCM as an adjunct to clinical diagnosis of solitary facial papules. We describe a series of patients with clinically and dermoscopically equivocal small facial papules for which a rapid HH-RCM examination pointed the clinician at the correct diagnosis.

Figure 1 Handheld RCM examination technique.

© 2013 European Academy of Dermatology and Venereology

Methods

This retrospective descriptive case series is derived from the population of patients who undergo skin cancer screening at a private practice in South Florida. Included in the series are patients presented with solitary pink, skin coloured or lightly pigmented facial papule that was suspicious for skin cancer based on equivocal clinical and dermoscopic attributes. All lesions reported were evaluated and imaged clinically, dermoscopically and with HH-RCM (see below) followed by biopsy. All patients consented to RCM imaging which is performed routinely in the clinic as an adjunct to diagnosis in equivocal cases.

Clinical images were obtained with NIKON D90 12.3 megapixels N16184 camera (Nikon Inc., Melville, NY, USA). Dermoscopic images were obtained with DermLiteII ProHR (DermLite, San Juan Capistrano, CA, USA) attached to Sony CyberShot 7.2 megapixels camera (Sony Electronics, San Diego, CA, USA). Dermoscopic images from cases 1, 3 and 4 were obtained with non-contact polarized mode; images from cases 2, 5 and 6 were obtained with contact non-polarized dermoscopy using alcohol as immersion fluid.

Handheld RCM imaging was performed with commercially available *in vivo* RCM system (Vivascope3000; CaliberID, Rochester, NY, USA). This system uses 830 nm (near-infrared) laser. HH-RCM provides horizontal resolution of 1.25 μm and vertical resolution of 5 μm at the Field Of View (FOV) centre, and maximal imaging depth of 350 μm, which corresponds to superficial reticular dermis. The image captured by HH-RCM system is a single frame 1 mm × 1 mm FOV. A drop of immersion oil (Crodamol STS; Croda Inc, Edison, NJ, USA) is applied to skin surface (Fig. 1a) to match the refractive index with the stratum corneum, thereby improving penetration depth and focus of light. RCM imaging along the horizontal (x-y) plane requires the operator to manually move the probe, while maintaining full contact with the skin and immersion oil (Fig. 1b). Using a button at the bottom side of the HH-RCM (Fig. 1c), individual RCM images can be captured. Using navigation buttons at the top-side (Fig. 1d), focal point depth can be changed, allowing for collection of images at variable points along the z-axis. An automated stepper function (Vivastack, Fig. 1e) allows for collection of a stack of RCM images at incremental depths from stratum corneum to superficial dermis. On the basis of our experience, we suggest the following manual operation. A right-handed operator would use his right thumb to press on navigation buttons at the top of the device (Fig. 1d, e), the right index finger to press on the image acquisition button (Fig. 1c) and the rest of the right palm and fingers to hold the RCM handle. The left hand index and middle fingers are used to stretch the skin around the lesion imaged (Fig. 1b), and when performing a stack, these fingers can gently tighten around the probe to stabilize it and prevent horizontal movement. An entire RCM imaging session takes approximately 4 min from patient positioning to scanning, capturing and saving of images.

All lesions included were biopsy-proven. Excised specimens were routinely fixed in formalin, embedded in paraffin and stained with hematoxylin-eosin. Diagnoses were issued by a board-certified dermatopathologist.

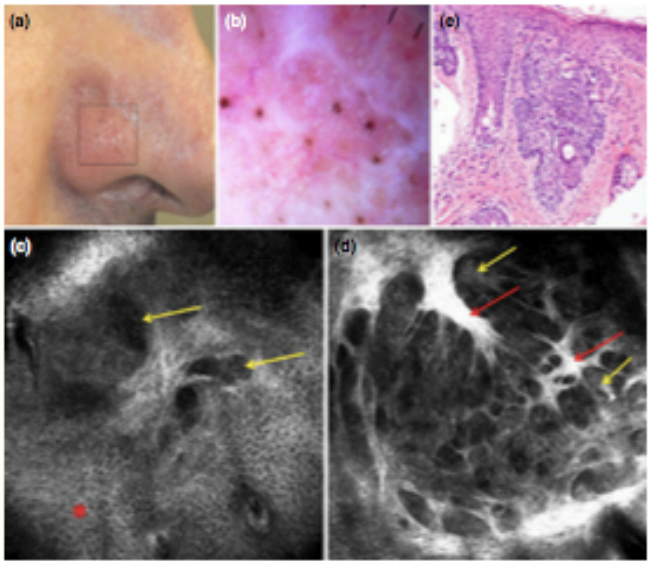

Figure 2 Patient #1. Basal cell carcinoma.

© 2013 European Academy of Dermatology and Venereology

Case Reports

Patient 1

A 59-year-old man reported that 6 years prior to the current visit, Mohs surgery was performed for BCC on the right nasal ala, and that 3 months ago, a new, asymptomatic lesion has appeared adjacent to the surgical scar. On examination, a 3 mm pink papule with central depression was observed (Fig. 2a). On dermoscopy, the papule displayed central depression surrounded by twisted looped vessels, chrystalline and rosette structures, with pink–white background (Fig. 2b). The differential diagnosis included recurrent BCC, SH, SCC and amelanotic melanoma. HH-RCM examination at the level of the basal layer of the epidermis and papillary dermis revealed dark silhouettes, which are hyporefractile areas outlined by more refractile surrounding epidermis or surrounding dermal collagen bundles. In addition, bright tumour islands, which are well-demarcated round, cord-like or lobulated bright cellular aggregates, separated by dark clefts from surrounding thickened collagen bundles, were observed in the dermis (Fig. 2c,d). RCM findings were consistent with the diagnosis of BCC. The lesion was removed by shave biopsy and the histopathological diagnosis was recurrent BCC (Fig. 2e); the residual neoplasm was subsequently removed by Mohs surgery.

Patient 2

A 70-year-old woman with history of NMSC presented for routine skin examination. The patient noticed a new lesion on the nose. On examination, a 2 mm papule with a darkly pigmented focus was noted on the right nasal ala (Fig. 3a). On dermoscopy, the lesion presented thin serpentine branched vessels and a blue clod, with pink–white background (Fig. 3b). Differential diagnosis included BCC, SH and melanoma. HH-RCM examination revealed regular honeycomb pattern at the spinous-granular level of the epidermis. At the dermo-epidermal junction (DEJ) and papillary dermis, bright tumour islands surrounded by thickened collagen bundles were observed; in addition, dark silhouettes were also observed (Fig. 3c). RCM findings were consistent with the diagnosis of BCC. The lesion was removed by shave biopsy and the histopathological diagnosis was BCC (Fig. 3d); the residual neoplasm was subsequently removed by Mohs surgery.

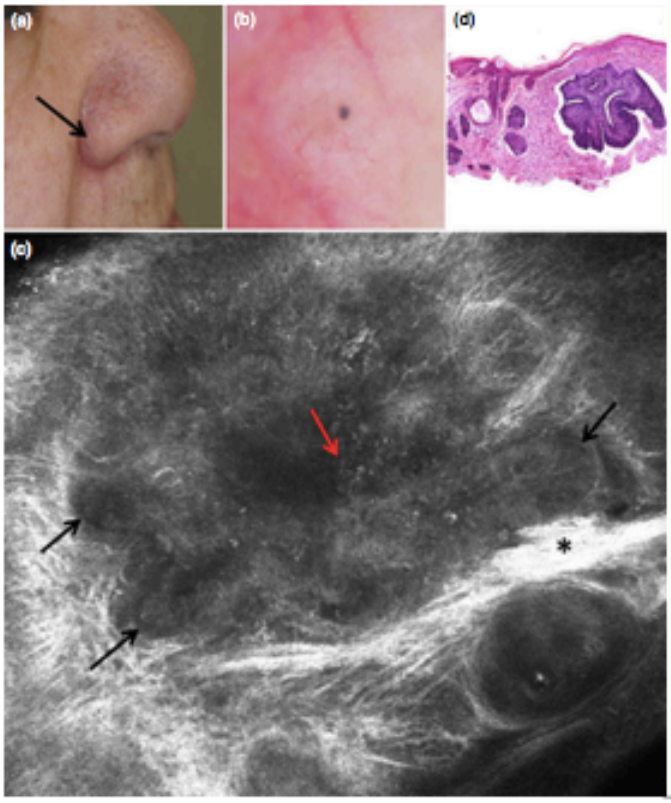

Figure 3 Patient #2. Basal cell carcinoma.

© 2013 European Academy of Dermatology and Venereology

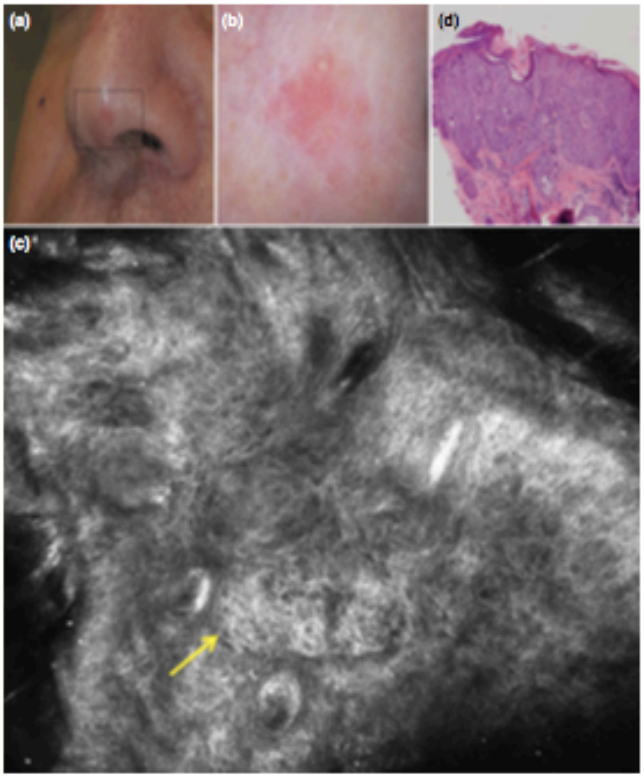

Figure 4 Patient #3. Squamous cell carcinoma *in situ*.

Patient 3

A 53-year-old man with history of melanoma and NMSC was concerned of a new lesion on the nose. Upon examination, a 5 mm erythematous scaly papule was noted on the nasal tip (Fig. 4a). Under dermoscopy, the lesion showed diffuse dotted vessels and yellowish scaly clods over pink–white background (Fig. 4b). Differential diagnosis included SCC, BCC and solar keratosis. HH-RCM probe examination at the spinous-granular level revealed an irregular honeycomb pattern (Fig. 4c), corresponding to the presence of atypical keratinocytes with pleomorphism. The RCM findings were suggestive of either SCC or solar keratosis. However, taken together with the clinical finding of a palpable lesion and the dermoscopic finding of dotted vessels, the lesion was more concerning for SCC. The lesion was removed by shave biopsy and the histopathological diagnosis was SCC *in situ* (Fig. 4d).The residual neoplasm was subsequently removed by Mohs surgery.

Patient 4

A 70-year-old woman with history of NMSC presented for skin cancer screening. The patient was not concerned of any lesion. During examination, the dermatologist noted a 2 mm skin colour papule with a focus of dark pigmentation on the chin (Fig. 5a). Under dermoscopy, the lesion had yellow lobular structures, blue clods and thin branching vessels (Fig. 5b). Differential diagnosis included BCC and SH. HH-RCM imaging at the superficial dermis level revealed morulae-like clusters, which are lobules of round to cuboidal cells with dark central nuclei and bright speckled cytoplasm (Fig. 5c), suggestive of sebaceous lobules. The surrounding dermis showed amorphous bright, broadened and reticulated collagen fibres compatible with solar elastosis. RCM findings were suggestive of SH. The lesion was removed by shave biopsy and histopathological diagnosis was indeed SH (Fig. 5d).

Patient 5

A 19-year-old man without history of skin cancer presented for examination of a new lesion on the cheek which concerned the patient. During examination, the dermatologist noted a 3 mm white, slightly depressed papule on the right malar area (Fig. 6a). Under dermoscopy, the lesion displayed milia-like cysts and thin branched vessels (Fig. 6b). Differential diagnosis

© 2013 European Academy of Dermatology and Venereology

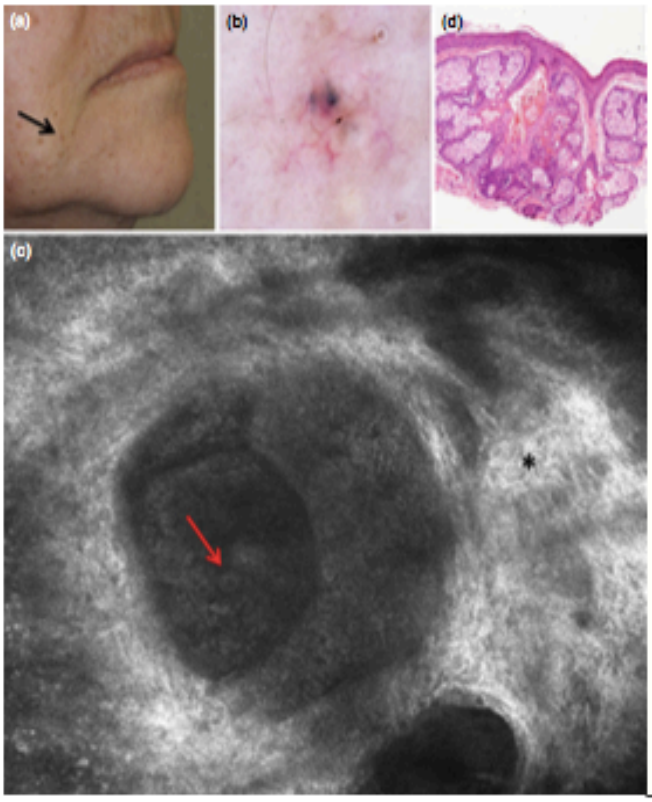

Figure 5 Patient #4. Sebaceous hyperplasia.

included BCC, trichoepithelioma (TE) and SH. On HH-RCM imaging, well-circumscribed, large, highly refractile, round structures, compatible with corneal cysts were seen at all epidermal layers; these structures are the RCM correlates of dermoscopically observed milia-like cysts. Deeper optical sections at the DEJ and superficial dermal levels showed bright tumour islands separated by dark clefts from surrounding collagen bundles. Of note, canalicular vessels, typical RCM finding in BCC, were not seen (Fig. 6c). The RCM findings were suggestive of a trichoblastic neoplasm, the differential diagnosis being between TE and BCC. Taken together, the patient's young age, white colour of the lesion and lack of increased vascularity on RCM were in favour of the diagnosis of TE. The lesion was removed by shave biopsy and histopathological diagnosis was desmoplastic TE (Fig. 6d).

Patient 6

A 65-year-old woman with history of melanoma and BCCs presented for skin cancer screening. The patient was concerned of a new lesion on the upper lip. During examination, a 2 mm pink-brownish papule was noted on the right upper lip (Fig. 7a). Dermoscopic examination revealed brown and blue clods and dots and linear serpentine vessels, surrounded by homogenous golden-brown areas (Fig. 7b). Differential diagnosis included pigmented BCC and melanocytic nevus. HH-RCM examination at the spinous-granular layers revealed regular honeycomb pattern. Bright junctional and dermal dense nests were seen at the DEJ and papillary dermis (Fig. 7c), compatible with nest of melanocytes. The RCM findings were highly suggestive of melanocytic nevus. However, given that this was a new melanocytic lesion in an elderly patient with history of skin cancer, the lesion was biopsied with a 2 mm punch biopsy specimen. Histopathological analysis confirmed the diagnosis of compound melanocytic nevus (Fig. 7d).

Discussion

In recent years, RCM has started to disseminate into public hospitals and even private practices in Europe and U.S.; this is likely due to technical improvement in the device and due to research showing an increase in accuracy of skin cancer diagnosis with RCM.[1–5]

© 2013 European Academy of Dermatology and Venereology

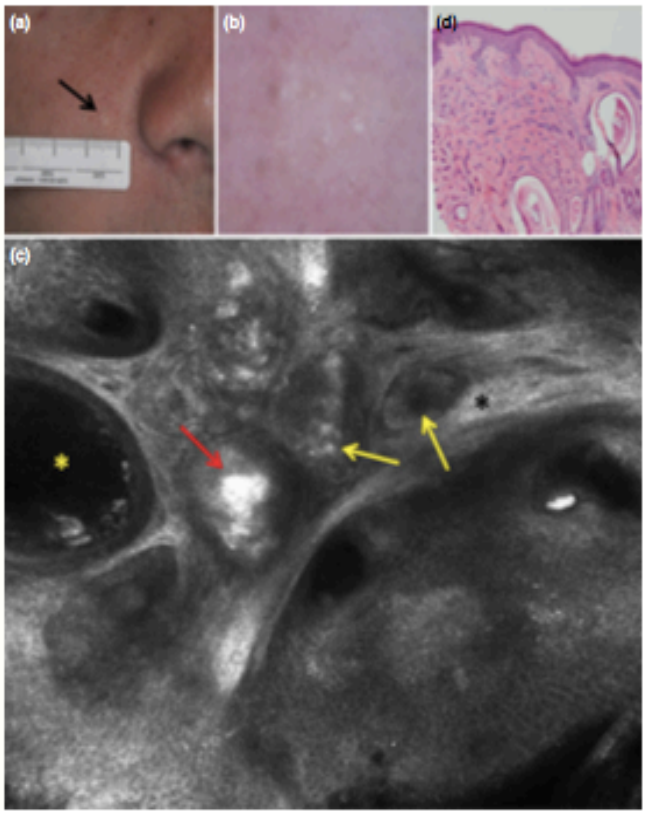

Figure 6 Patient #5. Trichoepithelioma.

The commercially available HH-RCM was introduced in 2011. The principle differences between the HH-RCM (Vivascope 3000) and the traditional wide-probe RCM (TWP-RCM, Vivascope 1500) are summarized (Table 1). In brief, with TWP-RCM, imaging requires skin fixation using disposable adhesive window, whereas HH-RCM can be applied to skin directly without fixation. Thus, with HH-RCM, commencement of lesion imaging is very fast and imaging of several sites (e.g. imaging several foci within a large lesion) is simple; in contrast, with TWP-RCM, displacing the probe to a different focus is more cumbersome. Taken together with the small diameter of the handheld probe, imaging with HH-RCM is faster than with TWP-RCM and allows reaching concave anatomical sites that are even difficult to access with contact dermoscopy.

Lateral and axial resolutions of HH-RCM are equivalent to those of TWP-RCM. However, whereas TWP-RCM can acquire images with a large FOV of up to 8 mm × 8 mm, akin to low magnification on histopathology, HH-RCM offers a more limited FOV up to 1 mm × 1 mm, akin to high magnification on histopathology. Thus, HH-RCM can be likened to core or tiny incisional optical biopsy, whereas TWP-RCM to excisional or wider incisional optical biopsy. An advantage of TWP-RCM is the built-in navigation system that is guided by the dermoscopic image of the lesion. The navigation system together with the tissue fixation, allows for systematic investigation and orientation within the tissue; suspicious foci within the dermoscopic image or in the RCM mosaic can be analysed at high magnification RCM. In contrast, HH-RCM navigation is currently more random and not guided by a dermoscopic image. Thus, orientation within the lesion, with respect to the dermoscopic findings, can be difficult and the foci investigated may not be the areas that harbour the most diagnostic RCM criteria.

A useful application of RCM is as an adjunct to clinical and dermoscopic evaluation of small, pink papules or nodules, particularly on the face where clinicians are more reluctant to perform unnecessary biopsies. For amelanotic lesions, the feature-poor dermoscopic image is usually not helpful in guiding RCM tissue investigation. Herein, we present a series of small, pink to lightly pigmented solitary facial lesions in which HH-RCM was useful in reaching the correct bedside diagnosis,

 © 2013 European Academy of Dermatology and Venereology

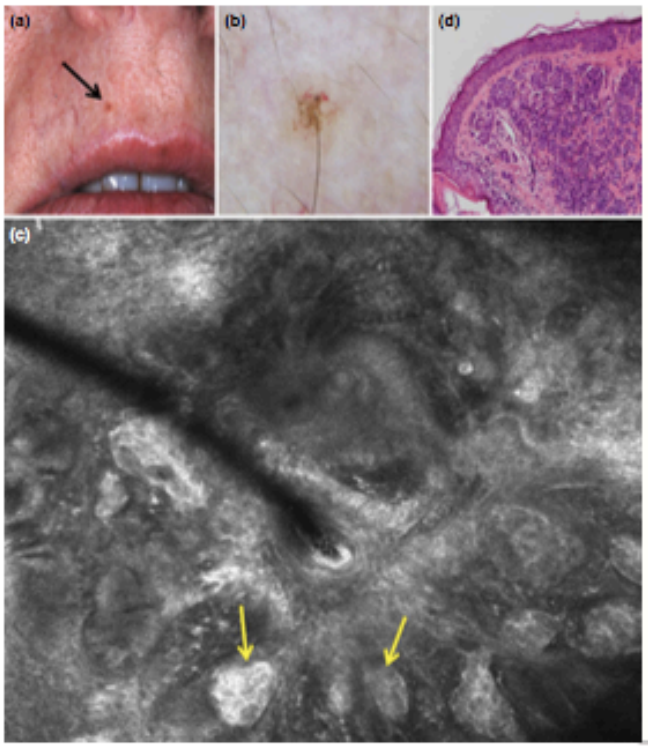

Figure 7 Patient #6. Melanocytic nevus.

Table 1 Differences between the HH-RCM probe and the TWP-RCM

	HH-RCM Probe	TWP-RCM
Individual RCM image FOV	1 mm × 1 mm	0.5 mm × 0.5 mm
Maximal FOV	1 mm × 1 mm	8 mm × 8 mm
Average imaging time	1–4 min	5–10 min
Automated capture functions	Stack of individual RCM images	Stack of individual RCM images Horizontal mosaic of "stitched" individual RCM images
Advantages	Access to contoured anatomic sites (e.g. facial region) Rapid examination of multiple areas of interest in the same subject	Wide FOV allows assessment of lesion at scan magnification for size, symmetry in brightness and distribution of structures Built-in RCM navigation that is guided by dermoscopic image of the lesion Tissue fixation allows for systematic navigation and orientation within the tissue
Limitations	Small FOV Orientation within the lesion can be difficult	Requires fixation with adhesive to approximately 10 × 10 mm of flat skin surface Limited access to curved anatomic sites

RCM, Reflectance Confocal Microscopy; FOV, Field of View; HH-RCM, handheld RCM; TWP-RCM, traditional wide-probe RCM.

despite equivocal clinical and dermoscopic attributes of lesions. In four cases, HH-RCM examination was diagnostic, whereas in two cases (patients 3 and 5) it narrowed the differential diagnosis; establishing the correct diagnosis in these two cases required integration of RCM findings with the clinical data. The basic RCM criteria for diagnosis of BCC, SCC, SH, TE and melanocy-

 © 2013 European Academy of Dermatology and Venereology

Table 2 Reflectance confocal microscopy criteria for facial papules evaluation, stratified by anatomic level of imaging

Anatomic level	BCC[6,13,14]	SCC[16]	Sebaceous hyperplasia [17,18]	Desmoplastic TE[15]	Compound melanocytic nevus[20]
Suprabasal Epidermis (Stratum corneum, Granular and Spinous layers)	Polarization of nuclei in spinous layer or regular honeycomb pattern; bright delicate dendritic structures occasionally seen (Langerhans cells)	Scale; irregular honeycomb pattern; round nucleated cells at suprabasal layers	Dilated follicular infundibulum with bright amorphous keratotic content	Regular honeycomb pattern	Regular honeycomb or cobblestone pattern
DEJ/Basal layer of epidermis	Dark silhouettes; bright tumor islands	Multiple round blood vessels within dermal papillae			Edged papillae; dense junctional nests, uniform in size and shape and regularly distributed
Dermis	Dark silhouettes outlined by surrounding dense collagen bundles; bright tumor islands separated from dense collagen bundles by peritumoral dark clefts; canalicular vessels	Multiple round blood vessel	Morulae-like clusters; broadened reticulated collagen	Bright tumor islands containing corneal cysts; tumor islands occasionally connected to follicular structures; bright parallel collagen bundles arranged tightly around the tumor islands	Dense dermal nests composed of cells with uniform morphology and refractility

BCC, Basal Cell Carcinoma; DEJ, Dermo-epidermal junction; SCC, Squamous Cell Carcinoma; TE, trichoepithelioma.

tic nevus stratified by anatomic level are summarized (Table 2); these HH-RCM criteria are similar to those described for TWP-RCM.[12]

In our experience, BCC is easily recognized with HH-RCM, even in large dermoscopically equivocal lesions. The main RCM features, dark silhouettes, bright tumour islands surrounded by dark clefts and canalicular blood vessels can be readily seen on HH-RCM.[6,13,14] Desmoplastic TE can be at times difficult to distinguish from morpheaform BCC on histopathological analysis. In a similar vein, desmoplastic TE shows RCM findings in common with BCC. Ardigo *et al.*[15] analysed four cases of TE with RCM. They observed features that were previously ascribed to BCC, such as presence of bright tumour islands as cords of bright cells with elongated nuclei. However, RCM features that were more characteristic of TE included connection between neoplastic aggregates and follicular structures; aggregates with corneal cysts seen as round, dark spaces filled with refractile material, corresponding to keratinizing cysts on histopathology and thick, highly refractile collagen bundles, wrapping the bright tumour islands. Desmoplastic TE revealed fewer, smaller and more sparsely distributed bright tumour islands on RCM examination than typically seen with BCC.

In SCC, atypia of keratinocytes in the suprabasal epidermis can be appreciated on HH-RCM as irregular honeycomb pattern, a disarranged epidermal pattern or bright round nucleated cells at the spinous and granular suprabasal layers.[6,16] In addition, round blood vessels looping through dermal papilla in SCC can be readily noted on HH-RCM. At present, RCM is limited in differentiating SCC *in situ* from solar keratosis, as both can show similar RCM attributes, although the changes tend to be more focal and subtle in solar keratosis.[16] Integration of RCM findings with clinical and dermoscopic criteria is helpful in differentiating SCC from solar keratosis, as shown in patient 3.

Sebaceous hyperplasia can clinically and dermoscopically mimic BCC; HH-RCM may be used to readily differentiate between them with the finding of morulae-like cluster in SH, described by Propperova *et al.*[17]. Similar RCM features were observed by Moscarella *et al.*[18] when imaging three sebaceous adenomas in patients with Muir–Torre syndrome.

Intradermal and compound nevi on the face are often feature-poor on clinical and dermoscopic examination. Differentiation of facial melanocytic nevi from BCC based on patient history and other subtle clues such as the dermoscopic vascular pattern can be challenging, whereas differentiation with RCM is usually straightforward, as nests of melanocytes are readily seen under RCM due to the strong reflectance of melanin.[6,19,20] However, HH-RCM may prove to be more limited for evaluation of nevus vs. melanoma; principle attributes for RCM evaluation of melanocytic neoplasms include overall pattern, symmetry in distribution of brightness and RCM structures and lateral circumscription, attributes that can only be assessed when the lesion is imaged *in toto*.

© 2013 European Academy of Dermatology and Venereology

In conclusion, the HH-RCM is a promising new, non-invasive imaging tool to perform a rapid bedside evaluation of skin lesions. For clinically and dermoscopically equivocal small pink to lightly pigmented papules on curved facial surface, HH-RCM may be particularly helpful in differentiating benign lesions from skin cancer. Given that this is a small case series, further study is needed to test the diagnostic accuracy of using HH-RCM for equivocal facial papules.

Acknowledgements

We thank Margaret Oliviero, ARNP for her contribution to the data collection.

References

1 Pellacani G, Guitera P, Longo C *et al.* The impact of in vivo reflectance confocal microscopy for the diagnostic accuracy of melanoma and equivocal melanocytic lesions. *J Invest Dermatol* 2007; **127**: 2759–2765.
2 Guitera P, Pellacani G, Longo C *et al.* In vivo reflectance confocal microscopy enhances secondary evaluation of melanocytic lesions. *J Invest Dermatol* 2009; **129**: 131–138.
3 Guitera P, Pellacani G, Crotty KA *et al.* The impact of in vivo reflectance confocal microscopy on the diagnostic accuracy of lentigo maligna and equivocal pigmented and nonpigmented macules of the face. *J Invest Dermatol* 2010; **130**: 2080–2091.
4 Braga JC, Scope A, Klaz I *et al.* The significance of reflectance confocal microscopy in the assessment of solitary pink skin lesions. *J Am Acad Dermatol* 2009; **61**: 230–241.
5 Rajadhyaksha M, Grossman M, Esterowitz D *et al.* In vivo confocal scanning laser microscopy of human skin: melanin provides strong contrast. *J Invest Dermatol* 1995; **104**: 946–952.
6 Guitera P, Menzies SW, Longo C *et al.* In vivo confocal microscopy for diagnosis of melanoma and basal cell carcinoma using a two-step method: analysis of 710 consecutive clinically equivocal cases. *J Invest Dermatol* 2012; **132**: 2386–2394.
7 Moscarella E, Zalaudek I, Agozzino M *et al.* Reflectance confocal microscopy for the evaluation of solitary red nodules. *Dermatology* 2012; **224**: 295–300.
8 Maier T, Satzler EC, Braun-Falco M *et al.* Reflectance confocal microscopy in the diagnosis of partially and completely amelanotic melanoma: report on seven cases. *J Eur Acad Dermatol Venereol* 2013; **27**: e42–e52.
9 Busam KJ, Hester K, Charles C *et al.* Detection of clinically amelanotic malignant melanoma and assessment of its margins by in vivo confocal scanning laser microscopy. *Arch Dermatol* 2001; **137**: 923–929.
10 Segura S, Pellacani G, Puig S *et al.* In vivo microscopic features of nodular melanomas: dermoscopy, confocal microscopy, and histopathologic correlates. *Arch Dermatol* 2008; **144**: 1311–1320.
11 Longo C, Farnetani F, Ciardo S *et al.* Is confocal microscopy a valuable tool in diagnosing nodular lesions? A study on 140 cases. *Br J Dermatol* 2013; **169**: 58–67.
12 Hofmann-Wellenhof R, Pellacani G, Malvehy J, Soyer HP. Reflectance Confocal Microscopy for Skin Diseases. Springer, Berlin, 2012.
13 Agero ALC, Busam KJ, Benvenuto-Andrade C, *et al.* Reflectance confocal microscopy of pigmented basal cell carcinoma. *J Am Acad Dermatol* 2006; **54**: 638–643.
14 Nori S, Rius-Díaz F, Cuevas J *et al.* Sensitivity and specificity of reflectance-mode confocal microscopy for in vivo diagnosis of basal cell carcinoma: a multicenter study. *J Am Acad Dermatol* 2004; **51**: 923–930.
15 Ardigo M, Zieff J, Scope A, *et al.* Dermoscopic and reflectance confocal microscope findings of trichoepithelioma. *Dermatology* 2007; **215**: 354–358.
16 Rishpon A, Kim N, Scope A *et al.* Reflectance confocal microscopy criteria for squamous cell carcinomas and actinic keratoses. *Arch Dermatol* 2009; **145**: 766–772.
17 Propperova I, Langley RB. Reflectance-mode confocal microscopy for the diagnosis of SH In vivo. *Arch Dermatol* 2007; **143**: 134.
18 Moscarella E, Argenziano G, Longo C *et al.* Clinical, dermoscopic and reflectance confocal microscopy features of sebaceous neoplasms in Muir-Torre syndrome. *J Eur Acad Dermatol Venereol* 2013; **27**: 699–705.
19 Scope A, Benvenuto-Andrade C, Agero AL *et al.* In vivo reflectance confocal microscopy imaging of melanocytic skin lesions: consensus terminology glossary and illustrative images. *J Am Acad Dermatol* 2007; **57**: 644–658.
20 Pellacani G, Cesinaro AM, Seidenari S. In vivo assessment of melanocytic nests in nevi and melanomas by reflectance confocal microscopy. *Mod Pathol* 2005; **18**: 469–474.

 © 2013 European Academy of Dermatology and Venereology

5.3 ARTIGO ORIGINAL 2

A pink papule on the back of an 82-year-old man: an example of the buttonhole sign on reflectance confocal microscopy.

Syril Keena T. Que, **Naiara Fraga-Braghiroli**, Jane M. Grant-Kels, Harold S. Rabinovitz, Margaret Oliviero, Alon Scope .

Dermatology Practical & Conceptual 2016; 6(3):1-2

Situação- Artigo Publicado

O artigo descreve a presença de numerosos vasos arredondados, agregados e destribuídos uniformemente na junção dermo-epidérmica - aqui denominados *buttonhole sign (sinal do buraco de botão)*, indicando os aspectos visualizados à microscopia confocal de reflectância.

Descrito pela primeira vez na literatura médica, neste artigo, este sinal ora representa um importante indício para o diagnóstico do carcinoma escamocelular (CEC) *in situ.*

Na estrutura do *sinal do buraco de botão*, os vasos assim distribuídos correspondem aos vasos glomerulares apreciados à dermatoscopia do carcinoma escamocelular, e representam as alças dos vasos dérmicos que atravessam repetidamente as papilas dérmicas.

Na MCR, a presença do sinal do buraco de botão associado a uma rede em favo de mel atípica nas camadas espinhosa e/ou granular da epiderme é altamente sugestiva do CEC.

DERMATOLOGY PRACTICAL & CONCEPTUAL
www.derm101.com

A pink papule on the back of an 82-year-old man: an example of the buttonhole sign on reflectance confocal microscopy

Syril Keena T. Que[1], Naiara Fraga-Braghiroli[2], Jane M. Grant-Kels[1], Harold S. Rabinovitz[2], Margaret Oliviero[2], Alon Scope[3]

1 Department of Dermatology, University of Connecticut Health Center, Farmington, CT, USA
2 Department of Dermatology, University of Miami Miller School of Medicine, Miami, FL, USA
3 Department of Dermatology, Sheba Medical Center and Sackler Faculty of Medicine, Tel Aviv University, Tel Aviv, Israel

Citation: Que SKT, Fraga-Braghiroli N, Grant-Kels JM, Rabinovitz HS, Oliviero M, Scope A. A pink papule on the back of an 82-year-old man: an example of the buttonhole sign on reflectance confocal microscopy Dermatol Pract Concept 2016;6(3): doi: 10.5826/dpc.0603a01

Received: December 2, 2015; Accepted: April 25, 2016; Published: July 31, 2016

Copyright: ©2016 Que et al. This is an open-access article distributed under the terms of the Creative Commons Attribution License, which permits unrestricted use, distribution, and reproduction in any medium, provided the original author and source are credited.

Funding: Dr. Scope's confocal microscopy research is supported by the European Commission Marie Curie FP7 Reintegration Grant (PIRG07-GA-2010-268359). Dr. Rabinovitz has received equipment and funding for a fellowship program from Lucid Inc.

Competing interests: Dr. Rabinovitz is an investigator in a study coordinated by Lucid Inc, manufacturer of a commercial confocal microscope. The authors have no conflicts of interest to disclose.

All authors have contributed significantly to this publication.

Corresponding author: Syril Keena Que, MD, University of Connecticut Health Center Department of Dermatology, 21 South Rd, Farmington, CT 06030, USA. Tel. 860. 679.4600. Email: keenaq@gmail.com

Clinical presentation

An 82-year-old man with Fitzpatrick skin type III presented for the evaluation of a lesion on the left upper back. A scaly pink papule was observed (Figure 1). The differential diagnosis included squamous cell carcinoma (SCC), actinic keratosis, basal cell carcinoma, and amelanotic melanoma.

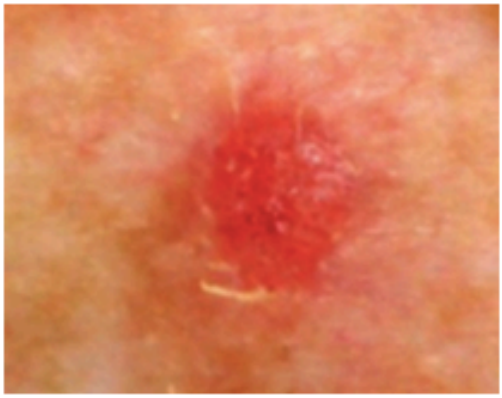

Figure 1. Squamous cell carcinoma *in situ*. Scaly pink papule on the left upper back. [Copyright: ©2016 Que et al.]

Dermoscopic appearance

On dermoscopy, multiple coiled blood vessels (also termed glomerular vessels) were scattered across the papule (Figure 2) [1].

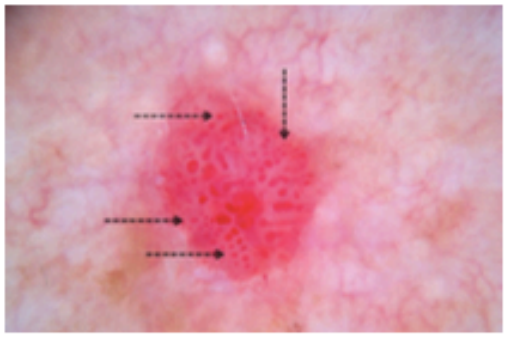

Figure 2. Squamous cell carcinoma *in situ*. Dermatoscopic image showing dotted and round blood vessels (*black arrows*) appearing centrally and around the periphery. [Copyright: ©2016 Que et al.]

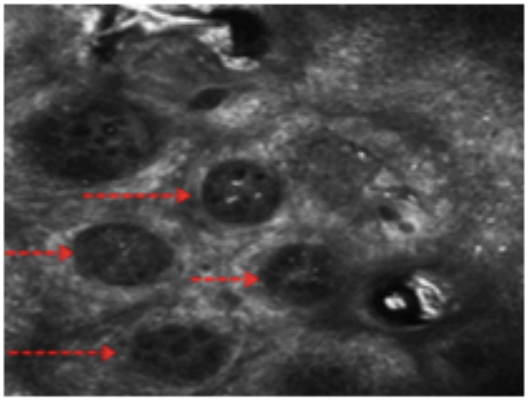

Figure 3. Squamous cell carcinoma *in situ*. At the level of the dermo-epidermal junction, reflectance confocal microscopy reveals round blood vessels ("buttonholes") traversing the dermal papillae ("buttons," *red arrows*). [Copyright: ©2016 Que et al.]

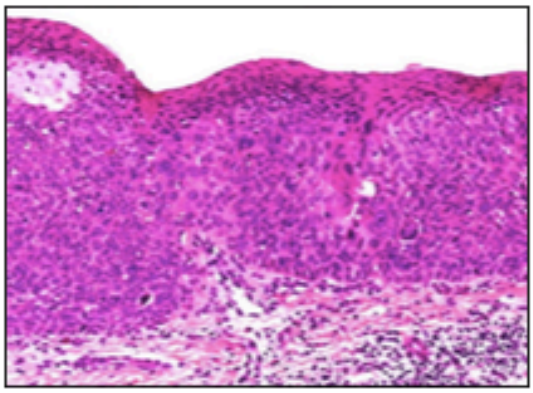

Figure 4. Histopathology reveals full-thickness cytological atypia with mitoses and acantholysis, consistent with squamous cell carcinoma *in situ*. [Copyright: ©2016 Que et al.]

Reflectance confocal microscopy appearance

Reflectance confocal microscopy (RCM) at the level of the dermo-epidermal junction shows dermal papillae appearing in cross-section as perfect circles, resembling "buttons." Round blood vessels traverse through the dermal papillae, appearing centrally and around the periphery as "buttonholes" (Figure 3). The surrounding epidermis is characterized by an atypical honeycomb pattern consisting of cells with variability in brightness and in the size of nuclei.

What is your diagnosis?

Diagnosis

Histopathology revealed SCC in situ (Figure 4). The "buttonholes" seen on RCM correlate with numerous tortuous blood vessels at the dermal papillae of the SCC in situ (Figure 5).

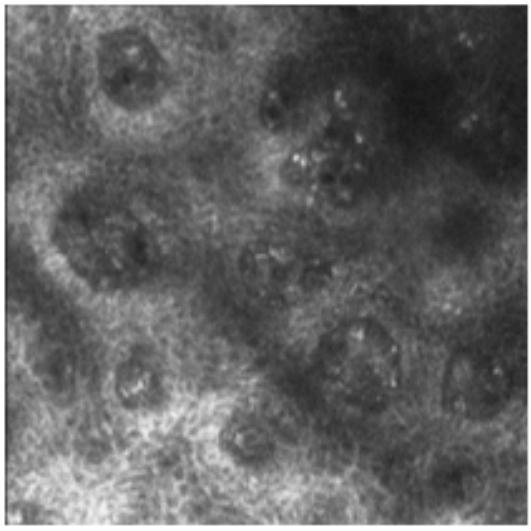

Figure 5. Psoriasis. At the level of the dermo-epidermal junction, reflectance confocal microscopy reveals round blood vessels ("buttonholes") traversing the dermal papillae (""buttons", *red arrows*). [Copyright: ©2016 Que et al.]

Discussion

A buttonhole sign in the presence of an atypical honeycomb pattern is an RCM clue for SCC. Previous articles have correlated dotted vessels on dermoscopy with sparsely distributed round vessels on RCM [2]. Here we report a new RCM diagnostic clue not previously reported—the presence of numerous round vessels in an SCC in situ with coiled vessels. The uniformity, clustered nature, and multitude of these round vessels reflect the way these vessels repeatedly loop through the dermal papillae. This finding is not specific for SCC and can be observed in conditions like psoriasis or clear cell acanthoma, when there are coiled or glomerular vessels seen under dermoscopy. However, in SCC the increased vascularity is seen under RCM in conjunction with irregularity of the honeycomb pattern of the spinous and granular layers of the epidermis.

References

1. Rishpon A, Kim N, Scope A, et al. Reflectance confocal microscopy criteria for squamous cell carcinomas and actinic keratoses. Arch Dermatol 2009 Jul;145(7):766-72. PMID: 19620557. DOI: 10.1001/archdermatol.2009.134.
2. Ahlgrimm-Siess V, Cao T, Oliviero M, et al. The vasculature of nonmelanocytic skin tumors on reflectance confocal microscopy: vascular features of squamous cell carcinoma in situ. Arch Dermatol 2011 Feb;147(2):264. PMID: 21339468. DOI: 10.1001/archdermatol.2010.416.

5.4 ARTIGO ORIGINAL 3

Reflectance Confocal Microscopy Features of Focal Dermal Mucinosis Differ from Those Described for Basal Cell Carcinoma: Report of Two Cases

Naiara Abreu Fraga-Braghiroli, Miesha Merati, Harold Rabinovitz, David Swanson, Alon Scope.

Dermatology 2015; 231:326–329

Situação- Artigo Publicado

O objetivo do presente artigo foi descrever os achados na MCR da mucinose dérmica focal e sua correlação com a histopatologia.

Uma vez que essa entidade mimetiza o carcinoma basocelular (CBC), tanto na clínica quanto na dermatoscopia, a descrição das características confocais dessa entidade permite evitar a necessidade de realização de um procedimento invasivo para que se obtenha o diagnóstico.

Os achados aqui descritos são: faixas de colágenos denso orientados de forma paralela na derme, focos de finas fibras de colágeno distribuídos aleatoriamente e separados por áreas escuras com ausência de estruturas, e ausência de silhuetas escuras ou ilhas tumorais.

Este estudo corrobora a premissa de que a MRC é uma tecnologia promissora no diagnóstico de lesões cutâneas e seu uso pode evitar procedimentos invasivos.

Dermatology

Case Report

Dermatology 2015;231:326–329
DOI: 10.1159/000437222

Received: January 5, 2015
Accepted after revision: June 8, 2015
Published online: August 22, 2015

Reflectance Confocal Microscopy Features of Focal Dermal Mucinosis Differ from Those Described for Basal Cell Carcinoma: Report of Two Cases

Naiara Abreu Fraga-Braghiroli[a] Miesha Merati[a] Harold Rabinovitz[a] David Swanson[b] Alon Scope[c, d]

[a]Skin and Cancer Associates, Plantation, Fla., [b]Dermatology Department, Mayo Clinic, Scottsdale, Ariz., and [c]Dermatology Service, Memorial Sloan-Kettering Cancer Center, New York, N.Y., USA; [d]Dermatology Department, Sheba Medical Center and Sackler Faculty of Medicine, Tel Aviv University, Tel Aviv, Israel

Key Words
Focal dermal mucinosis · Dermatoscopy · Reflectance confocal microscopy

Abstract
The purpose of this study was to describe the reflectance confocal microscopy (RCM) features of focal dermal mucinosis (FDM). The entity clinically and dermatoscopically mimics other diagnostic entities, most notably nonpigmented basal cell carcinoma. We describe two cases that highlight the dermatoscopic, RCM and histopathological attributes of FDM. RCM features such as dermal foci of dense collagen bundles oriented in the same direction, foci of haphazardly oriented thin collagen fibers separated by dark structureless areas and the absence of dark silhouettes and tumor islands are clues for FDM diagnosis. The FDM cases described here present consistent and particular RCM findings that appear to correlate well with the histopathological features of FDM. Therefore, RCM is a promising technology in diagnosing skin lesions and it use can avoid invasive procedures. © 2015 S. Karger AG, Basel

Introduction

Focal dermal mucinosis (FDM) is a benign diagnostic entity clinically presenting as a solitary papule or nodule. It is usually located on the face, neck, trunk, or proximal extremities of adults. Lesions are asymptomatic and skin-colored. As FDM is rarely encountered in clinical practice, it is often diagnosed at the bedside as a basal cell carcinoma (BCC), neurofibroma, intradermal nevus, or cyst. Histopathological examination confirms the specific diagnosis of FDM, which shows a dermal deposition of mucin – a mixture of acid mucopolysaccharides composed mostly of hyaluronic acid [1–3].

Reflectance confocal microscopy (RCM) is an advanced imaging tool that assists the dermatologist in noninvasively diagnosing solitary skin lesions, both pigmented and nonpigmented. RCM is currently in the process of dissemination into academic medical centers and even private practices.

Herein, we describe in 2 patients the RCM features of FDM, which appear different than previously published RCM attributes of BCC, the principal pathological entity in the differential diagnosis of FDM.

Description of Patients and Lesions

Patient 1

A 70-year-old woman presented for a routine 3-month dermatological examination. Her medical history was notable for multiple primary melanomas, including a melanoma 0.4 mm in depth on the left shin in 2006 and 2 in situ melanomas on the right and left lateral back in 2008. Her general medical history included hypertension and diabetes mellitus treated with metoprolol, lisinopril, diltiazem, and sitagliptin. The patient reported that she had first noticed a lesion on her upper back 3 months previously and that during this time the lesion had been stable in size and color, asymptomatic and without bleeding. On clinical examination, the dermatologist noted a 5-mm pink papule on the left upper back (fig. 1a, inset). Dermato-

KARGER 125

E-Mail karger@karger.com
www.karger.com/drm

© 2015 S. Karger AG, Basel
1018–8665/15/2314–0326$39.50/0

Naiara Abreu Fraga-Braghiroli, MD
Skin and Cancer Associates
201 NW 82nd Ave., Suite 103
Plantation, FL 33324 (USA)
E-Mail naiarafraga@yahoo.com.br

Downloaded by:
189.26.210.251 - 5/2/2017 9:44:25 PM

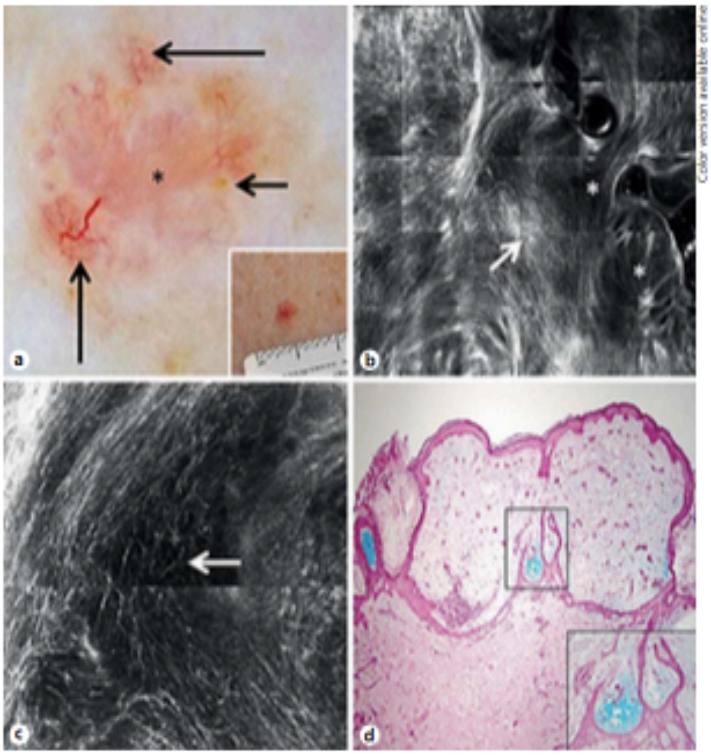

Fig. 1. a Under dermatoscopy, thin serpentine and branched vessels (long arrows), brown-yellowish globules (short arrow) and a pink-white background (asterisk) are seen. **Inset** Clinical image with a pink well-circumscribed papule. **b** RCM mosaic (3 × 3 mm) at the deeper papillary dermis level shows thin collagen fibers at variable density (arrow), including foci appearing as darker spaces in which the collagen fibers are sparse (asterisks). **c** The thin collagen fibers separated by darker spaces (arrow) are seen at higher magnification. **d** Histopathology section shows a well-circumscribed elevated dermal nodule. Colloidal iron stain. ×40. **Inset** The foci that show an accumulation of blue-stained mucin are likely to correlate with the darker areas on RCM.

scopic evaluation showed serpentine and branched vessels, brown-yellowish globules and a pink-white background (fig. 1a). The differential diagnosis based on the clinical and dermatoscopic findings included BCC, intradermal nevus and amelanotic melanoma.

Patient 2

A 62-year-old woman without a history of skin cancer presented for dermatological examination. She noticed 1 month prior to the visit an asymptomatic 4-mm skin-colored papule on her left shoulder; the lesion had been stable in size and color and without bleeding over this period. Her general medical history included breast cancer treated with cyclophosphamide and doxorubicin followed by pegfilgrastim, paclitaxel and trastuzumab; hypertension and hyperlipidemia were treated with valsartan, hydrochlorothiazide, metoprolol, and pravastatin. On clinical examination, there was a 4-mm pink-yellowish papule on the left shoulder (fig. 2a, inset). Dermatoscopy showed serpentine-branched vessels and a pink-yellowish background (fig. 2a). The differential diagnosis included BCC, intradermal nevus and amelanotic melanoma.

RCM Findings

In an attempt to make a more specific diagnosis for the lesions described, an RCM examination was performed using a commercially available RCM (VivaScope 1500; Caliber I.D., Rochester, N.Y., USA). In both cases, RCM examination revealed similar findings. A regular honeycomb pattern was observed at the level of the spinous-granular layers of the epidermis. At the deeper papillary dermis, there was an abnormal pattern composed of areas where thin collagen fibers at a low density and with haphazard orientation were separated by relatively dark spaces. Slightly broader, bright fusiform to dendritic structures were also observed amidst the thin collagen bundles (fig. 1b, c, 2b, c). In addition, there was increased blood flow in thin capillaries. In both cases, RCM examination did not support the diagnosis of BCC, nevus or melanoma. We did not observe the principal RCM attributes of BCC, namely, the presence of neoplastic aggregates seen as bright tumor islands or as dark silhouettes that are sharply outlines by thickened collagen bundles at the level of the dermoepidermal junction or upper dermis. In addition, we did not observe the presence of bright nucleated round or dendritic cells or the presence of bright cellular clusters – features of a melanocytic proliferation. However, we were not familiar with the particular RCM pattern seen in these 2 cases and could not make a definitive diagnosis.

Shave biopsies of both lesions were performed. Histopathological examinations showed a benign silhouette of an exoendophytic lesion. The epidermis was thin and flat, while hyperplastic follicular infundibula demarcated the deeper portion of the lesion in the dermis. The superficial dermis was characterized by abundant amounts of granular basophilic material, compatible with mucin. A proliferation of capillaries was also seen in the dermis. The dermal proliferation did not reveal an abnormal dermal accumulation of cells expressing CD34, Melan-A or keratin. The histopathological findings were diagnostic of FDM (fig. 1d, 2d). A colloidal iron stain was performed in both cases, highlighting the distribution of mucin in the dermis. There were foci where mucin was interspersed between thin collagen bundles, while in other areas there were mucin-filled spaces which displaced the collagen bundles (fig. 1d).

Downloaded by:
189.28.213.20 - 8/2/2017 5:44:26 PM

Table 1. Differences in the RCM features of FDM seen in the present cases and previously described RCM features of BCC

Anatomic level	FDM	BCC
Spinous-granular layer of the epidermis	Regular honeycomb pattern	Mostly polarized or regular honeycomb pattern; bright delicate dendritic structures occasionally seen (Langerhans cells)
Dermoepidermal junction and upper dermis	Foci where thin collagen fibers at a low density and with haphazard orientation are separated by relatively dark spaces	Dark silhouettes – dark areas which often have a polycyclic contour and are sharply outlined by surrounding dense collagen bundles; bright tumor islands with peripheral palisading of nuclei and surrounding dark clefts

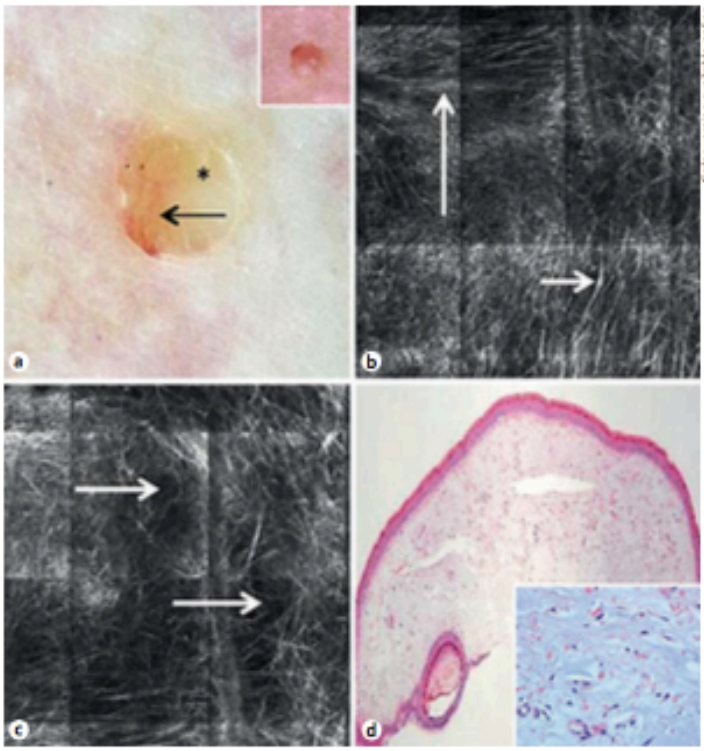

Color version available online

Fig. 2. a Under dermatoscopy thin serpentine branched vessels (arrow) and a pink-yellowish background (asterisk) are seen. **Inset** Clinical image with skin-colored papule. **b** RCM mosaic (1.5 × 1.5 mm) at the papillary dermis level shows thin collagen fibers at variable density and orientation (long arrow). The bright dendritic-shaped structures seen amidst the collagen are probably fibroblasts (short arrow). **c** RCM mosaic (1 × 1 mm) at the papillary dermis shows an area with dark spaces (arrows) and relatively sparse collagen fibers. **d** Histopathology section shows a well-circumscribed elevated dermal nodule with large empty spaces amidst the dermal stroma. HE. ×10. **Inset** Close up view of the dermis showing large empty space between dermal stroma and few fibroblasts.

Discussion

Cutaneous dermal mucinoses are a rare group of diseases whereby fibroblasts produce abundant mucin, which accumulates in the dermis. Variable classification schemes have been used in the literature. Briefly, mucinoses can manifest diffusely, displaying expansive plaques or multiple widespread papules, or focally. Diffuse mucinoses can be associated with a systemic disease (e.g. scleromyxedema with monoclonal gammopathy and pretibial myxedema with hyperthyroidism) or appear as a primary cutaneous disease [2, 4–6]. Focal mucinosis are those presenting solitary to few papules or nodules (e.g. acral persistent papular mucinosis whereby multiple flesh-colored papules develop exclusively on the back of the hands) and FDM presenting as a solitary papule or nodule. FDM is most common on the face, trunk or extremities [3, 7, 8]. While FDM is mostly a primary lesion that does not warrant a systemic workup, there is a reported case of FDMin a patient with hypothyroidism that resolved spontaneously after correction of thyroid hormone levels and a report of cases of FDM associated with diffuse cutaneous mucinoses [9–11]. In addition, Kempf et al. [12] reported 2 cases of trauma-induced FDM arising at the areola. Finally, nevus mucinosus describes a cluster of mucinous papules arranged in a zosteriform, blaschkoid or linear distribution.

The main significance of FDM, as reported in our case, is that it clinically and dermatoscopically mimics other diagnostic entities, most notably nonpigmented BCC. The dermatoscopic findings of serpentine and branched vessels with a pink-white to yellow background in the FDM cases described herein do not differentiate them from BCC. This is hardly surprising, as BCC is also comprised of an accumulation

Downloaded by
189.26.210.28 - 6/2/2017 5:44:35 PM

Table 2. FDM: RCM and histopathological findings

RCM	Histopathology
Dark spaces between thin collagen fibers	Mucin deposits amidst the dermal stroma
Fusiform to dendritic structures thicker than the surrounding collagen fibers	Spindle-shaped fibroblasts within the mucinous areas
Increased blood flow in thin capillaries is seen during real-time or video-mode imaging	Proliferation of capillaries in the dermis

of mucin (albeit around the neoplastic aggregates), abnormal fibroplasia and increased vascularity – features similar to those seen in FDM.

However, there are notable differences in the RCM features of FDM compared to those usually seen in BCC (table 1). The main RCM features of FDM were foci of haphazardly oriented thin collagen fibers separated by darker spaces. In contrast, BCC shows on RCM dark areas, termed dark silhouettes, which often have a polycyclic contour and are sharply outlined by surrounding dense collagen bundles. Other, even more distinct features of BCC include bright tumor islands, polarization of nuclei in the tumor islands and dark clefts that separate the tumor islands from the surrounding dense collagen bundles.

The correlations between the histopathological and RCM findings of FDM are highlighted in table 2. On hematoxylin and eosin-stained histopathological specimens, the presence of mucin is suspected by the finding of broad empty spaces between the thin collagen fibers. These findings are likely to correspond on RCM to the dark spaces separating the thin collagen bundles. It has previously been established that under RCM imaging of unprocessed dermis, collagen fibers appear bright [13], while mucin and elastic fibers appear dark [14, 15]. In contrast, ex vivo exposure of tissue to acetic acid ('acetowhitening') enhances and allows the detection of elastic fibers under RCM [14]. Finally, the slightly broader bright fusiform to dendritic structures on RCM examination probably correspond histopathologically to spindle-shaped fibroblasts within the mucinous area.

In conclusion, the 2 FDM cases present particular RCM findings that appear to correlate well with the histopathological features of FDM and are different than previously described RCM features of BCC. Further reports of RCM imaging of FDM will clarify the reproducibility of the RCM pattern described herein and the utility of RCM for diagnosing FDM with specificity.

Disclosure Statement

Dr. Rabinovitz is an investigator in a study coordinated by Lucid Inc., manufacturer of a commercial confocal microscope. He has received funding for a fellowship program and equipment from Lucid Inc. He is also a consultant and has received equipment from 3-Gen, manufacturer of a polarized dermatoscope. Drs. Fraga-Braghiroli, Merati, Swanson and Scope have no conflicts of interest to declare.

References

1 Weedon D: Skin Pathology. Brisbane, Churchill Livingstone-Elsevier, 2010.

2 Rongioletti F, Rebora A: Cutaneous mucinoses: microscopic criteria for diagnosis. Am J Dermatopathol 2001;23:257–267.

3 McDermott AL, Biswas C, Morgan K, Kay NJ: Focal mucinosis: clinical and histological features of an unusual condition. J Laryngol Otol 2003;117:408–409.

4 James WD, Berger TG, Elston DM: Andrews' Diseases of the Skin: Clinical Dermatology. Philadelphia, Saunders-Elsevier, 2006.

5 Wilk M, Schmoeckel C: Cutaneous focal mucinosis – a histopathological and immunohistochemical analysis of 11 cases. J Cutan Pathol 1994;21:446–452.

6 Lee WS, Lee JH, Oh DY, Seo JW, Rhie JW, Ahn ST: Cutaneous focal mucinosis arising from the chin. J Craniofac Surg 2010;21:1639–1641.

7 Jackson EM, English JC 3rd: Diffuse cutaneous mucinoses. Dermatol Clin 2002;20:493–501.

8 Nebrida ML, Tay YK: Cutaneous focal mucinosis: a case report. Pediatr Dermatol 2002;19:33–35.

9 Hernandez C, Fowler A, Gandhi MY: Multiple lesions of cutaneous focal mucinosis in a teenager. Skinmed 2007;6:301–303.

10 Ertam I, Karaca N, Ceylan C, Kazandi A, Alper S: Discrete papular dermal mucinosis with Hashimoto thyroiditis: a case report. Cutis 2011;87:143–145.

11 Rongioletti F, Amantea A, Balus L, Rebora A: Cutaneous focal mucinosis associated with reticular erythematous mucinosis and sclero-myxedema. J Am Acad Dermatol 1991;24:656–657.

12 Kempf W, von Stumberg B, Denisjuk N, Bode B, Rongioletti F: Trauma-induced cutaneous focal mucinosis of the mammary areola: an unusual presentation. Dermatopathology 2014;1:24–28.

13 Gareau DS: Feasibility of digitally stained multimodal confocal mosaics to simulate histopathology. J Biomed Opt 2009;14:034050.

14 Campo-Ruiz V, Patel D, Anderson RR, Delgado-Baeza E, González S: Evaluation of human knee meniscus biopsies with near infrared, reflectance confocal microscopy. A pilot study. Int J Exp Pathol 2005;86:297–307.

15 Ulrich M, Roewert-Huber J, González S, Rius-Diaz F, Stockfleth E, Kanitakis J: Peritumoral clefting in basal cell carcinoma: correlation of in vivo reflectance confocal microscopy and routine histology. J Cutan Pathol 2011;38:190–195.

Downloaded by:
189.26.213.20 - 6/2/2017 6:44:26 PM

5.5 ARTIGO ORIGINAL 4

Reflectance Confocal Microscopy Features of a Clonal Seborrheic Keratosis That Clinically and Dermoscopically Simulates Melanoma.

Naiara Abreu Fraga-Braghiroli, Miesha Merati, Harold Rabinovitz, Alon Scope.

Dermatology Surgery, 2015, 41(5): 662-665.

Situação- Artigo Publicado

O artigo demonstra a importância da microscopia confocal de reflectância como uma ferramenta diagnóstica de extrema utilidade na distinção de tumores equívocos de pele.

Os autores descrevem os achados confocais da ceratose seborréica clonal. Essa entidade apresenta características clínicas e dermatoscópicas similares ao melanoma maligno, como estruturas brancas brilhosas (crisálides) e véu branco-azulado.

Nesse estudo, a microscopia confocal evidenciou múltiplos agregados de células poligonais brilhosas ao nível da epiderme, correspondente a ninhos de queratinócitos basalóides pigmentados, associados a uma rede de favo de mel regular e alargamento dos espaços interpapilares na junção dermo-epidérmica. Não foram evidenciados quaisquer elementos sugestivos de malignidade.

Assim, a MCR revela aspectos morfológicos consistentes e constantes, com significativa correlação com os achados histopatológicos.

Routine prophylactic antibiotherapy cannot be advocated on such grounds. It is not harmless to the patients, can distress normal balance between pathogenic and nonpathogenic strains, and enhance selection of resistant strains.

Saying "we here present solid evidence that tissue filler gels do support the growth of bacteria into clusters (as biofilms) and that these might be the cause of most adverse events seen in patients with gel fillers" is not scientifically acceptable.

The authors prove that:

(1) When inoculating pus within tissues, it is possible to get an infection. That infection after tissue filler injections is possible. And that in vivo, the organism is capable of resisting a massive deliberate contamination.
(2) Closed infections are difficult to treat once developed. But, they know abscesses have to be drained and treated both locally and systemically.
(3) PAA is more prone to infections than other fillers.
(4) They should avoid injecting steroids within an infected area.
(5) In vitro results cannot necessarily be extrapolated, especially when contradicted by in vivo experiments.

Given all this, I feel reassured about fillers' safety, reinforcing that prophylaxis of infection is mandatory through strict aseptic injection technique but still confused about the aims of this nonobjective publication.

References

1. Alhede M, Er Ö, Eickhardt S, Kragh K, et al. Bacterial biofilm formation and treatment in soft tissue fillers. Pathog Dis 2014;70: 339–46.
2. Hil R. Injections of fillers for cosmetic treatment can open the door to bacteria. PRIME 2014;4. Available from: http://www.prime-journal.com/injections-of-fillers-for-cosmetic-treatment-can-open-the-door-to-bacteria/. Accessed on March 16, 2014.
3. Bjarnsholt T, Tolker-Nielsen T, Givskov M, Janssen M, et al. Detection of bacteria by fluorescence in situ hybridization in culture-negative soft tissue filler lesions. Dermatol Surg 2009;35: 1620–4.
4. Alijotas-Reig J, Miro-Mur F, Planells-Romeu I, Garcia-Aranda N, et al. Are bacterial growth and/or chemotaxis increased by filler injections? Implications for the pathogenesis and treatment of filler-related granulomas. Dermatology 2010;221:356–4.
5. Lemperle G, Nicolau PJ, Scheiermann N. Is there any evidence for biofilms in dermal fillers? Plast Reconstr Surg 2011;128:84e–85e.

PIERRE J. NICOLAU, MD
Past Consultant
Plastic Surgery and Burns Unit
Saint Louis University Hospital
Paris, France
Private Practice
Clinica Dr. Nicolau
Girona, Spain

The author has indicated no significant interest with commercial supporters.

Reflectance Confocal Microscopy Features of a Clonal Seborrheic Keratosis That Clinically and Dermoscopically Simulates Melanoma

Seborrheic keratosis (SK) is one of the most common benign skin neoplasms, typically appearing during the fourth decade of life. Of the histopathologic subtypes of SK, clonal SK is characterized by intraepidermal aggregates of pigmented basaloid keratinocytes (the Borst–Jadassohn phenomenon), which may also be associated with presence of melanocytes.[1]

The diagnosis of SK is straightforward in most cases; however, darkly pigmented SKs can be clinically challenging. Similarly, the common dermatoscopic features of SK, including comedo-like openings, milia-like cyst, sharp scalloped borders, and surface ridges and grooves, are readily recognized in most SKs.[1,2]

© 2015 by the American Society for Dermatologic Surgery, Inc. Published by Wolters Kluwer Health, Inc. Unauthorized reproduction of this article is prohibited.

Figure 1. Clonal SK, presenting clinically as an irregularly shaped black papule.

Reflectance confocal microscopy (RCM) is a diagnostic tool that uses an infrared laser technology for the diagnosis of skin lesions. The RCM criteria for SK include corneal cyst, cords with bulbous projections, polymorphous papillae, focally broadened honeycomb pattern, and keratin-filled invagination.[2] To the best of our knowledge, there is 1 previous publication describing the RCM features of clonal SK.[3]

Here, the authors describe a patient with a history of melanoma who presented with clonal SK with clinical and dermocospic features concerning with melanoma.

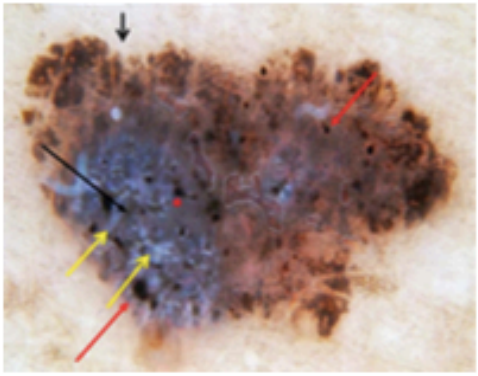

Figure 2. Clonal SK, dermoscopy. There are conflicting criteria: the scalloped and sharp border (short black arrow) and fissures (long black arrow) suggest the diagnosis of SK; however, the blue white veil (asterisk), black globules distributed throughout the lesion (red arrows), and crystalline structures (yellow arrows) are concerned with melanoma.

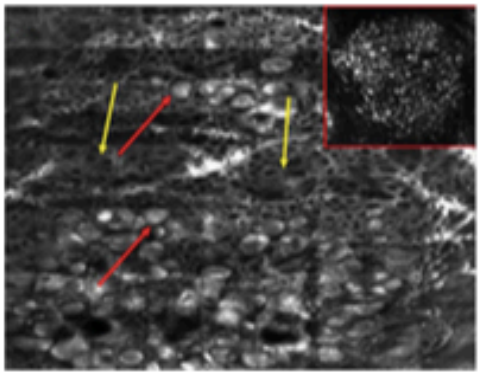

Figure 3. Clonal SK imaged with RCM at the level of the dermal-epidermal junction. Multiple bright clusters creating an overall clod pattern (red arrows); the ringed pattern enlarged interpapillary spaces (yellow arrows) separating edged papillae. A cluster of small, bright polygonal cell (compatible with pigmented keratinocytes) is highlighted (square).

An 82-year-old white man presented for a full body skin examination. He had recent history of melanoma in situ on plantar skin. On physical examination, a 7-mm black papule with irregular and sharp borders was noted on the right flank area (Figure 1). On dermatoscopic examination were appreciated a blue–white veil, multiple dark globules distributed throughout the lesion, sharp borders, fissures, and

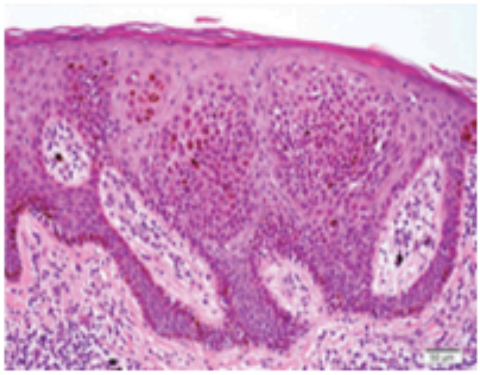

Figure 4. Clonal SK. A histopathology image (H&E, 20×) showing acanthotic epidermis with intraepidermal aggregates of pigmented keratinocytes.

© 2015 by the American Society for Dermatologic Surgery, Inc. Published by Wolters Kluwer Health, Inc. Unauthorized reproduction of this article is prohibited.

crystalline structures (Figure 2). The differential diagnosis included melanoma, pigmented basal cell carcinoma, SK, and collision of these neoplasms. On RCM imaging, the lesion displayed multiple clusters of bright cells' levels and enlarged interpapillary spaces at the basal epidermal (Figure 3); the overall RCM findings were in favor of a benign diagnosis, but the authors were not familiar with the pattern seen in this case and could not rule out that the bright aggregates were melanocytic in origin, raising the possibility of melanoma. Because of the concerning clinical and dermatoscopic features, the lack of conclusive RCM diagnosis, and the history of melanoma, an excisional biopsy with a 2-mm margin was performed. Histopathologic analysis showed an acanthotic epidermis with aggregates of pigmented basaloid keratinocytes within the epidermis, compatible with clonal SK (Figure 4).

Discussion

Longo and colleagues[3] described the dermatoscopic features of 9 clonal SKs; of which, 4 presented with a large, aggregated globular pattern simulating a melanocytic neoplasm and 5 showed smaller bluish globules loosely distributed in the lesion, resembling a basal cell carcinoma. Hirata and colleagues[4] described 2 cases of clonal SK that lacked the typical dermatoscopic features for SK; both cases had a globule-like pattern and no milia-like cyst or comedo-like openings. Conversely, Argenziano and colleagues[5] reported a melanoma in situ simulating SK on clinical and dermoscopic examinations.

The case described herein showed on dermatoscopy a blue–white veil, multiples dark globules distributed throughout the lesion, sharp borders, and crystalline structures. All of these findings are suggestive of melanoma, and although the lesion presented some features of SK, such as scalloped borders and fissures, the authors opted to biopsy the lesion to exclude melanoma by histopathologic examination. On retrospective dermatoscopic–pathologic correlation, the dark globules seen on dermoscopy correspond to aggregates of pigmented basaloid keratinocytes within the epidermis. The blue–white veil is likely due to densely pigmented keratinocytes in an acanthotic epidermis. The authors speculate that the crystalline structures are due to increased collagen in the superficial dermis because of trauma from excoriations.

Although our case had several dermoscopic features of melanoma, the overall RCM findings were in favor of a benign diagnosis. The most notable RCM features included multiple clusters of bright polygonal cells within the epidermis and enlarged interpapillary spaces at the dermal-epidermal junction level. Longo and colleagues recently described the RCM features of 3 cases of clonal SK; they found a regular epidermal pattern with keratin-filled invaginations. At the level of the basal layer of epidermis, there was an overall regular clod, which on closer inspection showed compact well-defined intraepidermal clusters of small, bright monomorphic polygonal cells, compatible with pigmented keratinocytes.[3] These RCM findings are similar to those seen in our case of clonal SK. Thus, RCM seems to show consistent features, which correlated well with the characteristic histopathologic findings in clonal SK.

Considering that case of clonal SKs with concerning dermoscopic features, RCM can assist in the correct diagnosis of this benign neoplasm. Studies with a larger number of cases will further outline the consistency of the RCM features of a clonal SK. Meanwhile, histolopathogic examination remains important in clonal SK cases suspicious for skin cancer.

References

1. Braun R, Rabinovitz H, Krischer J, Kreusch J, et al. Dermoscopy of pigmented seborrheic keratosis: a morphologic study. Arch Dermatol 2001;138:1556–60.

2. Ahlgrimm-Siess V, Cao T, Oliviero M, Lenrer M, et al. Seborrheic keratosis: reflectance confocal microscopy features and correlation with dermoscopy. J Am Acad Dermatol 2013;69:120–6.

3. Longo C, Zalaudek I, Moscarella, Lallas A, et al. Clonal seborrheic keratosis: dermoscopic and confocal microscopy characterization. J Eur Acad Dermatol Venereol 2013;28:1397–400.

4. Hirata H, Almeida F, Tomimori-Yamashita J, Enokihara MS, et al. "Globulelike" dermoscopic structures in pigmented seborrheic keratosis. Arch Dermatol 2004;140:128–9.

© 2015 by the American Society for Dermatologic Surgery, Inc. Published by Wolters Kluwer Health, Inc. Unauthorized reproduction of this article is prohibited.

5. Argenziano G, Rossiello L, Scalvenzi M, Staibano S, et al. Melanoma simulating seborrheic keratosis: a major dermoscopy pitfall. Arch Dermatol 2003;139:389–91.

Naiara Abreu Fraga-Braghiroli, MD
Miesha Merati, DO
Harold Rabinovitz, MD
Skin and Cancer Associations
Plantation, Florida

Alon Scope, MD
Department of Dermatology
Sheba Medical Center and Sackler Faculty of Medicine, Tel Aviv University
Tel-Aviv, Israel
Dermatology Service
Memorial Sloan-Kettering Cancer Center
New York, New York

H. Rabinovitz is an investigator in a study coordinated by Lucid Inc., manufacturer of a commercial confocal microscope. He has received funding for a fellowship program and equipment from Lucid Inc. He is also a consultant and has received equipment from 3-Gen, manufacturer of a polarized dermatoscope. The remaining authors have indicated no significant interest with commercial supporters.

© 2015 by the American Society for Dermatologic Surgery, Inc. Published by Wolters Kluwer Health, Inc. Unauthorized reproduction of this article is prohibited.

5.6 ARTIGO ORIGINAL 5

Accuracy of in vivo confocal microscopy for diagnosis of basal cell carcinoma: a comparative study between handheld and wide-probe confocal imaging.

R.P. Castro, A. Stephens, **N.A. Fraga-Braghiroli**, M.C. Oliviero, G.G. Rezze, H. Rabinovitz, A. Scope.

Journal of the European Academy of Dermatology and Venereology 2015, 29, 1164–1169

Situação- Artigo Publicado

O artigo teve como objetivo avaliar a sensibilidade e especificidade do tipo de equipamento *handheld* de Microscopia Confocal de Reflectância (HH-RCM) comparado com a MCR de sonda larga no diagnóstico do carcinoma basocelular (CBC).

A presença de ao menos 3 critérios para o CBC foi o limite estabelecido, sendo ao menos 1 deles representado pelas silhuetas escuras ou ilhas tumorais.

A MCR tradicional mostrou uma sensibilidade de 100% e especificidade de 78% no diagnóstico do CBC. O HH-RCM mostrou uma sensibilidade de 93% e especificidade de 78%. A presença de ilhas tumorais ou silhuetas escuras estavam presentes em todos os casos.

DOI: 10.1111/jdv.12780 JEADV

ORIGINAL ARTICLE

Accuracy of *in vivo* confocal microscopy for diagnosis of basal cell carcinoma: a comparative study between handheld and wide-probe confocal imaging

R.P. Castro,[1,*] A. Stephens,[2] N.A. Fraga-Braghiroli,[2] M.C. Oliviero,[2] G.G. Rezze,[1] H. Rabinovitz,[2] A. Scope[3,4]

[1]Department of Cutaneous Oncology, A.C. Camargo Cancer Center, São Paulo, SP, Brazil
[2]Skin and Cancer Associations, Plantation, FL, USA
[3]Dermatology Department, Sheba Medical Center and Sackler Faculty of Medicine, Tel Aviv University, Tel-Aviv, Israel
[4]Dermatology Service, Memorial Sloan Kettering Cancer Center, New York, NY, USA
*Correspondence: R. Castro. E-mail: rproastro@yahoo.com.br

Abstract

Background Reflectance confocal microscopy (RCM) increases specificity of identification of basal cell carcinoma (BCC). A smaller-diameter handheld RCM (HH-RCM) allows better access to limited anatomic locations.

Objective To compare accuracy of HH-RCM in identification of BCC to that of traditional wide-probe RCM (TWP-RCM).

Methods Patients presenting at least one lesion clinically and dermoscopically suspicious for BCC, were recruited from two dermatology skin cancer clinics. Prior to excision, we attempted to image all lesions with HH-RCM and TWP-RCM using a standardized protocol. RCM images were retrospectively evaluated, jointly by two blinded readers. For purposes of comparative RCM, sensitivity and specificity analysis, we used a threshold of ≥3 RCM criteria to identify BCC, whereby at least one criterion had to be presence of 'dark silhouettes' or 'bright tumor islands'.

Results Among 54 lesions imaged with both RCM devices, 45 were biopsy-proven BCCs. Comparison between TWP-RCM vs. HH-RCM was as follows: sensitivity (100% vs. 93%), specificity (78% for both probes), positive predictive value (96% vs. 95%), and negative predictive value (100% vs. 70%) respectively. Notably, both TWP-RCM and HH-RCM demonstrated the presence of 'dark silhouettes' or 'bright tumor islands' in all 45 BCCs.

Conclusion Both RCM probes demonstrate high PPV. TWP-RCM shows higher NPV, since its broader field-of-view probably allows more exhaustive search for BCC criteria. The RCM criteria threshold for BCC identification should be further tested.

Received: 17 May 2014; Accepted: 19 September 2014

Conflicts of interest

Dr Rabinovitz is an investigator in a study coordinated by Lucid Inc., manufacturer of a commercial confocal microscope. He has received funding for a fellowship programme and equipment from Lucid Inc. He is also a consultant and has received equipment from 3-Gen, manufacturer of a polarized dermatoscope. MC Oliviero is a consultant, speaker for Caliber ID, 3Gen LLC, Canfield and MelaSciences. The other authors have no conflicts of interest to declare.

Funding sources

None declared.

Introduction

Basal cell carcinoma (BCC) has become a major public health problem.[1] Patients who develop BCC often have severely sun-damaged skin which also presents multiple pigmented and pink benign neoplasms that can mimic BCC (e.g. seborrhoeic keratoses and intradermal nevi). A non-invasive imaging tool that increases specificity of identification of BCC can greatly aid the clinician in avoiding unnecessary removal of benign lesions.

To this end, reflectance confocal microscopy (RCM) is a high-resolution optical imaging tool that allows *in vivo*, non-invasive evaluation of skin lesions. The RCM features of BCC have been described and shown to be well correlated with the histopathological diagnostic criteria of BCC.[2–5] Previous studies have demonstrated the utility of RCM in the identification of BCC [6–8] and in differentiation from other pigmented and pink neoplasms.[9] Notably, these RCM studies have all been

 © 2014 European Academy of Dermatology and Venereology

used a threshold of ≥3 RCM criteria to identify BCC, whereby at least one of the criteria had to be the presence of 'dark silhouettes' or 'bright tumor islands'; these latter criteria denote the presence of neoplastic aggregates of BCC and hence need to be observed in all cases identified as BCC by RCM. The accuracy of this non-invasive method to identify BCC was later compared to the histopathologic diagnosis, which was used as the gold standard for diagnosis.

Statistical analysis was applied to compare TWP-RCM and HH-RCM imaging for lesions examined by both devices. Fisher's exact test was used to compare the frequency of identification of RCM criteria of BCC and also the number of cases displaying ≥3 RCM criteria. The paired *t*-test was used to compare the total number of criteria observed in each lesion, resulting in the mean number of criteria and standard deviation (SD) for each RCM probe. A *P* value less than 0.05 was considered significant. Statistical evaluation was carried out using a software (GraphPad Prism, GraphPad Software Inc., Jolla, CA, USA).

Results

Imaging with both TWP-RCM and HH-RCM was attempted in 92 lesions from 73 patients; however, 38 of the lesions (41%), mostly facial, were accessible only to HH-RCM imaging. Among 54 lesions imaged with both RCM devices, there were 45 biopsy-proven BCCs. These 45 biopsy-proven BCCs were found in 32 patients (63% males), whose average age was 65 years (range: 30–89 years); 24 (75%) of the patients had skin phototype II and 8 (25%) skin phototype III. The anatomic distribution of these 45 BCCs was head and neck – 9 (20%), torso – 26 (58%), upper extremities – 4 (9%) and lower extremities – 6 (13%).

Of the 54 lesions that could be imaged by both devices, TWP-RCM revealed 47 lesions with ≥3 RCM criteria of BCC, including the presence of 'dark silhouettes' or 'bright tumor islands' in all 47 cases; 45 (96%) of the 47 were biopsy-proven BCC, while the other two were lichen planus-like keratosis (LPLK) and amelanotic melanoma. Seven of the 54 lesions examined by TWP-RCM showed ≤2 RCM features and none of these 7 lesions showed 'dark silhouettes' or 'bright tumor islands'; none of the 7 lesions proved to be BCC on histopathology. The TWP-RCM sensitivity, specificity, positive predictive value (PPV) and negative predictive value (NPV) were 100%, 78%, 96% and 100%, respectively.

Of these same 54 lesions imaged with both RCM devices, HH-RCM revealed 44 lesions with ≥3 RCM criteria, including the presence of 'dark silhouettes' or 'bright tumor islands' in all 44 cases; 42 (95%) of 44 lesions were biopsy-proven BCCs and 2 (5%) were the LPLK and amelanotic melanoma that were also falsely identified as BCC with the TWP-RCM. Ten lesions had ≤2 RCM features; these included 3 (30%) biopsy-proven BCC, all of which showed 'dark silhouettes' and 7 (70%) non-BCC, none of which showed 'dark silhouettes' or 'bright tumor islands'. The sensitivity, specificity, PPV and NPV for this subgroup were 93%, 78%, 95% and 70%, respectively.

Table 1 RCM features observed in BCCs (n = 45) with TWP-RCM vs. HH-RCM

Features	TWP-RCM	HH-RCM	Comparison *P*-value
Dark silhouettes	21 (47%)	25 (56%)	0.52
Bright tumor islands	39 (87%)	37 (82%)	0.77
Streaming	16 (36%)	2 (4%)	0.0004
Peripheral palisading	15 (33%)	8 (18%)	0.15
Peritumoral clefts	37 (82%)	34 (76%)	0.61
Thickened collagen bundles	43 (96%)	42 (93%)	1.00
Linear blood vessels	43 (96%)	17 (38%)	<0.0001
Coiled blood vessels	3 (7%)	1 (2%)	0.62
Bright dendritic structures	20 (44%)	14 (31%)	0.28
Bright round cells	40 (89%)	30 (67%)	0.02
Mean number of RCM features	6.2	4.7	<0.0001
Presence of ≥3 RCM criteria of BCC*	45 (100%)	42 (93%)	0.24
Lesions not reaching threshold for RCM identification of BCC†	0 (0%)	3 (7%)	0.24

*At least one of criterion is the presence of 'dark silhouettes' or 'bright tumor islands'.

†≤2 RCM criteria of BCC, or absence of 'dark silhouettes'\'bright tumor islands'.

BCC, basal cell carcinoma; HH-RCM, handheld RCM; RCM, reflectance confocal microscopy; TWP-RCM, traditional wide-probe RCM.

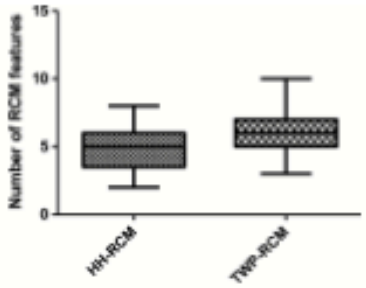

Figure 1 Comparison of RCM criteria of BCC for TWP vs. HH-RCM among 45 biopsy-proven BCCs imaged with both RCMs.

The frequency of each RCM criterion of BCC by imaging device (TWP-RCM vs. HH-RCM) is shown for the 45 biopsy-proven BCCs imaged with both RCMs (Table 1). Among the BCCs, the mean number of RCM criteria was higher for TWP-RCM than HH-RCM (6.2 ± 1.6 vs. 4.7 ± 1.6, $P<0.0001$) (Fig. 1). When comparing the frequency of observation of each RCM criterion among these 45 BCCs, a significant difference

© 2014 European Academy of Dermatology and Venereology

performed with the traditional wide-probe RCM (TWP-RCM, Vivascope 1500; CaliberID, Rochester, NY, USA). With the TWP-RCM, large images up to 8 × 8 mm can be acquired, akin to 3× lower magnification microscopy, allowing assessment of the entire lesion; these large mosaic images can also be correlated with the dermoscopic image that is taken with the RCM's built-in dermoscopic camera. However, the TWP-RCM is bulky and provides limited access to curved surfaces, such as the nose, ear and peri-orbital regions where BCC frequently arises. Recently, a handheld-RCM probe (HH-RCM, Vivascope 3000; CaliberID) has been introduced to clinical practice.[10] The HH-RCM has a smaller probe and is more accessible for application to the curved facial surfaces. Yet, HH-RCM offers a more limited field-of-view, up to 1 × 1 mm, and lacks a built-in dermoscopic camera; thus, accuracy of identification of BCC using HH-RCM needs to be proven and compared with that of TWP-RCM.

To this end, the aim of the study is to compare the accuracy of HH-RCM in identification of BCC to that of TWP-RCM.

Methods

The study protocol was approved by the Institutional Review Board of AC Camargo Cancer Center, São Paulo, Brazil. Patients included in the study were recruited from the population of women and men who underwent skin cancer screening at the outpatient dermatology clinic at a tertiary cancer center in São Paulo, Brazil and at a private practice that specializes in skin cancer treatment in South Florida, USA. Patients recruited were those presenting with one or more skin lesions that were deemed suspicious for BCC based on clinical and dermoscopic examination. Informed consent was obtained from each study participant.

Imaging protocol

All examinations, including clinical, dermoscopic and RCM imaging, were made by a dermatologist experienced with RCM examination (RPRC) with supervision by a skin cancer expert (GGR or HR). We attempted to image all lesions with HH-RCM and TWP-RCM using a standardized protocol. However, TWP-RCM imaging is restricted to anatomic locations that allow contact with the RCM fixating tissue ring; in some anatomic locations such as the eyelids, imaging with TWP-RCM is not feasible.

Handheld reflectance confocal microscopy imaging was performed with commercially-available *in vivo* RCM system (Vivascope3000; CaliberID) as previously described.[10] In brief, the HH-RCM uses 830 nm laser and is characterized by horizontal resolution of 1.25 μm, vertical resolution of 5 μm, and maximal imaging depth of about 250 μm which corresponds to the superficial reticular dermis. A drop of immersion oil (Crodamol STS; Croda Inc., Edison, NJ, USA) is applied to skin to match the refractive index of the RCM lens with the stratum corneum allowing penetration and focus of light. The images captured by HH-RCM are single 1 × 1 mm frames. An automated stack of sequential images can be obtained in the Z-axis, but movement in the horizontal X-Y plane depends on manually sliding the RCM probe on the skin surface.

TWP-RCM imaging was performed with a commercially available *in vivo* RCM system (Vivascope1500; CaliberID) as previously described.[11] Briefly, an adaptor metal ring is centred on the lesion and used to attach the TWP-RCM imaging probe to the skin. The images captured by TWP-RCM are single 500 × 500 μm frames. Individual RCM images can be sequentially collected in the horizontal X–Y plane using an automated stepper and stitched together by a dedicated software to create a mosaic image with a field-of-view of up to 8 × 8 mm ('Viva-block' image). An automated stack of sequential images can be obtained along the Z-axis.

A standardized RCM image acquisition protocol was followed:

- 4 × 4 mm mosaic images (acquired only with TWP-RCM) were obtained at three different anatomic depths, corresponding to stratum spinosum, dermal-epidermal junction (DEJ) and superficial dermis;
- Stacks of images (acquired using both HH-RCM and TWP-RCM) were obtained at 5 μm increments from the stratum corneum to a maximum depth of about 250 μm. The number of stacks varied between cases (mean 3.06, SD ± 1.83, range 1–12);
- Individual images (acquired using both HH-RCM and TWP-RCM) were captured when encountering appropriate RCM features for the identification of BCC; video files were also recorded when observing vascular patterns pertinent for the identification of BCC.

All lesions included were biopsy-proven. Excised specimens were routinely fixed in formalin, embedded in paraffin and stained with hematoxylin and eosin. Histopathological diagnosis was issued by a dermatopathologist who was blinded to RCM analysis.

Image evaluation and statistical analysis

All RCM images were evaluated jointly by two readers blinded to the results of the histopathological examination. Images were evaluated for the presence of previously-published RCM criteria for identification of BCC,[2,6,7] including: the presence of neoplastic aggregates, seen as 'dark silhouettes' or as 'bright tumor islands' at the level of the DEJ or upper dermis; 'streaming' polarization of nuclei in neoplastic aggregates along the same axis of orientation; 'peripheral palisading' of nuclei at the tumor islands' periphery; dark 'peritumoral clefts' around the tumor islands; fibrotic stroma with 'thickened collagen bundles'; dilated and tortuous 'linear blood vessels' and 'coiled blood vessels'; 'bright dendritic structures' within tumor islands; and 'bright round cells' in the stroma.

Since none of the RCM criteria is exclusively seen in BCC and for the purpose of exploring RCM sensitivity and specificity, we

© 2014 European Academy of Dermatology and Venereology

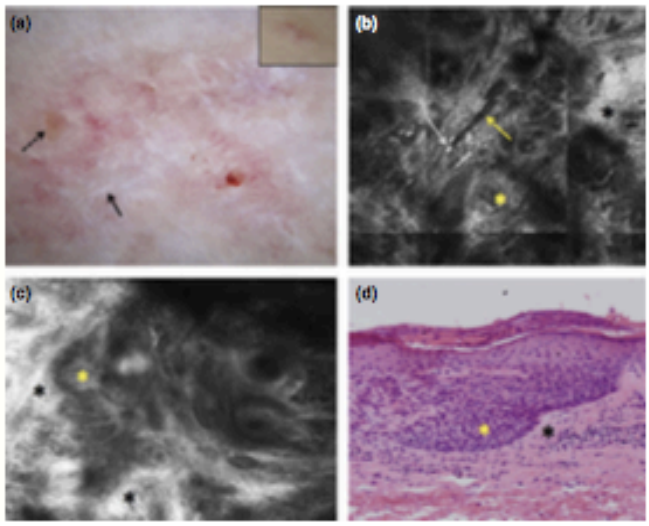

Figure 2 Dermoscopic image (a) showing pink-white shiny areas, small ulceration (dashed arrow), chrysalis (arrow) and short serpentine vessels. Both TWP-RCM (b, 1 × 1 mm) and HH-RCM (c, 0.5 × 0.5 mm) images at the superficial dermis level show bright tumor islands (yellow asterisk) and fibrotic stroma (black asterisk); however, only the TWP-RCM image (b) shows linear blood vessels (yellow arrow) and bright round cells (white arrow). Histopathology image (d, H&E, 20×), showing a neoplastic aggregate at the undersurface of the epidermis with peripheral palisading of crowded nuclei (yellow asterisk), the surrounding dermis displaying fibroplasia (black asterisk), and criteria diagnostic of BCC.

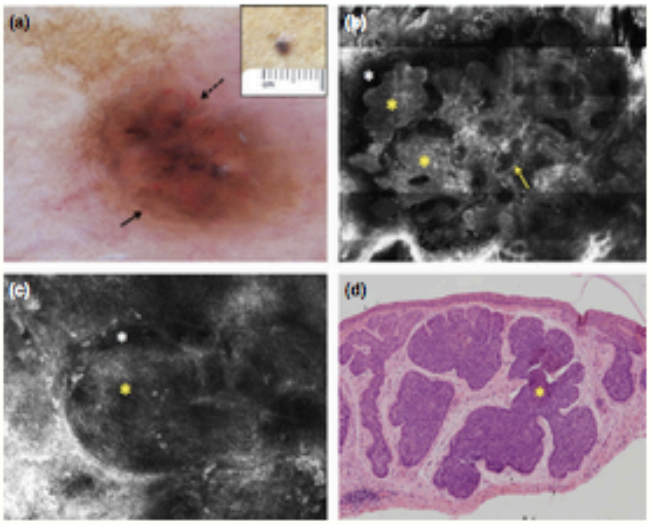

Figure 3 Dermoscopic image (a) showing brown-grey clods (arrow) and dots, pink-white shiny areas, looped vessels (dashed arrow) and peripheral network. TWP-RCM image (b) at the superficial dermis level (2.5 × 2.5 mm) shows aggregates of bright tumor islands (yellow asterisk), studded by bright round cells and surrounded by dark peritumoral cleft (white asterisk), which separate the aggregates from a fibrotic stroma. Looped vessels can also be seen (arrow). HH-RCM image (c) at level of the superficial dermis (0.5 × 0.5mm) shows a single bright tumor island (yellow asterisk), with few bright round cells, surrounded by a dark peritumoral cleft (white asterisk), which separate the aggregate from a fibrotic stroma. Histopathology image (d, H&E, 4X), shows a strikingly similar pattern to that seen with TWP-RCM, with basaloid neoplastic aggregates (yellow asterisk) with peripheral palisading of nuclei, which are separated from the surrounding fibroplastic dermis by a cleft, criteria diagnostic of BCC.

© 2014 European Academy of Dermatology and Venereology

was found for the presence of 'linear blood vessels', 'streaming' and 'bright round cells', all of which were identified with a higher frequency by TWP-RCM than HH-RCM: 96% vs. 38% ($P < 0.0001$), 36% vs. 4% ($P = 0.0004$), and 89% vs. 67% ($P = 0.02$), respectively (Figure 2).

Discussion

Previous studies have shown the clinical diagnostic accuracy of experienced dermatologists to be around 70%.[7] In our study, only 83% of clinically-suspect lesions proved to be BCC on histopathology, reflecting a PPV of 83%. Using a threshold of ≥3 RCM criteria for identification of BCC, PPV values were similarly high for both TWP-RCM (96%) and HH-RCM (95%). In other words, when RCM-based diagnosis of BCC is rendered, it is likely to be correct. However, the two RCM modalities differed in NPV values – 100% for TWP-RCM compared with 70% for HH-RCM. This means that, using the criteria for BCC identification that were employed herein, BCC can be virtually excluded using TWP-RCM, but not with HH-RCM. This difference is likely due to the more exhaustive scanning of the lesion, up to 8 × 8 mm field-of-view which is possible with TWP-RCM, compared to a much narrower field-of-view of up to 1 × 1 mm with HH-RCM (Fig. 3). The larger field of investigation afforded to the RCM reader by TWP-RCM probably makes the detection of 'linear blood vessels', 'streaming' and 'bright round cells' more likely than with the narrow field of view of HH-RCM, and may account for the observed difference in NPV. Notably, in *post hoc* analysis, diagnostic accuracy values of HH-RCM in our study could have been higher, if we had used a lower threshold for identification of BCC, namely ≥2 RCM criteria to identify BCC, with at least one of the criteria being the presence of 'dark silhouettes' or 'bright tumor islands'. Further study of the criteria threshold for RCM identification of BCC is needed.

The diagnostic accuracy of RCM in our study is in line with previous reports. Nori *et al.*[6] examined 83 BCCs with TWP-RCM and analysed 5 RCM features: presence of elongated monomorphic basaloid nuclei, polarization of nuclei, prominent inflammatory infiltrate, increased vasculature, and pleomorphism of the overlying epidermis indicative of actinic damage; presence of ≥2 RCM features had 100% sensitivity for BCC diagnosis, while ≥4 RCM features had specificity of 95.7% and sensitivity of 82.9%.[6] Polarization of nuclei was the most sensitive and specific RCM feature in the study by Nori *et al.*,[6] while in our study, polarization of nuclei ('streaming') was relatively infrequent, seen in 36% of BCCs with TWP-RCM and in only 4% of BCCs with HH-RCM. More recently, Gareau *et al.*[8] reported an overall sensitivity of 96.6% and specificity of 89.2% for detecting BCC *ex vivo* in Mohs excision specimens with RCM.[8] Guitera *et al.*[7] found 100% sensitivity and 88.5% specificity for BCC identification with RCM using the following criteria: polarized elongated features ('streaming'), telangiectasia and convoluted vessels, basaloid nodules (denoting the presence neoplastic aggregates) and epidermal shadowing (corresponding to 'peritumoral clefting').

Handheld RCM was more readily applicable to curved and narrow anatomic locations, frequently encountered when imaging facial lesions. Due to difference in accessibility in this anatomic region, HH-RCM imaging was successfully performed in all lesions in which imaging was attempted, while TWP-RCM was technically applicable in only 59% of lesions in which imaging was attempted. Interestingly, two facial lesions were inaccessible to contact dermoscopic imaging, but could be imaged with HH-RCM.

Our study has limitation. First, images were not independently reviewed by different dermatologists and thus we did not analyse for potential differences between observers. We plan to test inter-observer agreement on identification of RCM features of BCC with HH-RCM in a future study. Second, our dataset is relatively limited in size and originates from only two medical centres, and our findings need to be substantiated in larger datasets and generalized to more populations. Finally, additional RCM studies are needed to test the utility of each RCM criterion for identification of BCC.

In conclusion, HH-RCM is more frequently applicable to the curved facial area than TWP-RCM. Both TWP-RCM and HH-RCM demonstrate high PPV which enhances clinical diagnosis. TWP-RCM shows higher NPV than HH-RCM, probably due to a broader field-of-view of TWP-RCM which offers a more exhaustive tissue investigation for BCC criteria. The individual utility of each RCM criterion and the optimal combination of RCM criteria for BCC identification should be further tested.

Acknowledgements

We thank Prof. George W. Elgart, MD for his generous help in analysing histopathology images.

References

1 Wu S, Han J, Li WQ, Li T, Qureshi AA. Basal-cell carcinoma incidence and associated risk factors in U.S. women and men. *Am J Epidemiol* 2013; **178**: 890–897.

2 Agero AL, Busam KJ, Benvenuto-Andrade C *et al.* Reflectance confocal microscopy of pigmented basal cell carcinoma. *J Am Acad Dermatol* 2006; **54**: 638–643.

3 Segura S, Puig S, Carrera C, Palou J, Malvehy J. Dendritic cells in pigmented basal cell carcinoma: a relevant finding by reflectance-mode confocal microscopy. *Arch Dermatol* 2007; **143**: 883–886.

4 Ulrich M, Roewert-Huber J, Gonzalez S, Rius-Diaz F, Stockfleth E, Kanitakis J. Peritumoral clefting in basal cell carcinoma: correlation of in vivo reflectance confocal microscopy and routine histology. *J Cutan Pathol* 2011; **38**: 190–195.

5 González S, Tannous Z. Real-time in vivo confocal reflectance confocal microscopy of basal cell carcinoma. *J Am Acad Dermatol* 2002; **47**: 869–874.

6 Nori S, Rius-Diaz F, Cuevas J *et al.* Sensitivity and specificity of reflectance-mode confocal microscopy for in vivo diagnosis of basal cell carcinoma: a multicenter study. *J Am Acad Dermatol* 2004; **51**: 923–930.

7 Guitera P, Menzies SW, Longo C, Cesinaro AM, Scolyer RA, Pellacani G. In vivo confocal microscopy for diagnosis of melanoma and basal cell

© 2014 European Academy of Dermatology and Venereology

carcinoma using a two-step method: analysis of 710 consecutive clinically equivocal cases. *J Invest Dermatol* 2012; **132**: 2386–2394.
8 Gareau DS, Karen JK, Dusza SW, Tudisco M, Nehal KS, Rajadhyaksha M. Sensitivity and specificity for detecting basal cell carcinomas in Mohs excisions with confocal fluorescence mosaicing microscopy. *J Biomed Opt* 2009; **14**: 034012.
9 Braga JC, Scope A, Klaz I *et al.* The significance of reflectance confocal microscopy in the assessment of solitary pink skin lesions. *J Am Acad Dermatol* 2009; **61**: 230–241.
10 Fraga-Braghiroli NA, Stephens A, Grossman D, Rabinovitz H, Castro RP, Scope A. Use of handheld reflectance confocal microscopy for in vivo diagnosis of solitary facial papules: a case series. *J Eur Acad Dermatol Venereol* 2014; **28**: 933–942.
11 Rajadhyaksha M, Gonzalez S, Zavislan JM *et al.* In vivo confocal scanning laser microscopy of human skin II: advances in instrumentation and comparison with histology. *J Invest Dermatol* 1999; **113**: 293–303.

© 2014 European Academy of Dermatology and Venereology

6. DISCUSSÃO

6.1 TECNOLOGIA DA MICROSCOPIA CONFOCAL DE REFLECTÂNCIA

Desde seu advento em 1995, a microscopia confocal de reflectância vem sendo cada vez mais utilizada na prática dermatológica nos principais centros acadêmicos do mundo. Com o aprimoramento tecnológico na funcionalidade e dimensões das sondas, e subsequente disponibilização de equipamentos mais compactos, como o Vivascope 1500 (no ano 2000), e o Vivascope 3000 (em 2006), seu uso vem, progressivamente, revolucionando a abordagem médica das neoplasias cutâneas. Esta nova metodologia diagnóstica apresenta inúmeras vantagens. Dentre elas, permite a identificação instantânea das estruturas da pele de forma não invasiva, *in-vivo* e sem dano tecidual.

O modelo Vivascope 1500 utiliza a tecnologia de laser diodo infra vermelho (830 nm), com uma lente objetiva de x30, com uma resolução lateral de aproximadamente 1 micrômetro e uma resolução axial de 3 a 5 micrômetros. Ele atinge uma profundidade de cerca de 200-250 micrômetros, permitindo a visualização da derme papilar; em áreas com a epiderme mais delgada, como a face e mucosas, é possível analisar a derme reticular superficial.

A obtenção das imagens envolve o contato direto das lentes com a pele, que é previamente coberta com um óleo de imersão. No modelo de sonda larga, um anel de fixação é colocado sobre a lesão a ser estudada, entre a pele e as lentes. O processo de mapeamento criado pela MCR fornece uma imagem óptica de 0.5 X 0.5 mm^2 no ponto de interesse para exame da pele. A MCR escaneia a pele no sentido horizontal, produzindo múltiplas imagens individuais de 0.5 X 0.5 mm^2, que são subsequentes alinhadas formando um mosaico de até 8 x 8 mm^2. A profundidade precisa é controlada pelo software de navegação; a profundidade é selecionada pelo examinador, até a profundidade máxima de 250 micrômetros. O sistema de navegação da imagem da microscopia confocal é guiado pela imagem dermatoscópica da lesão, obtida após a colocação do anel de fixação e antes do acoplamento da lente, permitindo uma avaliação sistemática e orientada dentro do

tecido. Assim, focos suspeitos dentro da imagem dermatoscópica podem ser analisadas na imagem confocal correspondente em maior aumento.

O Vivascope 3000, é um modelo com uma pistola de fácil mobilização. A vantagem deste modelo é a sua sonda pequena, permitindo o acesso a áreas de difícil acesso com o Vivascope 1500. O processo de obtenção das imagens é mais rápido com o Vivascope 3000; porém, este apresenta como desvantagem o pequeno campo de captura de imagens de 1 X 1 mm^2, formando imagens empilhadas (sentido vertical), sem a possibilidade de visualização da arquitetura total de lesões maiores de 1 mm, não sendo possível a formação das imagens em mosaico no sentido horizontal.

6.2 CORRELAÇÃO ENTRE A HISTOLOGIA DA PELE NORMAL E OS ASPECTOS OBSERVADOS NA MICROSCOPIA CONFOCAL DE REFLECTÂNCIA

A identificação das estruturas na microscopia confocal se baseia na diferença de refração da luz das diferentes estruturas da pele, fornecendo uma imagem em preto e branco com variações de brilho.

Em 2015, descrevemos as características da pele normal visualizadas através das lentes da confocal (QUE et al., 2015).

As estruturas com alto índice de refração aparecem brilhosas e brancas, enquanto estruturas não reflectivas aparecem pretas. A melanina é a estrutura com maior contraste, com um índice de refração de 1,7, permitindo o reconhecimento de células individuais ricas em melanina, como melanócitos, ceratinócitos pigmentados e melanófagos. A queratina apresenta um índice de refração de 1,5, permitindo a visualização de neoplasias ceratinocíticas. Fibras de colágeno e células inflamatórias, como os neutrófilos, com índice de refração de 1,34, também aparecem brilhosas nas imagens da MCR. As fibras de colágeno se apresentam como estruturas em faixas lineares brilhosas na derme, e as células inflamatórias como pequenas estruturas brancas arredondadas e homogêneas. As células inflamatórias, apesar de possuírem um índice de refração menor do que a melanina,

ainda se apresentam como partículas brilhosas à MCR. Contudo, a maioria das doenças inflamatórias da pele até então estudadas utilizando a MCR foram lesões ricas em linfócitos, e os critérios para diferenciação entre linfócitos e neutrófilos não foram estabelecidos. (DEBARBIEUX et al, 2013). Gonzalez et al. (1999) demonstraram a presença de pequenas células brilhosas no *stratum corneum* e ao redor dos folículos pilosos, na avaliação da MCR em um paciente com foliculite, e correlacionou este achado com a presença de neutrófilos nas sessões histológicas convencionais.

A primeira camada da pele a ser avaliada é o *stratum corneum;* neste nível são visualizadas células anucleadas achatadas que se agregam formando ilhas separadas por fissuras escuras que representam os dermatoglifos. Essas células correspondem aos corneócitos anucleados que se destacam na microscopia confocal devido ao seu alto conteúdo de queratina. Logo abaixo, a cerca de 15 a 20 μm de profundidade, se encontra a camada granulosa. A este nível se encontram os ceratinócitos achatados, com grânulos internos, caracterizados na microscopia confocal por um núcleo central escuro circundado por um contorno brilhoso do citoplasma, devido aos grânulos de queratina aí localizados. A disposição dos ceratinócitos adjacentes uns aos outros nesta camada da pele forma um padrão conhecido como “favo de mel” típico ou regular. A camada espinhosa está localizada entre 20 a 100 μm de profundidade, e apresenta morfologia semelhante à da camada granular na MCR, com o padrão em favo de mel regular/típico, porém com ceratinócitos menores. A camada basal está localizada entre 40 e 130 μm de profundidade, e sua aparência à MCR varia de acordo com o fototipo de pele. Peles de fototipo III-IV apresentam o padrão em “pedras de calçamento” (*cobblestone*), formado por conjunto de ceratinócitos brancos brilhosos devido ao alto conteúdo de melanina supranuclear, dando um aspecto de alta iluminação ao redor do núcleo, em contraste com o restante do citoplasma que se apresenta relativamente mais escuro. Os ceratinócitos basais na pele fototipo I-II são menos pigmentados, e essas células não se apresentam tão brilhosas na microscopia confocal, sendo difícil visualizar os ceratinócitos basais em indivíduos de pele clara. Da mesma forma, os melanócitos na junção dermo-epidérmica (JDE) não são usualmente identificados em pele normal de indivíduos de pele clara não bronzeados. A imagem horizontal da

JDE é caracterizada por ceratinócitos basais brilhantes circundando as papilas dérmicas escuras, criando um padrão na MCR de anéis papilares dérmicos ou papilas demarcadas. A derme papilar e reticular superficial apresentam-se com baixa reflectividade e pode apresentar vasos sanguíneos e fibras de colágeno. A aparência na MCR da pele normal pode apresentar variações adicionais dependendo do local do corpo e da extensão do dano cutâneo devido a exposição solar crônica.

6.3 APLICABILIDADE DA MICROSCOPIA CONFOCAL DE REFLECTÂNCIA NO DIAGNÓSICOS DE LESÕES CUTÂNEAS EQUÍVOCAS E MONITORAMENTO PÓS TRATAMENTO

A MCR pode ser usada como ferramenta diagnóstica adjunta em lesões cutâneas que se apresentam equívocas ao exame clínico e na avaliação dermatoscópica, elevando a precisão na seleção das lesões que efetivamente tem indicação de biópsia, especialmente em áreas de difícil acesso cirúrgico, funcionalmente complexas e/ou cosmeticamente sensíveis (QUE et al., 2015). Cinotti et al. (2014) avaliaram o uso da MCR em 47 casos de lesões palpebrais, incluindo CBC, CEC e melanomas; o exame mostrou uma sensibilidade de 100% e especificidade de aproximadamente 70%. Derbabieux et al. (2014) analisaram 56 casos de máculas melanóticas labiais, sendo 10 deles melanomas macular. Eles corroboraram os achados previamente descritos por Erfan et al. (2012) de que a presença de células dendríticas esparsas na junção dermo-epidérmica é um achado comum em máculas melanóticas benignas em áreas fotoexpostas, sendo que a alta densidade dessas células, e/ou a presença de células arredondadas pagetóides, são achados associados ao melanoma de mucosa.

A MCR tem valioso papel adjunto na definição de margens cirúrgicas durante a cirurgia micrográfica de Mohs. Estudos evidenciaram uma sensibilidade de 86% à 96% e especificidade de 89 à 99% na identificação do carcinoma basocelular durante a cirurgia de Mohs. (GAREAU et al., 2009, BEN ASSAR et al., 2014).

Outra importante indicação da microscopia confocal é no monitoramento da resposta ao tratamento não cirúrgico das ceratoses actinícas, CEC, CBC e

melanoma em área foto-exposta. (CURIEL-LEWANDROWSKI et al., 2004; ULRICH et al., 2010; TORRES et al., 2004; NADIMINTI et al., 2010; AHLGRIMM-SIESS et al., 2009).

Em 2015, descrevemos aspectos característicos da ceratose seborréica clonal (CSC) vistos na MCR (FRAGA-BRAGHIROLI et al., 2015). Devido a alta pigmentação dessa neoplasia benigna da pele, seu diagnóstico clínico é muitas vezes desafiador, e seus achados dermatoscópicos se sobrepõem com os do melanoma maligno, como a presença do véu branco-azulado, múltiplos glóbulos escuros e estruturas brancas com brilho (antigamente descritas como crisálides). Clinicamente, a CSC faz diagnóstico diferencial com o melanoma, CBC pigmentado e tumores de colisão. A avaliação com a MCR demonstrou múltiplas células brilhosas poligonais agregadas na epiderme e alargamento dos espaços interpapilares na JDE. Não se observou achados sugestivo de malignidade, como presença de células dendríticas ou células arredondadas com padrão pagetóide. Os autores optaram por realizar uma biópsia excisional devido a história familiar de melanoma do paciente e pelos achados dermatoscópicos demasiadamente preocupantes. Os achados da MCR aqui descritos são similares aqueles apresentados por Longo et al. (2013) quando descreveram a MCR de 3 casos de CSC. Assim, a MCR demonstra achados da CSC consistentes, que se correlacionam com suas características histológicas. As células poligonais brilhosas agregadas correspondem aos agregados intraepidérmicos de ceratinócitos basais ricos pigmentados, conhecido como fenômeno de Borst-Jadassohn. Critérios adicionais para ceratose seborréica que também estão presentes na SSC são cistos córneos, invaginações ricas em ceratinas e áreas focais com padrão de favo de mel alargado na camada epidérmica, associados a cordões com projeções bulbosas e papilas polimorfas na JDE.

A mucinose dérmica focal (MDF) é uma entidade relativamente rara, porém clinicamente é semelhante ao CBC. Ela faz parte de um grupo de dermatoses mais abrangente, conhecido como mucinose dérmica cutânea, caracterizadas por fibroblastos que produzem abundante quantidade de mucina que se acumula na derme. A MDF, assim como o CBC, se apresenta como pápula solitária ou nódulo,

mais comumente na face, tronco e extremidades (McDERMOTT et al, 2003; NEBRIDA et al, 2002). A MDF apresenta-se à dermatoscopia com vasos serpenginosos associados a um fundo rosa-amarelado, não sendo possível sua diferenciação com o CBC, que também pode se apresentar de forma semelhante. Contudo, existem diferenças notáveis entre a MDF e o CBC na MCR. Descrevemos os principais achados da MDF, como a presença de estruturas fusiformes/dendríticas espessas, circundadas por fibras de colágeno finas orientadas ao acaso e separadas por espaços mais escuros na derme, associadas ao aumento do fluxo sanguíneo na microcirculação vista durante o exame ou no modo vídeo, devido à proliferação dos capilares dérmicos (FRAGA-BRAGHIROLI et al., 2015). Os espaços escuros correspondem ao depósito de mucina misturado ao estroma dérmico, visualizado à histopatologia com o uso de coloração especial para mucina; as células fusiformes correspondem aos fibroblastos imersos nas áreas com mucina. À análise com hematoxilina e eosina, a presença de mucina é suspeitada pela presença de espaços largos e vazios dentre as fibras de colágeno. Em contraste, o CBC apresenta à MCR áreas escuras, conhecidas como silhuetas escuras, com contornos policíclicos e delineadas por fibras de colágeno denso, além das ilhas tumorais e áreas escuras ao redor das ilhas tumorais separando-as das fibras de colágeno que as envolvem.

6.4 USO DO MODELO DE MICROSCOPIA CONFOCAL DE REFLECTÂNCIA COM PISTOLA PORTÁTIL (HANDHELD) NO DIAGNÓSTICO DE PÁPULAS FACIAIS INESPECÍFICAS E DO CARCINOMA BASOCELULAR

O modelo de microscopia confocal de reflectância com pistola portátil (handheld) (HH-RCM - Vivascope 3000, assim como o tradicional Vivascope 1500, utiliza a tecnologia de laser de diodo de 830 nanômetro. A pistola portátil com sonda pequena permite o acesso a áreas curvadas do corpo, além de poder ser aplicada diretamente à superfície cutânea, sem a necessidade do anel de fixação, tornando o exame da microscopia confocal mais fácil e rápido. Este modelo oferece um campo de visão de um milímetro, o que corresponde a visão histológica de pequeno aumento ao microscópio óptico. A MCR é uma ferramenta auxiliar importante na avaliação clínica e dermatoscópica de pápulas pequenas e nódulos, principalmente

na face, onde o médico clínico é mais relutante em indicar a realização de biópsias, que poderiam vir a se revelar desnecessárias. Os achados morfológicos da microscopia confocal utilizando-se o modelo Vivascope 3000 são os mesmos decritos no modelo tradicional.

Em 2014 descrevemos 6 (seis) casos de pápulas faciais brancas com características clínicas e dermatoscópicas não específicas, nos quais o uso da MCR permitiu o diagnótico preciso, confirmados em seguida pelo exame histopatológico (FRAGA-BRAGHIROLI et al., 2014). Dentre estes casos, foram diagnosticados 2 carcinomas basocelular (CBC), um tricoblastoma desmoplásico (TBD), um carcinoma escamocelular (CEC), uma hiperplasia sebácea (HS) e um nevo melanocítico intradérmico. O carcinoma basocelular, neoplasia maligna mais prevalente, é facilmente visualizado na MCR. Seus principais achados são: silhuetas escuras ao nível da JDE, ilhas tumorais brilhantes circundadas por espaços escuros, vasos canaliculares e colágeno espessado ao nível da derme papilar. O tricoblastoma desmoplásico é uma neoplasia benigna da pele, com aspectos clínicos e confocais semelhantes ao carcinoma basocelular. Os achados da MCR deste estudo estão de acordo com a descrição de Ardigo et al. (2007) quando relatou 4 casos de TBD. Os principais achados foram a presença de ilhas tumorais brilhantes compostas por cordões de células com núcleo alongado, semelhante ao CBC. Contudo, o TBD apresenta como características únicas as conexões entre os agregados neoplásicos e as estruturas foliculares; cistos córneos agregados, compostos por espaços escuros e arredondados preenchidos por material branco, correspondente aos cistos ceratinizados na histopatologia, além de faixas de colágeno espessadas envolvendo as ilhas tumorais. Estas ilhas, por sua vez, são menores, mais escassas e estão distribuídas mais espaçadamente quando comparadas ao CBC. As caracteríticas da MCR do CEC são compostas por uma epiderme com o padrão de favo de mel irregular, uma epiderme desorganizada e pela presença de células arredondadas e nucleadas nas camadas espinhosa e granular. Na JDE, alças de vasos sanguíneos são visualizadas como estruturas arredondadas brancas dentro da derme papilar. Assim como o TBD, a hiperplasia sebácea também pode se assemelhar ao CBC clinicamente e à dermatoscopia. Com o uso do Vivascope 3000, a HS pode ser rapidamente diferenciada. Suas principais

características na MCR são os agregados semelhantes à mórulas, descrito inicialmente por Propperova et al. (2007) e posteriormente por Moscarella et al. (2013). Os nevos intradérmicos e nevos compostos localizados na face são muitas vezes desafiadores posto que apresentam características clínicas e à dermatoscopia semelhantes ao CBC. Na MRC, a diferenção do nevo melanocítico do CBC é bem evidente e direta, uma vez que os ninhos de melanócitos são prontamente vizualizados na MCR devido ao forte poder de refração da melanina. (FRAGA-BRAGHIROLI et al., 2014) Descrevemos um caso de carcinoma basocelular pigmentado na pele negra; esta lesão, clinicamente, não apresentava achados específicos do CBC pigmentado devido ao fototipo da pele do paciente. A dermatoscopia apresentou estruturas em folhas ou roda de leme, presentes no CBC pigmentado. Contudo, somente após a realização do exame da MCR utilizando o modelo HH-RCM, as ilhas tumorais circundadas por espaços escuros foram visualisadas, confirmando o diagnótico do CBC pigmentado. (STEPHENS et al., 2013)

Estudos tem mostrado que a acurácia do diagnóstico clínico do CBC por dermatologistas experientes é de cerca de 70% (GUITERA et al., 2012). Compararamos a eficácia do Vivascope 3000 com o Vivascope 1500 no diagnóstico do CBC. Neste estudo 45 das 54 lesões clinicamente suspeitas de CBC foram confirmadas histologicamente, refletindo um valor preditivo positivo de 83%. As mesmas 54 lesões foram avaliadas com ambos modelos de MCR**;** o HH-RCM revelou 44 lesões com mais de 3 critérios para o CBC, incluindo a presença de silhuetas tumorais escuras ou ilhas tumorais brilhantes; destas, 42 lesões (95%) foram histologicamente comprovadas como CBC, 1 (uma) como ceratose liquenóide (liquen-plano like keratosis) e 1 (uma) como melanoma amelanótico. Os principais achados da MCR relacionados ao CBC foram: silhuetas tumorais escuras, ilhas tumorais, espaços em fenda peritumoral, polarização dos ceratinócitos epidérmicos supra-tumorais, polarização dos núcleos das células tumorais periféricas, faixas de colágeno espessadas, vasos sanguíneos lineares, vasos sanguíneos canaliculares, células dendríticas e células redondas brilhantes. O diagnóstico do CBC pela MCR foi feito na presença de ao menos 3 desses critérios descritos, sendo ao menos um deles a ocorrência de ilhas tumorais ou silhuetas tumorais. O número médio de

achados na MCR tradicional foi da ordem de 6.2, enquanto no modelo handheld foi de 4.7. O modelo de MCR tradicional evidenciou pelo menos 3 critérios do CBC em 100% dos casos histologicamente confirmados de CBC **;** o modelo *handheld* evidenciou ao menos 3 achados em 93% dos casos histologicamente confirmados. O modelo tradicional diagnosticou todos os casos de CBC, já o modelo *handheld* não foi capaz de diagnosticar 3 casos de CBC. Quando comparado a frequência de observação de cada achado na MCR dos 45 casos de CBC, com ambos os modelos, uma significância estatística foi encontrada para a presença dos vasos sanguíneos lineares, polarização dos ceratinócitos epidérmicos supra-tumorais, e células redondas brilhantes; todos foram identificados mais frequentemente com o modelo de MCR tradicional do que com o HH-RCM (96% vs. 38% ($P < 0.0001$), 36% vs. 4% ($P = 0.0004$), e 89% vs. 67% ($P = 0.02$), respectivamente. Utilizando-se o critério da presença de ao menos 3 achados para o diagnóstico do CBC, o valor preditivo positivo para o modelo MCR tradicional foi de 96% e para o HH-RCM foi de 95%, indicando que, se o diagnóstico do CBC foi feito pela MCR, este é provavelmente correto. Contudo**,** o valor preditivo negativo foi de 100% para o MCR tradicional, enquanto para o HH-RCM foi de 70%. Assim, utilizando os critérios adotados, o modelo de MCR tradicional foi capaz de excluir o diagnóstico do CBC com precisão. Esta diferença está provavelmente relacionada com o maior campo de visão do modelo MCR tradicional (CASTRO et al., 2015). A acurácia diagnóstica deste estudo foi compatível com estudos anteriores. Nori et al. (2004) relataram uma sensibilidade de 100% no diagnóstico do CBC quando adotado o critério de 2 ou mais achados na MCR utilizando o modelo tradicional; a sensibilidade do estudo foi de 82.9% e a especificidade foi de 95.7% quando adotado o critério da presença de 4 ou mais achados. Gareau et al. (2009) reportaram a sensibilidade de 96.6% e especificidade de 89.2% com o uso da MCR tradicional na detecção do CBC *ex vivo* durante a cirurgia de Mohs. Guitera et al. (2012) encontraram sensibilidade de 100% e especificidade de 88.5% na identificação do CBC na MCR tradicional, utilizando os achados classicamente descritos para o CBC na microscopia confocal (polarização dos ceratinócitos supra-tumorais, telangiectasias e vasos tortuosos, ilhas tumorais e silhuetas tumorais escuras/espaços em fenda peritumoral).

6.5 ASPECTOS MORFOLÓGICOS DO CARCINOMA ESCAMOCELULAR PIGMENTADO E DESCRIÇÃO DO PADRÃO DE VASCULATURA DO CARCINOMA ESPINOCELULAR NA MICROSCOPIA CONFOCAL DE REFLECTÂNCIA

O carcinoma espinocelular é o segundo tipo de câncer de pele mais prevalente, depois do CBC, e alguns estudos recentes indicam que sua incidência vem se aproximando à do CBC. O CEC representa 20% a 50% de todos os cânceres de pele (ROGERS et al., 2015). Dados do Rochester Epidemiology Project, realizado pela Mayo Clinic, demonstraram um aumento de 263% na incidência do CEC cutâneo nos Estados Unidos entre os anos de 1976 a 1984, e entre 2000 e 2010 (MUZIC et al., 2017). Este aumento é atribuído ao envelhecimento da população e ao aprimoramento do diagnóstico clínico de neoplasias cutâneas, consequente ao desenvolvimento de novas tecnologias disponíveis para o atendimento médico. Karia et al. (2013) relataram que no acompanhamento de 12.572 pessoas com CEC cutâneo, 5.604 desenvolveram metástase nodais; no estudo de 8.791 pacientes, 3.932 morreram devido ao CEC cutâneo no ano de 2012. Dado ao aumento significante na incidência do CEC cutâneo e seu potencial para um desfecho letal, o CEC passou a ser considerado um problema de saúde pública. A utilização de ferramentas diagnósticas não invasivas, como a MRC, permite um diagnóstico da neoplasia em estágio inicial, direciona a conduta terapêutica com estratégias de atendimento médico que podem reduzir significativamente a evolução para agravamento dos casos.

Os critérios diagnósticos do carcinoma espinocelular na MCR foram inicialmente descritos por Rispon e colaboradores, em 2009 com avaliação de 38 lesões cutâneas histologicamente comprovadas como CEC. Os principais achados descritos foram**:** a presença de escamas na camada córnea, presentes em 95% dos casos; padrão em favo de mel atípico ou irregular das camadas granular e espinhosa; células arredondadas e nucleadas brilhosas nas camadas granular e espinhosa, presentes em 55% dos casos. As escamas correspondem, histologicamente, à presença de ortoqueratose ou paraqueratose. A presença de células poligonais nucleadas na camada córnea corresponde à paraqueratose. Este achado não é específico do CEC, podendo ocorrer em outras dermatoses com alto

índice de proliferação celular, como a psoríase. A presença do padrão em favo de mel atípico é específico das neoplasias de ceratócitos, visto em todos os casos de ceratose actínica e CEC. Enquanto o CEC apresenta extensa atipia ou desarranjo da camada epidérmica, as ceratoses actínicas revelam um desarranjo focal e um padrão de favo de mel levemente alterado. As células arredondadas nucleadas presentes nas camadas granulosa e espinhosa correspondem aos ceratinócitos disceratóticos. Gonyaley e colaboradores (2008) descreveram achados semelhantes na MCR do CEC.

Descrevemos a presença pequenos círculos brilhosos ao redor das pápulas dérmicas ao nível da JDE como um achado exclusivo do carcinoma escamocelular pigmentado (FRAGA-BRAGHIROLI et al., 2013). Esta entidade se apresenta clinicamente de forma inespecífica podendo se assemelhar ao lentigo solar ou a ceratose liquenóide (liquen-plano like keratosis*)*, ambas condições benignas. A MCR do CEC pigmentado é caracterizada por um padrão de favo de mel atípico nas camadas granulosa e espinhosa da epiderme, associado a presença dos pequenos círculos brilhosos ao redor das papilas dérmicas. Estes anéis são compostos por pequenas células brilhantes na MCR, que, histologicamente, representam os ceratinócitos pigmentados atípicos basais ricos em melanina, rodeando as papilas dérmicas ao nível da junção dermo-epidérmica.

O padrão de distribuição dos vasos ao nível da JDE e derme papilar fornecem pistas relevantes para o diagnóstico do CEC cutâneo. Descrevemos o sinal do “buracos de botão” na MCR, que, associado ao padrão de favo de mel atípico ao nível epidérmico, representam achados importantes no diagnóstico do CEC *in situ* (Que et al., 2016). O sinal do buracos de botão é representado pela presença de numerosos vasos arredondados e agregados na JDE, visualizados como círculos perfeitos numa visão transversal das papilas dérmicas, assemelhando-se a botões. A uniformidade, distribuição, e numerosidade dos vasos agregados refletem a forma como os vasos formam alças dentro das papilas dérmicas. Este achado corresponde aos vasos glomerulares visualizados à dermatoscopia. Histopatologicamente, o sinal do buracos de botão corresponde aos numerosos vasos sanguíneos tortuosos vistos ao nível das papilas dérmicas. Ahlgrimm-Siess V et al. (2011) correlacionaram os

vasos em pontos, observados na dermatoscopia do CEC, com a presença de vasos arredondados esparsamente distribuídos na JDE que aparecem na MCR. Apesar da presença isolada do sinal do buracos de botão à MCR não ser um achado específico do CEC, sua ocorrência associada ao padrão de favo de mel atípico da camada espinhosa direciona o diagnóstico para o CEC. Rispon et al. (2009) mostraram que 39% dos 38 casos de CEC analisados no seu estudo, não apresentavam vasos visíveis à dermatoscopia; no entanto, a MCR se mostrou particularmente útil no diagnóstico desses casos de CEC, uma vez que foi possível visualizar os vasos arredondados na derme superficial. Este fato se deve, provavelmente, pela maior penetração da luz infra vermelha da MCR, que tem o potencial de penetrar mais profundamente na pele do que a luz do dermatoscópio. As ceratoses actínicas apresentam um menor número de vasos na derme superficial e estes se distribuem mais esparsamente do que no CEC.

6.6 LIMITAÇÕES DA MICROSCOPIA CONFOCAL DE REFLECTÂNCIA E PERSPECTIVAS FUTURAS

Umas das limitações da microscopia confocal é a possibilidade de analisarmos as estruturas microanatômicas somente até a profundidade de 250 micrômetros, correspondendo ao alcance até a derme papilar. Alterações na derme reticular e os tumores que invadem a profundidade não podem ser avaliados adequadamente, resultando em exames falso negativos. Entretanto, em áreas onde a epiderme apresenta pouca espessura, parte da derme reticular também pode também ser avaliada. Em lesões com espessamento importante da epiderme, incluindo lesões acrais, a visão da MCR fica limitada à epiderme.

Outros fatores que também podem comprometer a qualidade do imagem da MCR são a presença de hiperceratose, a presença de resíduos de cremes com partículas com alta refração como protetores solar, e também a superfície não uniforme da pele que resulta na formação de bolhas, que constituem artefato.

A MCR requer treinamento do avaliador, que deve ter um robusto conhecimento em dermatopatologia uma vez que a identificação e a interpretação dos achados da MCR se correlacionam com as estruturas observadas nos exames

da histopatologia. Assim, o examinador pode se deparar com o desafio de distinguir estruturas e células com índice de refração semelhantes, a exemplo de melanócitos e células de Langerhans na camada espinhosa.

Cabe considerar, ainda, que o alto investimento necessário para aquisição do aparelho de MCR, também pode ser um fator limitante para sua utilização em grande escala nos tempos atuais.

Estudos têm mostrado a MCR como uma ferramenta auxiliar no diagnóstico de doenças cutâneas inflamatórias e infecciosas, como psoríase, dermatite de contato, lúpus eritematoso discóide e onicomicose, além de neoplasias como o linfoma cutâneo de células T (HOOGEDOON et al., 2015). Contudo, faltam estudos conduzidos com metodologia adequada para identificar a acurácia da MCR na distinção dos diferentes tipos de células inflamatórias. O uso da tecnologia da microscopia confocal pode vir a se mostrar interessante no diagnóstico de doenças endêmicas, como na leishmaniose cutânea e hanseníase, enfermidades ainda prevalentes no Brasil.

Uma série de novos projetos no âmbito do desenvolvimento tecnológico parecem promissores para o uso futuro da MCR. Aparelhos de MCR que capturam imagens da pele utilizando um escaneamento em linha, ao invés do escaneamento de um ponto, já estão sendo desenvolvidos. Isso reduzirá o tempo de obtenção de imagem, além de reduzir o tamanho e custo do aparelho. Máquinas de microscopia confocal com software programado para o reconhecimento automatizado de detalhes da anatomia da pele e da histopatologia também estão sendo estudadas, com possibilidade de reconstrução das imagens em 3 dimensões (KURUGOL et al., 2011, GAREAU et al., 2011). Por fim, imagens de confocal fluorescentes, que se revelam após a injeção de contraste intradérmico *in vivo*, como a verde-indocianina, também estão em fase de testes, com o objetivo de melhorar a identificação das estruturas visualizadas através da MCR (JONAK et al., 2011, SKVARA et al., 2011).

7. CONCLUSÕES

1. A Microscopia Confocal de Reflectância (MCR) é uma ferramenta adjunta no diagnóstico não invasivo de neoplasias cutâneas.
2. Os aspectos morfológicos observados à Microscopia Confocal de Reflectância na avaliação das estruturas da pele, mostram equivalência com os achados histológicos, no diagnóstico das neoplasias cutâneas, permitindo plena comparação entre as imagens da microscopia confocal e as imagens histopatológicas.
3. O uso da Microscopia Confocal de Reflectância no diagnóstico de neoplasias cutâneas poupa o paciente de procedimentos invasivos, evitando a dor, ansiedade e risco de complicações, como infecções e cicatrizes inerentes a um procedimento cirúrgico.
4. O equipamento de Microscopia Confocal de Reflectância com pistola portátil (*handheld*) (HH-RCM - Vivascope 3000) demonstra vantagens pela facilidade de acesso a áreas anatômicas curvadas, podendo ser aplicado diretamente à superfície cutânea, sem a necessidade do anel de fixação, tornando o exame da microscopia confocal mais factível e mais rápido.
5. O equipamento portátil de Microscopia Confocal de Reflectância (HH-RCM) é capaz de revelar aspectos morfológicos que permitem diagnosticar, com precisão, pápulas solitárias faciais inespecíficas, dentre elas o carcinoma basocelular, tricoblastoma desmoplásico, carcinoma escamocelular, hiperplasia sebácea e o nevo melanocítico intradérmico.
6. O equipamento tradicional para realização da Microscopia Confocal de Reflectância (Vivascope 1500), assim como o modelo portátil HH-RCM, demonstram um alto valor preditivo positivo no diagnóstico do carcinoma basocelular. O modelo tradicional mostra um valor preditivo negativo maior que o modelo portátil, devido ao seu campo de visão mais largo, oferecendo uma visão da arquitetura total das lesões maiores de 1 mm.
7. A Microscopia Confocal de Reflectância se mostrou precisa no diagnóstico de ceratose seborréica clonal, enquanto que, ao exame clínico e à dermatoscopia, aparenta aspecto semelhante ao melanoma maligno da pele.

8. A mucinose dérmica focal, apesar de clinicamente se assemelhar ao carcinoma basocelular, mostra características na microscopia confocal que permitem o diagnóstico diferencial do CBC.
9. A Microscopia Confocal de Reflectância permite caracterizar o carcinoma escamocelular pigmentado pela presença do padrão de favo de mel atípico nas camadas granulosa e espinhosa da epiderme, associado a presença dos pequenos círculos brilhosos ao redor das papilas dérmicas.
10. O padrão de distribuição dos vasos ao nível da junção dermo-epidérmica (JDE) e derme papilar é relevante para o diagnóstico do carcinoma escamocelular (CEC) cutâneo.
11. O sinal do “buracos de botão” observado na Microscopia Confocal de Reflectância, associado ao padrão de favo de mel atípico ao nível epidérmico, é importante no diagnóstico do carcinoma escamocelular (CEC) in situ.

REFERÊNCIAS

AHLGRIMM-SIESS, V. et al. The vasculature of nonmelanocytic skin tumors on reflectance confocal microscopy: vascular features of squamous cell carcinoma in situ. **Arch. Dermatol**., v. 147, n. 2, p. 264, 2011.

AHLGRIMM-SIESS, V. et al. Monitoring efficacy of cryotherapy for superficial basal cell carcinomas with in vivo reflectance confocal microscopy: a preliminary study. **J. Dermatol. Sci**., v. 53, p. 60-64, 2009.

ARDIGO, M. et al. Dermoscopic and reflectance confocal microscope findings of trichoepithelioma. **Dermatology,** v. 215, p. 354–358, 2007**.**

BENN ASSAR, A. et al. Ex vivo fluorescence confocal microscopy for fast evaluation of tumour margins during Mohs surgery. **Br. J. Dermatol.,** v. 170, p. 360-365, 2014**.**

CASTRO, R. et al. Accuracy of in vivo confocal microscopy for diagnosis of basal cell carcinoma: a comparative study between handheld and wide-probe confocal imaging. **JEAVD,** v. 29, p. 1164-1169, 2015.

CINOTTI, E. et al. The role of in vivo confocal microscopy in the diagnosis of eyelid margin tumors: 47 cases. **J. Am. Acad. Dermatol.,** v. 71, p. 912-918.e2, 2014.

CURIEL-LEWANDROWSKI, C. et al. Use of in vivo confocal microscopy in malignant melanoma: an aid in diagnosis and assessment of surgical and nonsurgical therapeutic approaches. **Arch. Dermatol.,** v. 140, p. 1127-1132, 2004.

DAVIDOVITS, P.; EGGER, M. D. Scanning laser microscope. **Nature,** v. 223, n**.** 5208, p. 831, 1969.

DAVIDOVITS, P.; EGGER, M. D. Scanning laser microscope for biological investigations. **Appl. Optics.,** v; 10, n. 7, p. 1615–1619, 1971.

DEBARBIEUX, S. et al. Reflectance confocal microscopy characteristics of eight cases of pustular eruptions and histopathological correlations. **Skin Res. Technol.,** v. 19, p. e444–e452, 2013.

DEBARBIEUX, S. et al. Reflectance confocal microscopy of mucosal pigmented macules: a review of 56 cases including 10 macular melanomas. **Br. J. Dermatol.,** v. 170, p. 1276-1284, 2014.

ERFAN, N. et al. Labial melanotic macule: a potential pitfall on reflectance confocal microscopy. **Dermatology**, v. 224, p. 209– 211, 2012.

FRAGA-BRAGHIROLI, N. et al. Use of handheld reflectance confocal microscopy for in vivo diagnosis of solitary facial papules: a case series. **JEAVD**, v. 28, p. 933-942, 2014.

FRAGA-BRAGHIROLI, N. et al. Small brown circles: An important diagnostic clue for pigmented squamous cell carcinoma. **J. Am. Acad. of Dermatol.,** v. 69, n. 4, p. 161-163, 2013.

FRAGA-BRAGHIROLI, N. et al. Reflectance confocal microscopy features of a clonal seborrheic keratosis that clinically and dermoscopically simulates melanoma. **Dermatol. Surg.**, v. 41, n. 5, p. 662-665, 2015.

FRAGA-BRAGHIROLI et al. Reflectance confocal microscopy features of focal dermal mucinosis differ from those described for basal cell carcinoma: report of two cases. **Dermatology**, v. 231, p. 326-329, 2015.

GAREAU, D. Automated identification of epidermal keratinocytes in reflectance confocal microscopy. **J. Biomed. Opt.** v.16, n. 3:030502, 2011.

GAREAU, D.S. et al. Sensitivity and specificity for detecting basal cell carcinomas in Mohs excisions with confocal fluorescence mosaicing microscopy. **J. Biomed. Opt.**, v. 14, n. 3 :034012, 2009.

GONZALEZ, S. et al. Changing Paradigms in Dermatology: Confocal Microscopy in Clinical and Surgical Dermatology. **Clin. Dermatol.**, v. 21, p. 359-369, 2003.

GONZALEZ, S. et. al. Confocal reflectance imaging of folliculitis in vivo: correlation with routine histology. **J. Cutan. Pathol.**, v. 26: p. 201–205, 1999.

GONYALEY, S., GILL, M., HALPERN, A.C. **Reflectance confocal microscopy of cutaneous tumors: an atlas with clinical, dermoscopic and histological correlations**. New York, NY: Inf. HealthCare, 2008. p. 30-75.

GUITERA, P. et al. In vivo confocal microscopy for diagnosis of melanoma and basal cell carcinoma using a two-step method: analysis of 710 consecutive clinically equivocal cases. **J. Invest. Dermatol.**, v. 132, p. 2386–2394, 2012.

HOOGEDOON, L. et al. The value of in vivo reflectance confocal microscopy in the diagnosis and monitoring of inflammatory and infectious skin diseases: a systematic review. **Brit. J. Dermatol.,** v.172, p: 1222–1248, 2015.

JONAK, C. et al. Intradermal indocyanine green for in vivo fluorescence laser scanning microscopy of human skin: a pilot study**. PLoS One.**, v. 6: e23972, 2011.

KARIA, P.S., HAN, J., SCHMULTS, C.D. Cutaneous squamous cell carcinoma: estimated incidence of disease, nodal metastasis, and deaths from disease in the United States, 2012. **J. Am. Acad. Dermatol.**, v. 68, p. 957-966, 2013.

KURUGOL, S. et al. Pilot study of semiautomated localization of the dermal/epidermal junction in reflectance confocal microscopy images of skin. **J. Biomed. Opt.**, v. 16:036005, 2011.

LONGO, C. et al. Clonal seborrheic keratosis: dermoscopic and confocal microscopy characterization. **J. Eur. Acad. Dermatol. Venereol., v.** 28, p. 1397– 1400, 2013.

MC DERMOTT, A.L. et al. Focal mucinosis: clinical and histological features of an unusual condition. **J. Laryngol. Otol**., v. 117:p. 408–409, 2003.

MINSKY, M. Microscopy apparatus. U.S. Patent No. 3013467, 7 Nov. 1957.

MOSCARELLA, E. et al. Clinical, dermoscopic and reflectance confocal microscopy features of sebaceous neoplasms in Muir-Torre syndrome. **J. Eur. Acad. Dermatol. Venereol.**,v. 27:,p. 699–705, 2013.

MUZIC J.G. et al. Incidence and trends of basal cell carcinoma and cutaneous squamous cell carcinoma: a population-based study in Olmsted County, Minnesota, 2000 to 2010. **Mayo Clin. Proc.**, v. 92, p. 890-898, 2017.

NEBRIDA, M.L., TAY, Y.K. Cutaneous focal muci- nosis: a case report. **Pediatr. Dermatol.**, v. 19, p. 33–35, 2002.

NADIMINTI, H. et al. Use of reflectance confocal microscopy to monitor response of lentigo maligna to nonsurgical treatment. **Dermatol. Surg.**, v. 36, p. 177-184, 2010.

NEDA, S. et al. In vivo reflectance confocal microscopy image interpretation for the dermatopathologist. **J. Cutan. Pathol.** p. 1–11, 2017.

NORI, S. et al. Sensitivity and specificity of reflectance-mode confocal microscopy for in vivo diagnosis of basal cell carcinoma: a multicenter study. **J. Am. Acad. Dermatol.**, v. 51, p. 923–930, 2004.

PETRAN, M. et al. Tandem-Scanning Reflected-Light Microscope. **J. Optic. Soc. Amer.**, v. 58, n. 5, p. 661–664, 1968.

PETRAN, M., HADRAVSKY, M. Method and arrangement for improving the resolving, power and contrast. November 1967, granted 30. June 1970.

PROPPEROVA, I., LANGLEY, R.B. Reflectance-mode confocal microscopy for the diagnosis of SH In vivo. **Arch. Dermatol.**, v. 143, p. 134, 2007.

QUE, SK. et al. Through the looking glass: Basics and principles of reflectance confocal microscopy. **J. Am. Acad. Dermatol**., v. 73, n.2, p. 276-282, 2015.

QUE, SK. et al. A pink papule on the back of an 82-year-old man: an exemple of the buttonhole sign on reflectance confocal microscopy. **Dermatol. Pract. Concept**., v. 6, n. 3, p. 1-2, 2016.

RAJADHYAKSHA, M. et al. In vivo scanning laser microscopy of human skin: Melanin provides strong contrast. **J. Invest. Dermatol.**. v. 104, n. 6, p. 946-952, 1995.

RISHPON, A. et al. Reflectance confocal microscopy criteria for squamous cell carcinomas and actinic keratoses. **Arch. Dermatol.**, v. 145, p. 766-772, 2009.

ROGERS, H.W. et al. Incidence estimate of nonmelanoma skin cancer (keratinocyte carcinoma in the U.S population, 2012. **JAMA Dermatol.**, v. 215, p. 1081-1086, 2015.

STEPHENS, A. et al. Spoke wheel-like structures in superficial basal cell carcinoma: A correlation between dermoscopy, histopathology, and reflective confocal microscopy. **J. Am. Acad. Dermatol**., v. 69, n. 5, p. 291-221, 2013.

SKVARA, H. et al. In vivo fluorescence confocal microscopy: indocyanine green enhances the contrast of epidermal and dermal structures. **J. Biomed. Opt.**, v. 16, p. 096010, 2011.

TORRES, A. et al. 5% imiquimod cream and reflectance-mode confocal microscopy as adjunct modalities to Mohs micrographic surgery for treatment of basal cell carcinoma. **Dermatol .Surg.**; v. 30, p. 1462-1469, 2004.

ULRICH, M. et al. Reflectance confocal microscopy for noninvasive monitoring of therapy and detection of subclinical actinic keratoses. **Dermatology,** v. 220, p. 15-24, 2010.

9. ANEXOS

9.1 ANEXO I. Termo de consentimento

Skin and Cancer Associates
Center For Dermatology

Richard S. Greene, M.D.
Joel M. Wilentz, M.D.
Joseph A. Arena, M.D.
Garry B. Gewirtzman, M.D.
Harold S. Rabinovitz, M.D.

David M. Sharaf, M.D.
Daniel J. Wolf, M.D.
Mark S. Nestor, M.D., Ph.D.
Daniel Rivin, M.D.
Brian J. Katz, M.D.

CHART #_____

Consent for Photographs/Digital Images/RCM

1. I do hereby authorize the taking of images for research, educational purposes and for possible publication. Regarding publication, the patient will not be able to be identified from the photographs/images.
2. Many times these images remain as part of your permanent medical record. Sometimes they are deleted.
3. I understand that all information will remain confidential according to HIPAA Laws. The only information which may but not always be released includes initials, birth date, sex and location of lesion. Only researchers and agencies working with Skin and Cancer Associates will have access to your images and the above limited personal information.
4. You have the right to refuse to sign this permission form.

Signature of Patient/ Legal Guardian: _____

Date: _____

Witness: _____

Date: _____

This Office is Regulated to 64B8-9.009 Standard of Care for Office Surgery, and Such Notice is Prominently Posted.

Q 201 N.W. 82nd Ave. • Suite 501 • Plantation, FL 33324 • (954) 473-6750
Q 201 N.W. 82nd Ave. • Suite 103 • Plantation, FL 33324 • (954) 693-9648
Q 2100 E. Hallandale Beach Blvd. • Suite 100 • Hallandale, FL 33009 • (954) 454-1066
Q 2925 Aventura Blvd. • Suite 205 • Aventura, FL 33180 • (305) 933-5950 • (305) 933-6716
Q 7301 Palmetto Park Rd. W. • Suite 200B • Boca Raton, FL 33180 • (561) 417-8413
Q 4302 Alton Road • Suite 960 • Miami Beach, FL 33140 • (305) 674-6865

Skin and Cancer Associates
CENTER FOR DERMATOLOGY

Harold S. Rabinovitz, M.D.
Mohs Micrographic Surgery

201 N.W. 82nd Avenue
Suite 103
Plantation, Florida 33324
(954) 693-9648

Consent for Publication of Identifying Material in The JAMA Network Journals

I give my permission for the following material to appear in the pript, online and licensed versions of The JAMA Network Journals and for The JAMA Network Journals to grant permission to third parties to reproduce this material.

Title or subject of article or photograph, video or audio

I understand that my name will not be published but that complete anonymity cannot be guaranteed.

Please check the appropriate box below after reading each statement.

❑ I have read the manuscript or a general description of what the manuscript contains and reviewed all photographs, illustrations, video or audio files (if included) in which I am included that will be published.

❑ I have been offered the opportunity to read the manuscript and to see all photographs, Illustrations, video or audio files (if included) in which I am included, but I waive my right to do so.

Signed _____ Date _____

Print Name _____

If you are granting permission for another person, what is your relationship to that person?

_____

The JAMA Network Journals

JAMA
JAMA Dermatology
JAMA Facial Plastic Surgery
JAMA Internal Medicine
JAMA Neurology
JAMA Opthamology
JAMA Otolaryngology-Head & Neck Surgery
JAMA Psychiatry
JAMA Pediatrics
JAMA Surgery

9.2 ANEXO II – Parecer do Comitê de Ética (Institutional Review Board)

UNIVERSITY OF Miami
SCHOOL OF MEDICINE

NOT HUMAN SUBJECT RESEARCH

October 1, 2009

James Grichnik, MD PhD
University of Miami
Department of Dermatology
Medical Campus

STUDY TITLE: Retrospective feature analysis of cutaneous dermoscopic and confoncal microscopy images.

IRB ACTION DATE: 10/01/09

On October 1, 2009, an IRB Administrative Designee reviewed the information you provided to the Human Subject Research Office (HSRO) and determined that your project does not constitute human subject research. Based on the information submitted for review, you only plan to access images from an archive, which do not contain any of the 18 specific identifiers noted in the privacy Rule. As such, it is not subject to IRB review under 45 CFR 46.

The materials submitted and considered for review of this project included:
1. Non-Human/Non-Research Determination Application Dated September 30, 2009

This review and determination is based only on the information provided to the HSRO and is not valid if the proposed project is not exactly as described, or if additional information (including grants, contracts or other information) have been withheld.

The HSRO must be notified if the proposed activity changes and becomes research. Research involving human subjects must receive IRB review and approval prior to implementation.

If you have any questions, please call the HSRO at (305) 243-3195.

Sincerely,

Amanda Coltes-Rojas, MPH, CIP
Director
Regulatory Affairs & Educational Initiatives

10. APÊNDICES

Artigos completos publicado em co-autoria sobre temas relacionados à Tese

Spoke wheel–like structures in superficial basal cell carcinoma: A correlation between dermoscopy, histopathology, and reflective confocal microscopy

Alexis Stephens, DO,[a] Naiara Fraga-Braghiroli, MD,[a] Margaret Oliviero, ARNP,[a] Harold Rabinovitz, MD,[a] and Alon Scope, MD[b,c]

Plantation, Florida; New York, New York; and Tel Aviv, Israel

CLINICAL PRESENTATION

A 62-year-old man with Fitzpatrick skin phototype VI presented for the evaluation of a lesion on his scalp. A 5-mm, poorly defined, skin-colored papule speckled with multiple dark brown dots was observed (Fig 1). The clinical differential diagnosis included pigmented basal cell carcinoma (BCC), solar lentigo, seborrheic keratosis, and melanoma on sun-damaged skin.

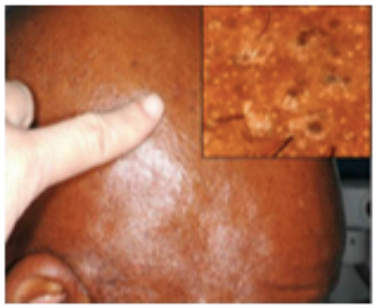

Fig 1. Superficial basal cell carcinoma. Poorly defined, skin-colored papule with multiple dark brown dots on the scalp.

DERMOSCOPIC APPEARANCE

Under the dermatoscope, multiple spoke wheel–like structures were seen (Fig 2; *arrows*). Spoke wheel–like structures have been defined as well circumscribed, brown radial projections meeting at a darker brown central hub.[1] Spoke wheel–like structures are a highly specific dermoscopic finding of pigmented BCC, with a reported specificity of 100%.[2]

From the Skin and Cancer Associates,[a] Plantation, Florida; Dermatology Department,[b] Sheba Medical Center and Sackler Faculty of Medicine, Tel Aviv University; and the Dermatology Service,[c] Memorial Sloan-Kettering Cancer Center, New York.

Funding sources: None.

Dr Rabinovitz and Ms Oliviero are investigators in a study coordinated by Caliber I.D., manufacturer of a commercial confocal microscope. Dr Rabinovitz has received funding for a fellowship program and equipment from Canfield I.D. He is also a consultant and has received equipment from 3Gen and Canfield, manufacturer of a polarized dermatoscope.

Reprint requests: Harold Rabinovitz, MD, Skin and Cancer Associates, 201 NW 82nd Ave, Ste 103, Plantation, FL 33324. E-mail: Harold@ADMCORP.com.

J Am Acad Dermatol 2013;69:e219-21.
0190-9622/$36.00

© 2013 by the American Academy of Dermatology, Inc.

http://dx.doi.org/10.1016/j.jaad.2013.04.038

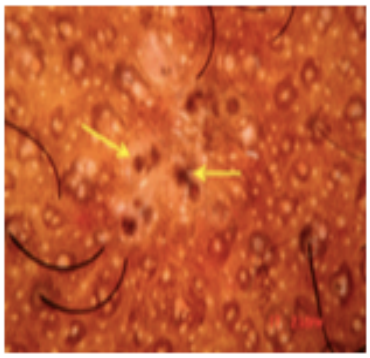

Fig 2. Superficial basal cell carcinoma. Dermoscopy image showing multiple spoke wheel–like structures.

REFLECTIVE CONFOCAL MICROSCOPY APPEARANCE

For additional diagnostic confirmation, a reflectance confocal microscopic (RCM) examination was performed, revealing stellate-shaped bright tumor islands surrounded by a dark area at the level of the dermoepidermal junction (Fig 3). Of note, some of the projections of the bright tumor islands were connected to the basal layer of the epidermis (Fig 3; *arrows*).

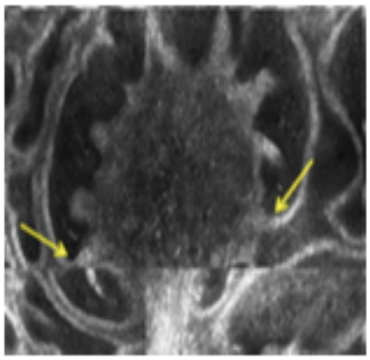

Fig 3. Superficial basal cell carcinoma. Reflectance confocal microscopy (1.5 mm × 1.5 mm) reveals a stellate-shaped bright tumor island at the dermoepidermal junction with projections connected to the basal layer of the epidermis (*arrows*).

HISTOPATHOLOGIC DIAGNOSIS

A shave biopsy specimen was obtained, and the subsequent histopathologic examination confirmed the diagnosis of superficial BCC (Fig 4). The histopathologic findings that correspond to the spoke wheel–like structures seen under dermoscopy and the stellate-shaped bright tumor islands seen under RCM are neoplastic basaloid aggregates in the papillary dermis that emanate from the undersurface of the epidermis, displaying multiple connections to the base of the epidermis (Fig 4; *arrows*).

J Am Acad Dermatol
Volume 69, Number 5

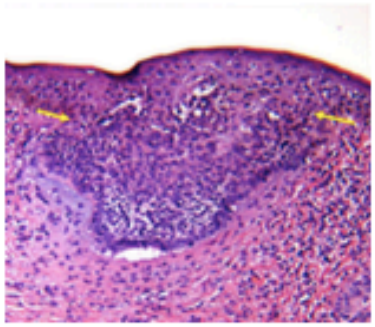

Fig 4. Superficial basal cell carcinoma. The histopathologic examination reveals neoplastic basaloid aggregates in the papillary dermis that emanate from the undersurface of the epidermis, revealing multiple connections to the base of the epidermis (*arrows*). These histopathologic results correspond to the spoke wheel–like structures seen under dermoscopy and reflectance confocal microscopy. (Hematoxylin–eosin stain; original magnification: ×100.)

KEY MESSAGE

Spoke wheel–like structures, a highly specific dermoscopic structure for the diagnosis of superficial BCC, correlate histopathologically and confocally with neoplastic basaloid aggregates that display multiple connections to the base of the epidermis.

REFERENCES

1. Kaya G, Braun RP. Histopathological correlation in dermoscopy. In: Marghoob AA, Braun RP, Kopf AW, editors. Atlas of dermoscopy. 1st ed London: Taylor & Francis; 2005. pp. 23-7.
2. Menzies SW, Westerhoff K, Rabinovitz H, Kopf AW, McCarthy WH, Katz B. Surface microscopy of pigmented basal cell carcinoma. Arch Dermatol 2000;136:1012-6.

Small brown circles: An important diagnostic clue for pigmented squamous cell carcinoma

Naiara Fraga-Braghiroli, MD,[a] Alexis Stephens, DO,[a] Margaret Oliviero, ARNP,[a] Harold Rabinovitz, MD,[a] and Alon Scope, MD[b,c]
Plantation, Florida; Tel Aviv, Israel; and New York, New York

CLINICAL PRESENTATION

A 70-year-old woman presented for a periodic skin examination. A pink-brown plaque was identified on the left thigh; the clinical differential diagnoses included solar lentigo and lichen planus–like keratosis because of the sharp borders, homogeneous brown color, and absence of scales (Fig 1).

Fig 1. Pigmented squamous cell carcinoma. Pink-brown plaque on the left thigh.

DERMATOSCOPIC APPEARANCE

On dermatoscopy, small brown circles were seen at the periphery of the lesion (Fig 2; *arrow*); this dermatoscopic finding added a differential diagnosis of pigmented squamous cell carcinoma (SCC).[1]

From Skin and Cancer Associates,[a] Plantation; Department of Dermatology,[b] Sheba Medical Center and Sackler Faculty of Medicine, Tel Aviv University, Tel Aviv; and the Dermatology Service,[c] Memorial Sloan-Kettering Cancer Center, New York.

Funding sources: None.

Dr Rabinovitz and Ms Olivieiro are investigators in a study coordinated by Caliber ID, manufacturer of a commercial confocal microscope. Dr Rabinovitz has received funding for a fellowship program and equipment from Canfield ID. He is also a consultant and has received equipment from 3Gen and Canfield.

Reprint requests: Harold Rabinovitz, MD, Skin and Cancer Associates, 201 NW 82nd Ave, Ste 103, Plantation, FL 33324. E-mail: Harold@ADMCORP.com.

J Am Acad Dermatol 2013;69:e161-3.
0190-9622/$36.00

© 2013 by the American Academy of Dermatology, Inc.

http://dx.doi.org/10.1016/j.jaad.2013.04.024

Fig 2. Pigmented squamous cell carcinoma. Dermatoscopic image shows brown circles at the periphery of the lesion (higher magnification seen at *inset*) and a pink-white background.

Reflective confocal microscopy appearance

To better differentiate these diagnostic entities, reflectance confocal microscopy (RCM) examination was performed. RCM revealed an atypical honeycomb pattern at the spinous layer.[2] In addition, multiple small bright circles were observed at the dermoepidermal junction (DEJ; Fig 3, *arrows*), which correlated with the small brown circles seen on dermatoscopy; these bright circles were comprised of small bright cells, which represent pigmented basal keratinocytes, rimming the dermal papillae. These RCM findings supported the diagnosis of SCC.

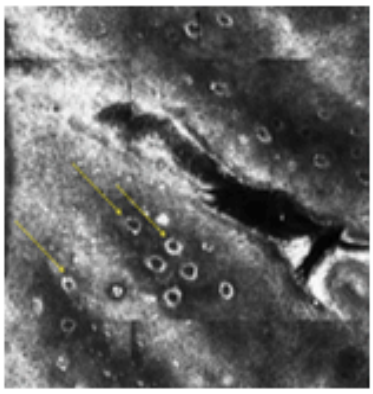

Fig 3. Pigmented squamous cell carcinoma. Reflectance confocal microscopy image (1.5 × 1.5 mm) reveals an atypical honeycomb pattern at the spinous layer (*asterisk*). In addition, multiple small bright circles are seen at the dermoepidermal junction (*arrow*).

HISTOLOGIC DIAGNOSIS

A shave biopsy specimen was obtained, and the histopathologic examination revealed an acanthotic epidermis with crowding and disordered arrangement of nuclei and large, pleomorphic nuclei (Fig 4), findings that are diagnostic of SCC in situ. Of note, there were foci in which the DEJ revealed an undulated pattern composed of rete ridges and dermal papillae. The small brown circle seen under dermatoscopy and the bright circles seen under RCM correlate on histopathology with atypical pigmented basal keratinocytes along the rete ridges in these foci.

J Am Acad Dermatol
Volume 69, Number 4

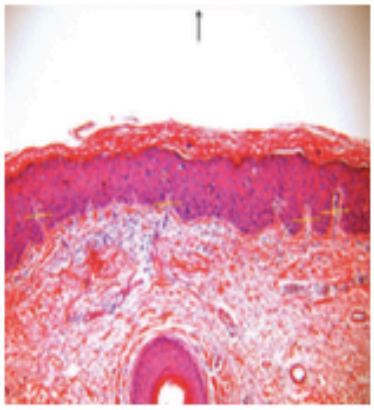

Fig 4. Pigmented squamous cell carcinoma. On histopathology, there is an acanthotic epidermis with crowding and disordered arrangement of nuclei and large, pleomorphic nuclei (hematoxylin–eosin stain; original magnification, ×100). Basal pigmented keratinocytes at foci in which the dermoepidermal junction has an undulated pattern are the correlates of the brown rings seen on dermatoscopy and bright rings seen on reflectance confocal microscopy.

KEY MESSAGE

Small brown circles are an important dermatoscopic feature for the diagnosis of pigmented SCC.

REFERENCES

1. Rosendahl C, Cameron A, Argenziano G, Zalaudek I, Tschandl P, Kittler H. Dermoscopy of squamous cell carcinoma and keratoacanthoma. Arch Dermatol 2012;148:1386-92.
2. Rishpon A, Kim N, Scope A, Porges L, Oliviero M, Braun R, et al. Reflectance confocal microscopy criteria for squamous cell carcinomas and actinic keratoses. Arch Dermatol 2009;145:766-72.